



TECHNISCHE UNIVERSITÄT MÜNCHEN

Wissenschaftszentrum Weihenstephan für Ernährung, Landnutzung und Umwelt (WZW)

Lehrstuhl für Biochemische Pflanzenpathologie

COPPER AMINE OXIDASE 8 (CuAO8) participates in the regulation of nitric oxide production during salt stress in seedlings of *Arabidopsis thaliana*

Felicitas Barbara Groß

Vollständiger Abdruck der von der Fakultät Wissenschaftszentrum Weihenstephan für Ernährung, Landnutzung und Umwelt der Technischen Universität München zur Erlangung des akademischen Grades eines

Doktors der Naturwissenschaften

genehmigten Dissertation.

Vorsitzender: Univ.-Prof. Dr. Claus Schwechheimer

Prüfer der Dissertation: 1. Univ.-Prof. Dr. Jörg Durner
2. apl. Prof. Dr. Erich Glawischnig

Die Dissertation wurde am 28.9.2016 bei der Technischen Universität München eingereicht und durch die Fakultät Wissenschaftszentrum Weihenstephan für Ernährung, Landnutzung und Umwelt am 1.12.2016 angenommen.

Publications related to this thesis:

Groß F, Durner J, Gaupels F. (2013) Nitric oxide, antioxidants and prooxidants in plant defence responses. *Front Plant Sci* **4**: 419

Groß F, Rudolf E, Thiele B, Durner J, Astier J. (2016) COPPER AMINE OXIDASE 8 (CuAO8) affects nitric oxide production in *Arabidopsis thaliana* seedlings by regulating arginase activity. (in preparation)

Other publications:

Wojtera-Kwiczor J, **Groß F**, Leffers HM, Kang M, Schneider M, Scheibe R. (2013) Transfer of a Redox-Signal through the Cytosol by Redox-Dependent Microcompartmentation of Glycolytic Enzymes at Mitochondria and Actin Cytoskeleton. *Front Plant Sci* **3**: 1–19

I. Table to content

I. TABLE TO CONTENT	2
II. SUMMARY	6
III. ABBREVIATIONS.....	7
IV. LIST OF FIGURES AND TABLES.....	9
1. INTRODUCTION.....	11
1.1 Importance and functions of nitric oxide (NO) in plants	11
1.2 NO synthesis in plants	12
1.2.1 Reductive pathway.....	13
1.2.1.1 Nitrate reductase dependent NO production.....	13
1.2.1.2 Xanthine oxidoreductase dependent NO production.....	15
1.2.1.3 Non-enzymatic reduction of nitrite to NO.....	15
1.2.2 Oxidative pathway	15
1.2.2.1 Structure and function of the mammalian NOS isoforms.....	16
1.2.2.2 NOS-like activity in plants.....	17
1.3 Polyamine metabolism.....	18
1.3.1 Amine oxidases.....	19
1.3.1.1 Copper dependent amine oxidases (CuAOs).....	20
1.3.1.2 FAD- dependent amine oxidases (PAOs).....	20
1.3.1.3 LDS1-like (LDL) proteins	21
1.4 Aim of the thesis	22
2. RESULTS	23
2.1 Identification of new genes involved in NO production	23
2.2 Reduced NO production in root tips of <i>cuao8-1</i> and <i>cuao8-2</i> seedlings in response to INA.....	26
2.3 General characterization of <i>CuAO8</i> and CuAO8	28
2.3.1 Loss of <i>CuAO8</i> mRNA and CuAO8 protein in <i>cuao8-1</i> and <i>cuao8-2</i>	28
2.3.2 Copper amine oxidase activity of CuAO8.....	28
2.3.3 Cytosolic and plasma membrane localization of GFP-CuAO8.....	31
2.3.4 Reduced primary root growth of <i>cuao8-1</i> and <i>cuao8-2</i>	32

2.4	Reduced NO production of <i>cuao8-1</i> and <i>cuao8-2</i> during salt stress	34
2.4.1	Reduced NO production in <i>cuao8-1</i> and <i>cuao8-2</i> root tips during salt stress	34
2.4.2	Reduced NO production in <i>cuao8-1</i> and <i>cuao8-2</i> cotyledons during salt stress	35
2.5	Reduced H₂O₂ production in root tips of <i>cuao8-1</i> and <i>cuao8-2</i> during salt stress	36
2.6	Increased amount of putrescine in <i>cuao8-1</i> and <i>cuao8-2</i> during salt stress	37
2.7	Decreased amount of free arginine in <i>cuao8-1</i> and <i>cuao8-2</i> during salt stress	38
2.8	Influence of Arginase activity on NO production in <i>cuao8-1</i> and <i>cuao8-2</i>.....	40
2.8.1	Increased arginase activity in <i>cuao8-1</i> and <i>cuao8-2</i> seedlings	40
2.8.2	Arginine supplementation restored <i>cuao8-1</i> and <i>cuao8-2</i> phenotype	41
2.9	Influence of NR activity on NO production in <i>cuao8-1</i> and <i>cuao8-2</i>	42
2.9.1	Increased nitrogen content in <i>cuao8-1</i> and <i>cuao8-2</i>	42
2.9.2	NR activity is not altered in <i>cuao8-1</i> and <i>cuao8-2</i>	44
3.	DISCUSSION	46
3.1	CuAO8 - a classical copper amine oxidase	46
3.2	CuAO8 knockout affects NO production in <i>A. thaliana</i> by altering arginase activity	47
3.3	Mammalian and plant arginine catabolism – a comparison.....	49
3.4	How could CuAO8 affect arginase activity?	51
3.5	Regulation of nitrate reductase (NR) by CuAO8.....	52
3.6	Is CuAO8 involved in the prevention of oxidative stress?	53
4.	OUTLOOK.....	56
5.	MATERIAL AND METHODS	57
5.1	Material.....	57
5.1.1	Plant Material.....	57
5.1.2	Bacteria	59
5.1.3	Kits.....	59
5.1.4	Buffers and solutions	60
5.1.5	Antibiotics.....	61
5.1.6	Media	61
5.1.7	Chemicals.....	62

5.1.8	Antibodies	63
5.1.9	Resins, columns, membranes	64
5.1.10	Enzymes	64
5.1.11	Vectors	64
5.1.12	Oligonucleotides	64
5.1.13	General Instruments	66
5.1.14	Webtools and software	67
5.2	Methods.....	68
5.2.1	Plan cultivation	68
5.2.1.1	Cultivation on soil.....	68
5.2.1.2	Cultivation under sterile conditions	68
5.2.2	General NaCl treatment of five day old seedlings	68
5.2.3	Molecular methods.....	68
5.2.3.1	Genomic DNA isolation (CTAP method).....	68
5.2.3.2	RNA extraction and cDNA synthesis	69
5.2.3.3	Polymerase chain reaction	69
5.2.3.4	BP reaction Gateway system	69
5.2.3.5	LR reaction Gateway system	69
5.2.3.6	Restriction digest	70
5.2.3.7	Ligation	70
5.2.3.8	Plasmid isolation.....	70
5.2.3.9	Agarose-gel electrophoresis.....	70
5.2.3.10	Extraction of DNA from Agarose Gels	70
5.2.3.11	Preparation of chemically competent <i>E. coli</i> DH5 α cells.....	70
5.2.3.12	Preparation of electro competent <i>A. tumefaciens</i> GV3101 pMP90.....	70
5.2.3.13	Transformation of chemical competent <i>E. coli</i> DH5 α	71
5.2.3.14	Transformation of electro competent <i>A. tumefaciens</i> GV3101 pMP90.....	71
5.2.3.15	Quantitative PCR	71
5.2.4	Phenotyping methods.....	72
5.2.4.1	Flowering time	72
5.2.4.2	Primary root growth.....	72
5.2.4.3	Chlorophyll breakdown	72
5.2.5	Biochemical methods.....	73
5.2.5.1	SDS-Page	73
5.2.5.2	Western Blot	73
5.2.5.3	Determination of protein concentration with Bradford	73
5.2.5.4	Total protein extraction for CuAO8 knockout analysis	73
5.2.5.5	Determination of putrescine, spermidine and spermine contents by HPLC	74
5.2.5.6	Amino acid analysis by LC-MS-MS.....	74
5.2.5.7	Measurement of nitrite and nitrate contents.....	75
5.2.5.8	Nitrate reductase activity measurement	75
5.2.5.9	Transient protein expression of CuAO8-His ₆ in <i>N. benthamiana</i>	76
5.2.5.10	Protein purification of CuAO8.....	76

5.2.5.11	CuAO8 activity measurement.....	77
5.2.5.12	Arginase activity measurement.....	77
5.2.5.13	Quantification of NO and H ₂ O ₂ production in seedling root tips	78
5.2.5.14	Quantification of NO production in cotyledons.....	78
5.2.5.15	Transient expression and localization of GFP-CuAO8 in <i>N. benthamiana</i>	79
6.	SUPPLEMENT	80
7.	LITERATURE	84
	DANKSAGUNG.....	97
	CURRICULUM	98
	EIDESTATTLICHE ERKLÄRUNG.....	100

II. Summary

Spatially and temporally controlled production of NO was shown to be essential for the plant's response to abiotic and biotic stresses but also during development. There are two main NO production routes in plants: i) enzymatic (i.e. nitrate/nitrite reductase) or non-enzymatic reduction of nitrite to NO and ii) oxidation of arginine, presumably resulting in the formation of citrulline and NO. The latter reaction is catalyzed by NO-synthases in mammals, but homologous proteins seem to be not present in higher plants. In general, information on enzymes involved in the arginine dependent oxidative pathway is lacking.

The aim of this project was to identify and characterize new proteins involved in NO formation in *Arabidopsis thaliana*. Therefore, 24 T-DNA insertion lines had previously been selected, based on homology to mammalian enzymes involved in NO production. These mutants were then screened for disturbed NO production in root tips after dichloroisonicotinic acid (INA, known NO elicitor) treatment, leading to the identification of the *cuao8* mutant, which is lacking a copper amine oxidase (CuAO) and displayed 50% reduced NO formation compared to wild-type (WT). Furthermore, NO formation during salt stress was severely compromised in two independent *CuAO8* knockout lines (*cuao8-1/cuao8-2*).

Transient expression of GFP-CuAO8 and subsequent laser scanning confocal microscopy revealed that CuAO8 localizes to the cytosol and the plasma membrane. Recombinantly expressed CuAO8 displayed classical amine oxidase activity being able to deaminate agmatine, putrescine, spermidine and spermine thereby producing H₂O₂ and ammonium. The highest reaction rate was measured for putrescine, suggesting that putrescine might be the main substrate of CuAO8 *in vivo*. Supporting this, *cuao8* displayed increased amounts of putrescine during salt stress, whereas the other polyamine levels were similar to those in WT plants.

Quantitative comparison of the amino acid contents in *cuao8* and WT by LC-MS-MS revealed slightly decreased arginine levels in *cuao8-1* and *cuao8-2*. Consistently, arginase activity, which consumes arginine, was two-fold higher than in WT. Inhibition of arginase as well as arginine supplementation rescued NO production during salt stress, demonstrating that arginine dependent NO production was disturbed in *cuao8-1* and *cuao8-2*. Moreover, exogenously added arginine and GSNO (a physiological NO donor) restored the primary root growth defect in both mutants, suggesting that the root-growth phenotype was caused by a compromised arginine dependent NO formation. Finally, NR activity was similar in WT, *cuao8-1* and *cuao8-2* allowing the conclusion that NR-dependent NO formation did not contribute to the NO deficient phenotype.

In summary, the decreased NO production in *cuao8-1* and *cuao8-2* is likely caused by enhanced arginase activity, which depletes the arginine pool leaving less substrate for the arginine dependent NO production. These results revealed an unknown regulatory mechanism of CuAO8 on NO production in plants and connect polyamine metabolism with NO synthesis.

III. Abbreviations

AAO: Aldehyde oxidase

ADC: Arginine decarboxylase

AG: Aminoguanidine

AIH: Agmatine iminohydrolase

AO: Amine oxidase

A. tumefaciens: Agrobacterium tumefaciens

BP: Band pass filter

CDPK: Calcium-dependent protein kinase

Col-0: Columbia 0

CPA: N-carbamoylputrescine amidohydrolase

cPTIO: 2-(4-Carboxyphenyl)-4,4,5,5-tetramethylimidazoline-1-oxyl-3-oxide

CT: Fractional cycle number at threshold

CuAO: Copper amine oxidase

CV: Column volumes

DAF-FM DA: 2',7'-dichlorofluorescein diacetate

DAR-4M AM: Diaminorhodamine-4M AM solution

DCF-DA: 2',7'-dichlorodihydrofluorescein diacetate

DNA: Deoxyribonucleic acid

E. coli: Escherichia coli

E-cup: Eppendorf cup

Em: Emission

Ex: Excitation

FAD: Flavin adenine dinucleotide

FMOC-Cl: Fluorenylmethoxycarbonyl chloride

H₄F: Tetrahydrofolate

GABA: γ -aminobutyric acid

GFP: Green fluorescent protein

GOI: Gene of interest

GSNO: S-nitrosoglutathione

His6-tag: Hexa-histidine-tag

HPLC: High-performance liquid chromatography

H₄B: Tetrahydrobiopterin

INA: 2,6-dichloro: isonicotinic acid/2,6: Dichloropyridine-4-carboxylic acid

LC-MS: Liquid chromatography coupled to mass spectrometry

LDL: Lysine specific demethylase

LP: Long pass filter

MS-medium: Murashige & skoog medium

NADPH: Nicotinamide adenine dinucleotide phosphate

Ni-NOR: Nitrite/NO reductase

NO: nitric oxide

NOHA: N-hydroxy-l-arginine

NOS: Nitric oxide synthase

NR: Nitrate reductase

ODC: Ornithine decarboxylase

PA: Polyamines

PAGE: Polyacrylamide gel electrophoresis

PAO: Polyamine oxidase/FAD-dependent amine oxidase

PBS: Phosphate buffer saline

PCR: Polymerase chain reaction

PI: Propidium iodide

PM-NR: plasma-membrane bound nitrate reductase

PTM: Posttranslational modification

Put: Putrescine

RNA: Ribonucleic acid

RNS: Reactive nitrogen species

ROS: Reactive oxygen species

SEM: Standard error of the mean

Spd: Spermidine

Spm: Spermine

WT: Wild type

XDH: Xanthine dehydrogenase

XOR: Xanthine oxidoreductase

IV. List of Figures and tables

Figures

Figure 1: Sources of NO in plants.....	13
Figure 2: NO synthesis from Arginine.....	16
Figure 3: Polyamines anabolism and catabolism in plants.....	19
Figure 4: INA induced NO production in root tips of different <i>A. thaliana</i> mutant lines.....	25
Figure 5: INA induced NO production in Col-0, <i>cuao8-1</i> and <i>cuao8-2</i> root tips.....	27
Figure 6: Verification of the complete knockout of <i>CAO8</i> in <i>cuao8-1</i> and <i>cuao8-2</i> T-DNA insertion lines on mRNA and protein level.....	28
Figure 7: Expression system and purification of CuAO8-His ₆	29
Figure 8: Amine oxidase activity test of recombinant CuAO8.....	30
Figure 9: Subcellular localization of GFP-CuAO8 and PI in epidermal cells of <i>N. benthamiana</i>	31
Figure 10: Subcellular localization of GFP-CuAO8 and FM4-64 in mesophyll and epidermal cells of <i>N. benthamiana</i>	32
Figure 11: Flowering time, root length and senescing phenotype of detached leaves in the dark were observed in Col-0, <i>cuao8-1</i> and <i>cuao8-2</i>	33
Figure 12: NaCl induced NO production in Col-0, <i>cuao8-1</i> and <i>cuao8-2</i> root tips.....	35
Figure 13: NaCl induced NO production in Col-0, <i>cuao8-1</i> and <i>cuao8-2</i> in cotyledons of five day old seedlings.....	36
Figure 14: NaCl induced H ₂ O ₂ production in Col-0, <i>cuao8-1</i> and <i>cuao8-2</i> root tips.....	37
Figure 15: Effect of NaCl treatment on free polyamine levels in five day old seedlings of Col-0, <i>cuao8-1</i> and <i>cuao8-2</i>	38
Figure 16: Representative distribution of amino acids in five day old seedlings.....	38
Figure 17: Overview of the metabolic network between PAs and amino acids and the influence of NaCl treatment on the amino acid levels in Col-0, <i>cuao8-1</i> and <i>cuao8-2</i>	39
Figure 18: Arginase enzyme activity and the effect on the arginase inhibitor <i>nor</i> -NOHA on NO production in root tips during NaCl treatment.....	41
Figure 19: NO production of Col-0, <i>cuao8-1</i> and <i>cuao8-2</i> after co-application of NaCl stress and arginine as well as relative root growth of Col-0, <i>cuao8-1</i> and <i>cuao8-2</i> on only ½ MS plates or with GSNO, arginine and GABA supplementation.....	42
Figure 20: Nitrite and nitrate contents in five day old seedlings of Col-0, <i>cuao8-1</i> and <i>cuao8-2</i> after salt stress.....	43
Figure 21: Nitrate reductase activity and mRNA level of <i>NIA1</i> and <i>NIA2</i> in five day old seedlings after NaCl stress.....	45
Figure 22: Catabolism of arginine in plants.....	49
Figure 23: Arginine catabolism in <i>A. thaliana</i> and mammals.....	51
Figure 24: Hypothetical model how CuAO8 might limit the amplitude of the oxidative burst during salt stress.....	55

Supplemental Figures

Supplemental Figure 1: Effect of NaCl treatment on free polyamine levels in five day old seedlings of Col-0, <i>cuao8-1</i> and <i>cuao8-2</i>	80
Supplemental Figure 2: Relative mRNA level of arginase 1 and 2 in five day old seedlings.....	82
Supplemental Figure 3: Results of the TargetP software predicting for possible localization of CuAO8 based on N-terminal pre-sequences.....	82
Supplemental Figure 4: Multiple sequence alignment of CuAO8 and CuAO2.....	83

Tables:

Table 1: <i>A. thaliana</i> T-DNA insertion lines which were screened for disturbed NO production after INA treatment.....	24
Table 2: Plant Material.....	57
Table 3: Bacteria strains.....	59
Table 4: Applied Kits.....	59
Table 5: Buffers and solutions.....	60
Table 6: Antibiotics.....	61
Table 7: Media.....	61
Table 8: Chemicals.....	62
Table 9: Antibodies.....	63
Table 10: Resins, columns, membranes.....	64
Table 11: Enzymes.....	64
Table 12: Vectors.....	64
Table 13: Oligonucleotides.....	65
Table 14: General instruments.....	66
Table 15: Applied fluorescent dyes for the visualization of NO and H ₂ O ₂	78
Table 16: Applied microscope settings (Zeiss, cLSM 510 META).....	79

Supplemental Tables:

Supplemental table 1: Amount of proteinogenic amino acids in five day old seedlings.....	80
Supplemental table 2: Amount of proteinogenic amino acids in five day old seedlings after 6h control treatment (buffer).....	81
Supplemental table 3: Amount of proteinogenic amino acids in five day old seedlings after NaCl treatment.....	81

1. Introduction

1.1 Importance and functions of nitric oxide (NO) in plants

NO is a colorless gaseous molecule, which is industrially produced by the reaction of N₂ with O₂ and serves as substrate for the synthesis of important industrial and economical chemicals. On the other hand, NO is commonly known as an air pollutant mainly generated by incomplete oxidation of fuels. Despite the severe ecological problems caused by atmospheric NO and its toxicity to animals, endogenously produced NO also fulfills important functions as a signaling molecule in living organisms. Although NO contains an unpaired electron, it is rather stable compared to other biological radicals like superoxide or the hydroxyl-radical, therefore being suitable as a short- to medium-range biological messenger. NO is proposed to be a very ancient signaling molecule in evolution since it is ubiquitously found in pro- and eukaryotes and is present in even the simplest organism like slime mould, Hydra or the American horseshoe crab, which have changed little during 500 million years of evolution (Feelisch and Martin, 1995). Feelisch and Martin (1995) suggested that NO was possibly part of the first intercellular signaling cascade since NO can diffuse rapidly across membranes, circumventing the need of membrane carriers, which were invented later during evolution. NO is of particular importance in mammals where it was identified as a critical signaling molecule in the nervous, cardiovascular and immune system as well as in tumor growth regulation (Campbell et al., 2014; see review: Bogdan, 2015). In plants, the first evidence presenting *in vivo* existence of NO was published in 1979 demonstrating NO emission of soybean leaves after herbicide treatment (Klepper, 1979). The importance of NO in plants was initially shown during the response to pathogen infection. NO potentiated the hypersensitive response, initiated the expression of defense genes and induced the release of cyclic GMP (cGMP) and cyclic ADP-ribose, which are important second messengers being involved in diverse cellular signaling cascades (Delledonne et al., 1998; Durner et al., 1998).

NO bioactivity in plants is transduced by (i) the activation of second messengers in particular cGMP and (ii) by the production of *reactive nitrogen species* (RNS) leading to posttranslational modifications (PTMs) of proteins (“redox-signaling”). Both pathways are important for the plant to cope with abiotic and biotic stress conditions as well as for controlling developmental processes. NO action by cGMP release was shown to be involved in stomata closure, induction of defense genes expression, orientation of pollen tube growth, adventitious root formation and root gravitropism (see review: Gross and Durner, 2016). For instance, stomata closure is mediated by ABA induced NO production leading to cGMP dependent Ca²⁺ release, which in turn regulates Ca²⁺ sensitive K⁺ and Cl⁻ channels (Garcia-Mata et al., 2003). Furthermore, auxin induced NO formation also results in cGMP dependent Ca²⁺ release which promotes adventitious root formation during vegetative propagation (Pagnussat et al., 2003).

Redox signaling describes the PTM of proteins by NO and RNS which may regulate enzyme activity, protein-protein interactions or the subcellular localization of the target protein. Three different NO-dependent PTMs are described: i) Direct coordination of NO to metal centers (metal nitrosylation), ii) addition of a nitro-group to tyrosine residues mediated by peroxynitrite (ONNO^-), the reaction product of NO and superoxide (tyrosine nitration) and iii) formal addition of NO to cysteine residues (S-nitrosylation) probably mediated by S-nitrosoglutathione (GSNO, reaction product of glutathione and NO) or N_2O_3 (reaction product of NO and O_2). S-nitrosylation seems to be of particular importance in plants. For instance, S-nitrosylation of the cytosolic glyceraldehyde-3 phosphate dehydrogenase (GAPDH) inhibits its catalytic activity, initiates its nuclear translocation and also induces its interaction with F-actin and the mitochondrial voltage dependent anion channel (VDAC) (Holtgreffe et al., 2008; Wojtera-Kwiczor et al., 2013). Another example is the targeted degradation of the transcription factor ABI5 by E3 ligases upon S-nitrosylation, regulating the initiation and promotion of seed germination (Albertos et al., 2015). NO mediated N-terminal cysteine modifications are also important for targeted protein degradation by the N-end rule pathway. The plant specific transcriptional regulator group VII ethylene response factors (ERFs) are degraded upon N-terminal S-nitrosylation which was shown to be critical for seed germination, stomatal closure and hypocotyl elongation (Gibbs et al., 2014).

NO is associated with many more processes in the plant. However, the proteins, which are targeted by NO to mediate these functions remain largely elusive. For example, elevated NO levels in *A. thaliana* led to the inhibition of primary root growth (Fernandez-Marcos et al., 2011), which was connected with decreased levels of the auxin transporter PIN1 and abnormalities in the architecture of the root apical meristem. However, the direct target protein of NO in this process was not identified. Moreover, NO influences the floral transition by suppressing *CONSTANS* and *GIGANTEA* gene expression and enhancing the expression of *FLOWERING LOCUS C* (He et al., 2004). Again, the molecular mechanism, how NO might regulate the expression of these genes awaits further research. More work is needed to decipher exact molecular pathways of NO in plants and to push NO research from a rather descriptive to a more mechanistic direction. From this perspective it is of particular importance to resolve the important issue of NO biogenesis in plants, since - despite the unambiguous importance of NO - it is rather unclear how NO is actually synthesized in plants. .

1.2 NO synthesis in plants

NO synthesis in plants can generally be classified into two pathways, the reductive and the oxidative pathway (Figure 1). The reductive pathway is dependent on nitrite as primary substrate which is reduced to NO. This reduction can occur (i) enzymatically catalyzed by a cytosolic nitrate reductase (NR) or a plasma-membrane associated nitrite reductase (Ni-NOR), and (ii) non-enzymatically at the mitochondrial and chloroplastic electron transport chain or in the apoplast at low pH and high nitrite concentrations. There is further evidence for an oxidative pathway of NO production, which presumably

involves the oxidation of arginine to citrulline, thereby releasing NO. In animals, this reaction is catalyzed by three different NOS isoforms, in higher plants, however, no such enzymes have been identified so far and evidence for this pathway is rather indirect.

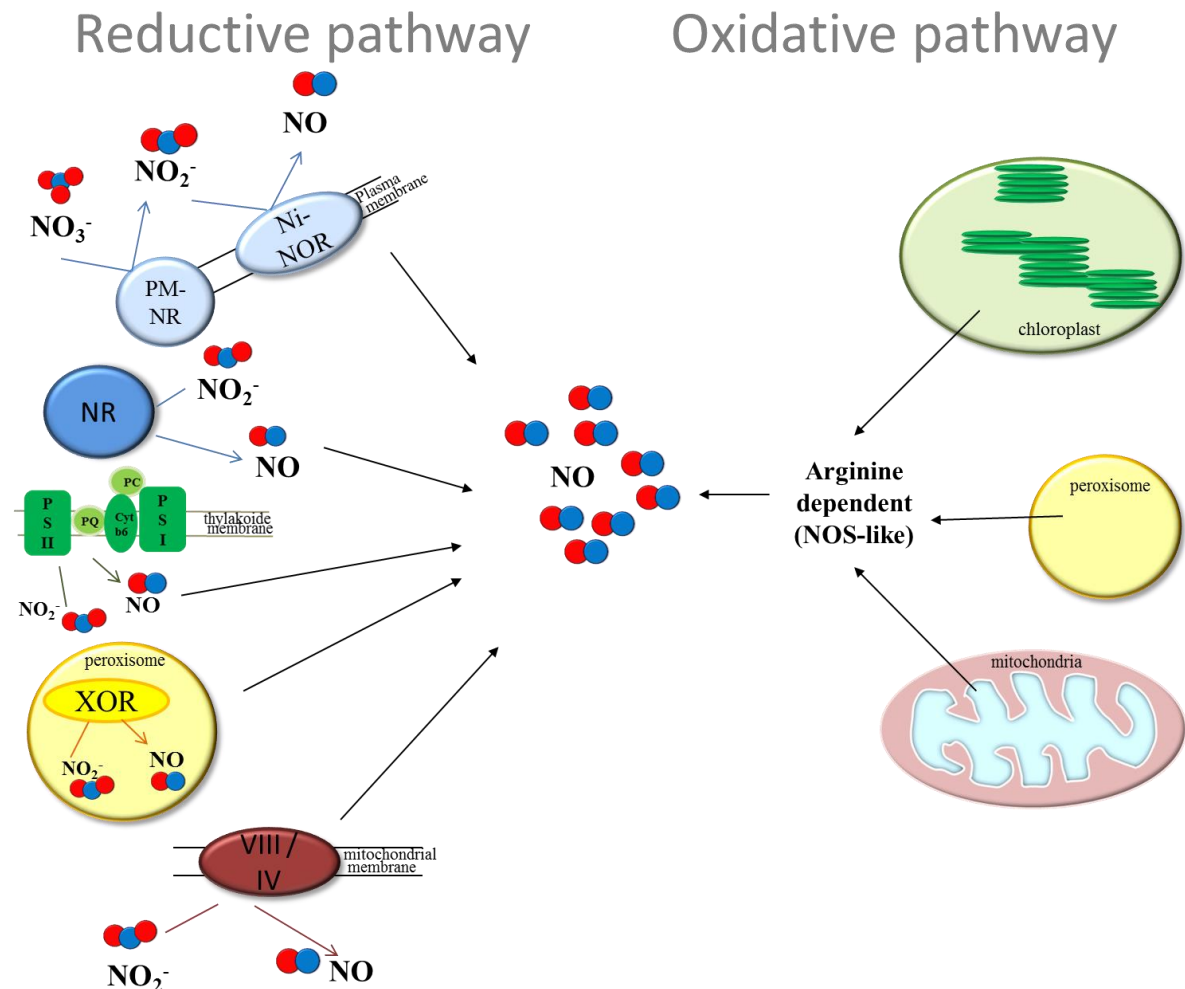


Figure 1: Sources of NO in plants. NO production in plants is generally separated into a reductive and oxidative pathway. The reductive pathway describes the reduction of nitrite to NO either non-enzymatically at the mitochondrial and chloroplastidic electron transport chain or enzymatically catalyzed by NR, Ni-NOR and XOR. The oxidative pathway describes an arginine-dependent NO production where no enzyme has been found yet but arginine addition to several organelles induced NO production which could be abolished by mammalian NOS inhibitors. NR: cytosolic nitrate reductase. PM-NR: plasma-membrane bound nitrate reductase, Ni-NOR: plasma-membrane bound nitrite/NO reductase; XOR: Xanthine oxidoreductase; Arg: arginine; NO₃⁻: nitrate; NO₂⁻: nitrite; NO: nitric oxide; PS: Photosystem; PQ: Plastoquinone; PC: Plastocyanine; cyt b6: cytochrome b6f.

1.2.1 Reductive pathway

1.2.1.1 Nitrate reductase (NR) dependent NO production

NRs catalyze the NAD(P)H dependent reduction of nitrate to nitrite which constitutes the first step of nitrate assimilation. Four different NRs are described in plants: two cytosolic NR isoforms are ubiquitously expressed (NIA1, NIA2) and two plasma membrane

anchored NRs (PM-NRs) are specifically expressed in the apoplast of roots. One of the PM-NRs is highly similar to the cytosolic NR whereas the other one shows homology with a NR involved in bacterial respiration (Eick and Stöhr, 2012).

Cytosolic NRs consists of eight segments combined to three functional domains with a total size of 100 kDa: the flavin adenine dinucleotide (FAD) domain, the heme-iron domain and the molybdenum-molybdopterin (Mo-MPT/Mo-Co) domain (see review: Campbell, 1999). These three functional domains are connected via two hinge regions: *hinge 1* connects the heme-iron and the Mo-Co domain and *hinge 2* connects the FAD and the heme-iron domain. The first step of nitrate reduction is the oxidation of NAD(P)H which takes place at the FAD domain. The redox potentials of the FAD, heme-iron and Mo-Co domain in the holo-enzyme lead to a “downhill” flow of the electrons through the iron-heme domain to the Mo-Co domain where the irreversible nitrate reduction occurs (Campbell, 1999). The NR activity is post-translationally regulated via serine 543 in the *hinge 1* region, which can be phosphorylated, allowing the binding of a 14-3-3 dimer. In combination with millimolar concentrations of divalent cations like Mg^{2+} this phosphorylation results in the inactivation of NR (Weiner and Kaiser, 2000). The half-life of NR is relatively short, reflecting rapid proteasome-dependent degradation of this protein. This implies that NR activity might also be tightly controlled by regulating NR protein abundance through transcriptional and posttranslational mechanisms. Examples include adaptation of NR abundance in response to varying nitrate levels, cytokinins or glutamine (Yu and Sukumaran, 1998; Weiner and Kaiser, 1999; Migge et al., 2000b; Konishi and Yanagisawa, 2011).

Additionally, cytosolic NR is also described to be capable to produce superoxide anion using oxygen as a substrate (Barber and Kay, 1996). Furthermore, an even more important additional activity of NR is catalyzing the NAD(P)H dependent reduction of nitrite to NO, which depends on the presence of light, small oxygen tensions and high nitrite concentrations (Dean and Harper, 1988; Rockel et al., 2002; Planchet et al., 2005). Nitrite accumulation occurs under anaerobic conditions or during phases of low photosynthetic activity (darkness). NR reduces nitrite to NO at the same active site where nitrate reduction occurs but the efficiency of this reaction is much lower (< 1% of the total enzyme activity). NR dependent NO production has been demonstrated to be important in a number of physiological and pathophysiological processes: an *A. thaliana* double knockout line of *NIA1* and *NIA2* displayed severe reduction of NO production during *Pseudomonas syringae* infection and cold stress acclimation leading to an altered hypersensitive response and reduced cold stress tolerance (Modolo et al., 2006; Zhao et al., 2009). Furthermore, *nialnia2* double mutants displayed delayed floral development and altered stomatal closure, two processes in which NO was shown to be critically involved (Desikan et al., 2002; He et al., 2004; Seligman et al., 2008).

In contrast to the cytosolic NR, apoplastic root PM-NRs cannot directly produce NO by nitrite reduction. Instead, under hypoxic conditions, PM-NR reduces nitrate to nitrite which is then further reduced to NO by the associated plasma-membrane bound nitrite/NO reductase (Ni-NOR) (Stöhr et al., 2001). However, until now, Ni-NOR activity

was only found in tobacco and barley roots and the responsible protein for Ni-NOR activity has not been identified. Moreover, the physiological relevance of this NO production pathway has to be further elucidated (Eick and Stöhr, 2012).

1.2.1.2 Xanthine oxidoreductase dependent NO production

The capacity of animal xanthine oxidoreductase (XOR) to reduce nitrite to NO in an NADH dependent manner was demonstrated in the late 90ties (Millar et al., 1998; Zhang et al., 1998; Godber et al., 2000). Mammalian XORs consist of two subunits (145 kDa), each possessing two non-identical iron-sulfur redox centers and each binding one molybdenum and one FAD cofactor. XOR exists as two interconvertible forms: the xanthine dehydrogenase and the xanthine oxidase. Under aerobic conditions, animal XOR catalyzes the oxidation of hypoxanthine to xanthine and xanthine to uric acid thereby producing NAD^+ and molecular oxygen. Under hypoxic conditions, XOR can reduce nitrite to NO by using xanthine or NADH as electron donors. In plants, the existence of two interconvertible forms of XOR has been demonstrated in peroxisomes of pea leaves (Corpas et al., 2008). However, the ability of plant XOR to reduce nitrite to NO has not yet been proven.

1.2.1.3 Non-enzymatic reduction of nitrite to NO

NO formation by nitrite reduction can also occur non-enzymatically in the mitochondria, chloroplast and in the apoplast. In the mitochondria, NADH oxidation transfers electrons into the mitochondrial electron transport chain where they are delivered – especially under conditions of low oxygen concentrations - to the electron acceptor nitrite thereby producing NO (Tischner et al., 2004; Planchet et al., 2005). Inhibitor studies suggest that this reaction takes place at the cytochrome c oxidase or –reductase domain (complex III or IV). This mechanism might ensure the supply of ATP and reduction equivalents under hypoxic conditions (Kozlov et al., 1999; Stoimenova et al., 2007). Furthermore, chloroplasts of soybeans were also able to produce NO after external addition of nitrite (Jasid et al., 2006). The molecular mechanism has not yet been elucidated, but the electrons are probably derived from the photosynthetic electron transport chain at photosystem II or the plasto-quinone pool, as suggested by inhibitor studies. Non-enzymatic NO production by nitrite reduction was also detected in the apoplast. Aleurone layers of barley produced NO under acidic conditions upon nitrite addition which could be promoted by the addition of phenolic compounds (Bethke et al., 2004).

1.2.2 Oxidative pathway

Although nitrite dependent NO production seems to play a fundamental role in several developmental processes and stress responses, there are many indications in literature pointing to an additional arginine dependent way of NO production in plants. This pathway is poorly described and in particular involved enzymes have not been identified. In mammals, NOS proteins catalyze the oxidation of arginine to citrulline, thereby

releasing NO, however, a homologous protein has not been found until now in higher plants.

1.2.2.1 Structure and function of the mammalian NOS isoforms

In mammals there are three NOS isoforms: the neuronal NOS (nNOS/NOS1), the endothelial NOS (eNOS/NOS3) and the inducible NOS (iNOS/NOS2). The nNOS and eNOS are expressed constitutively and both enzyme activities are dependent on the intracellular Ca^{2+} concentrations. The expression of iNOS is induced during the immune response and independent of the intracellular Ca^{2+} levels (see review: Daff, 2010). All NOSes are active as homodimers and catalyze the conversion of arginine to NO and citrulline via two consecutive monooxygenation reactions requiring O_2 and NAD(P)H (Figure 2). NOSes consist of a C-terminal reductase domain (NOSred) and an N-terminal oxygenase domain (NOSoxy) connected by a calmodulin (CaM) binding motif. The domain organization of iNOS, eNOS and nNOS is highly similar and consists of a dimerized oxygenase domain flanked by two separated reductase domains (Campbell et al., 2014). The NOSred domain contains binding sites for NAD(P)H and the cofactors FAD and FMN and the NOSoxy domain possesses a cytochrome P-450 type heme-center and binding sites for the co-factor tetrahydrobiopterin (H_4B) and the substrate arginine. The catalysis starts at the NOSred domain, where NAD(P)H oxidation reduces FAD. The electrons are then transferred to the FMN subdomain by direct interaction with the FAD/NAD(P)H subdomain (Campbell et al., 2014). The electron transfer from the FMN to the NOSoxy domain is probably initiated by CaM binding leading to a conformational change of the NOSred domain. The electrons are then transferred to the heme-center of the NOSoxy domain where arginine and H_4B bound (active site). Here, two electrons are transferred to the guanidinium group of arginine which is then hydrolyzed to N-hydroxy-L-arginine (NOHA) (Marietta et al., 1998). The NOHA generally remains bound to the active site (Daff, 2010). Now, another electron is needed to oxidize NOHA to NO and citrulline. The H_4B co-factor acts as an electron donor during oxygen activation and is very important for the last step, the NO release. Here, H_4B has to recapture an electron from the ferrous nitrosyl complex (heme center) in order to trigger NO release (Daff, 2010).

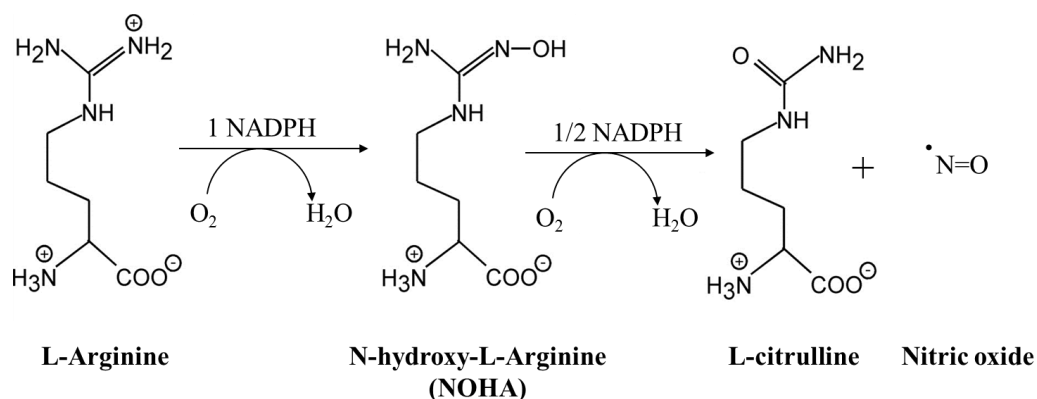


Figure 2: NO synthesis from Arginine (modified from Daff, 2010).

1.2.2.2 *NOS-like activity in plants*

In 2003, a putative NOS protein was identified (NOS1) displaying typical NOS activity (Guo et al., 2003). The corresponding *A. thaliana* T-DNA insertion line showed impaired NO production, organ growth and stomatal movement, which could be rescued by NO-donor treatment (Guo et al., 2003). The gene sequence of *NOS1* displayed no sequence similarities to mammalian NOS but resembled a NOS from snail. However, neither the constitutively reduced NO formation in *nos1* nor the NOS-like activity of recombinant NOS1 could be reproduced by other groups (Kolbert et al., 2008; Tun et al., 2008). In 2006, it was demonstrated that NOS1 displays GTPase activity with RNA binding capacity instead of a NOS-like activity (Moreau et al., 2008). Therefore NOS1 was renamed to NO associated-1 (NOA1).

Despite a lot of effort, a homolog of the mammalian NOS has not yet been identified in higher plants. The analysis of the genomes of 1087 land plants and 265 algae species revealed no typical NOS sequence in land plants but 15 NOS-like sequences in algae (Jeandroz et al., 2016). In accordance with this study, a protein with 45% sequence identity and a similar overall folding structure to the mammalian NOS was identified in the algae *Ostreococcus tauri*. This protein was capable to produce NO from arginine, using the same cofactors as the mammalian NOS (Foresi et al., 2010). However, this study did not take into account that a NOS-like enzyme might assemble from several different polypeptides, instead of being encoded in one gene. In fact, several lines of evidence point towards the existence of a NOS-like activity in higher plants, which depends on arginine as substrate/precursor for NO production. First, the conversion of externally added radioactive arginine to citrulline was detected in plants, proving the existence of a plant enzymatic activity similar to the mammalian NOS (Durner et al., 1998; Barroso et al., 1999; Zeidler et al., 2004; see review: Gupta et al., 2011). Moreover, different inhibitors of the mammalian NOS - most of them are arginine derivatives - inhibited the arginine to citrulline conversion and NO production in plants. Finally, an antibody directed against murine iNOS immunoreacted with a peroxisomal pea protein, suggesting the existence of a plant homolog of iNOS (Barroso et al., 1999). However, the specificity of the antibody was questioned due to several cross reactions with non-related peptides (Butt et al., 2003).

Furthermore, NOS-like activity was detected in different cellular organelles (Figure 1). Arginine addition to chloroplasts of soybeans initiated NO production, which required the same cofactors as mammalian NOS-catalyzed NO synthesis. This NO production was completely abolished by NOS inhibitors (Jasid et al., 2006). NOS-like activity was also detected in purified pea peroxisomes, which was again sensitive towards NOS inhibitors. In contrast to NOS-like activity in chloroplasts, this activity was found to be Ca^{2+} dependent (Barroso et al., 1999). Similarly, NOS-like activity was measured in barley mitochondria, however, in this study different NO detection methods revealed inconsistent results (Gupta and Kaiser, 2010). In conclusion, several NO production sites were described, suggesting that arginine dependent NO synthesis is strictly spatially controlled.

1.3 Polyamine metabolism

Polyamines (PA) are low molecular weight aliphatic cations found in eukaryotes, bacteria and archaea. They are synthesized from amino acids and are mostly linear with flexible carbon chains containing two or more amino groups. The most common PAs are the diamine putrescine, the triamine spermidine and the tetraamine spermine. Due to their positive charge they can bind to RNA, DNA and macromolecules thereby modulating cellular processes like cell division, gene expression, protein synthesis and stress response (Kaur-Sawhney et al., 1980; Flores and Galston., 1982; Pollard et al., 1999; see review: Miller-Fleming et al., 2015). In plants, PAs are involved in flowering, germination, pollen tube growth and cell proliferation and are ubiquitously produced in all cells and tissues (Liu et al., 2006; Roach et al., 2015; Sanchez-Rangel et al., 2016; see review: Kusano et al., 2008). Moreover, PAs accumulate during exposure to salt, ozone, heavy metal or pathogens and promote plant stress tolerance (Navakoudis et al., 2003; Yoda, 2006; Quinet et al., 2010). Interestingly, external addition of polyamines to seedlings of *A. thaliana* induced NO production suggesting an interconnection between PAs and arginine dependent NO production (Tun et al., 2006).

The common substrate for PA biosynthesis in all organisms is arginine (Figure 3A). PAs are synthesized via two different pathways, but depending on the plant species only one of these pathways may be used. The first pathway involves conversion of arginine to ornithine and then to putrescine, which is catalyzed by arginase and ornithine decarboxylases (ODC). This biosynthetic pathway occurs in a wide variety of organisms. The second pathway for PA synthesis is initiated by decarboxylation of arginine to agmatine catalyzed by arginine decarboxylase (ADC). Agmatine is then converted to N-carbamoyl-putrescine and subsequently to putrescine catalyzed by agmatine iminohydrolase (AIH) and N-carbamoylputrescine amidohydrolase (CPA), respectively. Putrescine is converted into spermidine and spermine by incorporation of an amino-propyl group provided by S-adenosyl-methionine. Interestingly, the *A. thaliana* genome does not contain a gene for ODC and this circumstance has only been reported in one other organism, the protozoan eukaryote *Trypanosoma cruzi* (Hanfrey et al., 2001). Therefore, *A. thaliana* can synthesize PAs only via agmatine and N-carbamoylputrescine.

PAs are catabolized by oxidative deamination catalyzed by either copper dependent amine oxidases (CuAO) or FAD-dependent amine oxidases (PAO). The respective aldehydes are precursors for secondary metabolites or for γ -aminobutyric acid (GABA) being involved in signaling, for instance during salt stress (Renault et al., 2010; Renault et al., 2011).

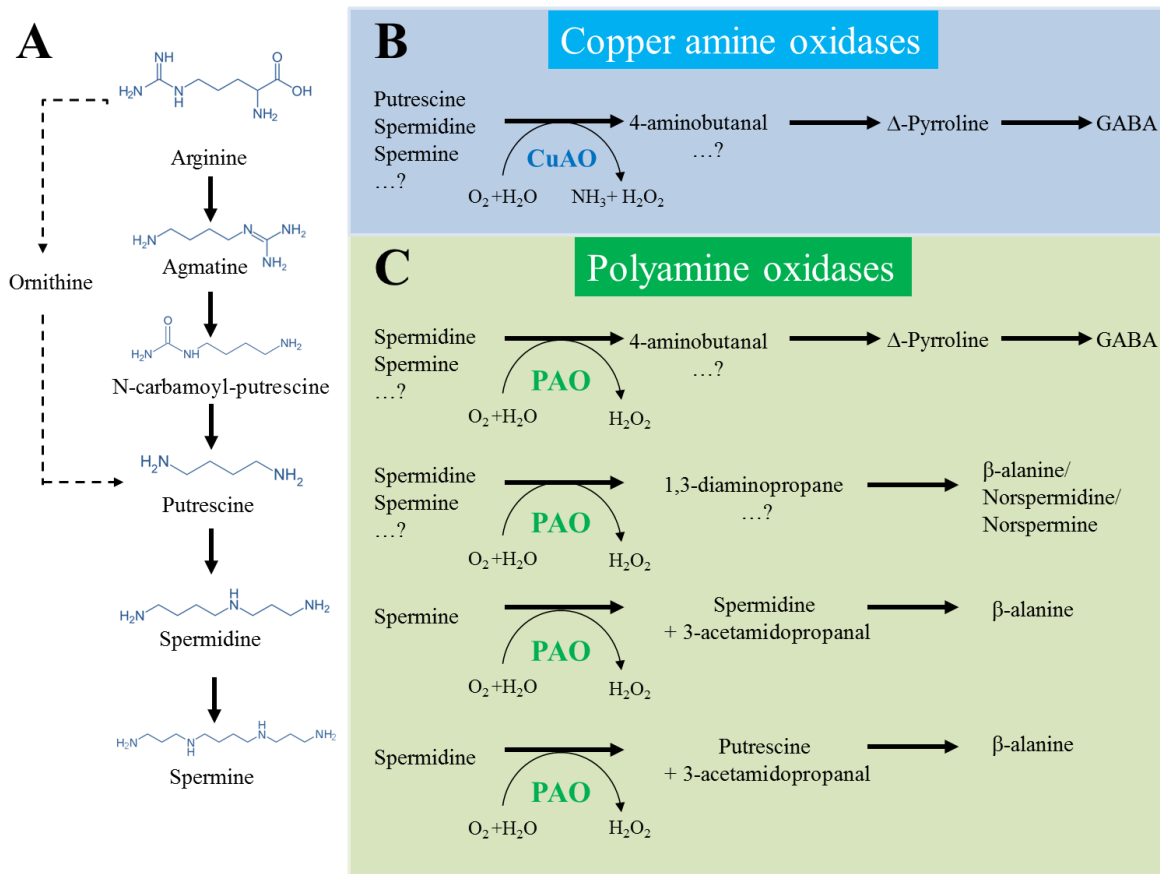


Figure 3: Polyamines anabolism and catabolism in plants. (A) Polyamines synthesis starting with arginine. (B) Deamination of di-/polyamines catalyzed by CuAOs. (C) Deamination of polyamines catalyzed by PAOs. CuAO: Copper amine oxidases, PAO: Polyamine oxidases/FAD-dependent amine oxidase, GABA: γ -aminobutyric acid. Figure modified from: Kusano et al., 2008; Tiburcio et al., 2014.

1.3.1 Amine oxidases (AOs)

AOs are characterized by the presence of a specific amine oxidase domain and are classified based on their cofactor requirements and the corresponding catalytic mechanism. Copper-dependent AOs (CuAO/DAO/AO in plants or CAO/DAO in animals) need a Cu^{2+} ion cofactor to deaminate amines, whereas PAOs display an FAD-dependent catalytic mechanism. The third family (LSD1-like) does contain an amine oxidase domain similar to PAOs (Shi et al., 2004), however, amine oxidase activity could not be demonstrated for these proteins (Forneris et al., 2005). Changes in the CAO activity are involved in a variety of human diseases like diabetes mellitus, Alzheimer or inflammatory disorders (see review: Klema and Wilmot, 2012). In *Arabidopsis* AO activity is for instance involved in the protoxylem differentiation in *Arabidopsis* roots or participate in the transition from the vegetative to the reproductive growth (Kim et al., 2014; Ghuge et al., 2015a).

1.3.1.1 Copper-dependent amine oxidases (CuAOs)

CuAOs were found in pro- and eukaryotes and catalyze the conversion of primary amines to the corresponding aldehyde and ammonia coupled with the reduction of O₂ to H₂O₂ (Figure 3B). CuAOs act as homodimers (70-80 kDa subunit size), binding one Cu²⁺ and one 2,4,5-trihydroxyphenylalanine quinone (TPQ) cofactor per subunit (Koyanagi et al., 2000; Shepard and Dooley, 2015). The TPQ cofactor is generated by a post-translational modification of a tyrosine created by a self-catalytic mechanism (Cai and Klinman, 1994). Deamination of putrescine and spermidine by CuAOs results in the production of 4-aminobutanal with concomitant release of NH₃ and H₂O₂. 4-Aminobutanal is then further metabolized to GABA via the production of Δ -pyrroline (Figure 3B). Despite of the low sequence homology (20 – 40%), CAOs from mammals, yeast, bacteria, fungi and plants adopt an archetypical fold forming the CAO active site (Klema and Wilmot, 2012).

The *A. thaliana* genome contains ten annotated CuAO genes, from which four are characterized by now (AtAO1, AtCuAO1-3) (Møller and McPherson, 1998; Planas-Portell et al., 2013). AtAO1 and AtCuAO1-3 are differentially expressed during development, wounding or hormone treatment and are found to be localized in the apoplast or peroxisome. All four CuAOs accept putrescine and spermidine as substrate *in vitro*, however, the deamination rate for the different PAs varies substantially. The ability of Arabidopsis CuAOs to deaminate other amines has not been tested until now. However, apple AOs were capable to deaminate several mono- and diamines apart from PAs, suggesting that plant CuAOs have similar substrate preferences as their mammalian counterparts (Zarei et al., 2015). In mammals, CAOs deaminate almost all cellular primary amines, for instance histamines, serotonin, dopamine, benzylamine but also the “classical” polyamines putrescine, spermidine and spermine (Klema and Wilmot, 2012).

1.3.1.2 FAD-dependent amine oxidases (PAOs)

PAOs were identified in yeast, plants and animals and catalyze the deamination of secondary amine groups of polyamines. PAOs are active as monomeric enzymes ranging in size from 53-60 kDa and contain a non-covalently bound FAD (see review: Moschou et al., 2012). PAOs are distinguished into two groups based on their function. One group catalyzes the terminal oxidation of spermidine and spermine to 4-aminobutanal and 1,3-diaminopropane thereby producing H₂O₂ (Figure 3C). This group was only found in plants (barley, maize, rice) and bacteria until now (Cervelli et al., 2000; Cervelli et al., 2001; Tavladoraki et al., 2006). The second group catalyzes the back-conversion of thermospermine to spermine, spermidine and putrescine, thereby releasing 3-acetoaminopropanal and H₂O₂. Interestingly, in contrast to maize, barley and rice, all five PAOs of *A. thaliana* were reported to be only involved in the back-conversion pathway (Tavladoraki et al., 2006; Kamada-Nobusada et al., 2008; Moschou et al., 2008; Takahashi et al., 2010; Fincato et al., 2012). *A. thaliana* PAOs possess distinct tissue and developmental expression patterns and are localized in the peroxisome and cytosol.

1.3.1.3 *LSD1-like (LDL) proteins*

Mammalian Lysine Specific Demethylase 1 (LSD1) possesses histone demethylase activity specifically for histone H3 lysine 4 modifications and functions as a transcriptional co-repressor. LSD1 is found in yeast, animals and plants and consists of three domains, where the C-terminal domain shows significant homology to the PAO family (Shi et al., 2004). Although a PAO domain is identified, amine oxidase activity could not be detected (Forneris et al., 2005). LSD1 protein is an integral component of mammalian histone deacetylases complexes in which they may cooperate to remove acetyl and methyl groups from histones. In *A. thaliana* four homologs of LSD1 were identified, called FLD or LSD1-like (LDL) proteins, which promote flowering by repressing *FLOWERING LOCUS C* and *D* (*FLC/FLD*) expression (He et al., 2003; Jiang et al., 2007).

1.4 Aim of the thesis

Nitric oxide (NO) is an important signaling molecule in plants involved in a variety of stress responses as well as developmental processes. One production route of NO is based on the reduction of nitrite, which can occur enzymatically by nitrate reductase or non-enzymatically. On the other hand several lines of evidence suggest that NO can also be synthesized by oxidation of arginine. In mammals, this reaction is catalyzed by NO-Synthases (NOS), however, homologous proteins have not been identified in higher plants. Therefore, information on proteins involved in the arginine dependent NO production in plants is strongly limited.

The aim of this work was to identify new proteins involved in the NO production in plants. 24 previously selected *A. thaliana* T-DNA insertion lines were to be tested for disturbed NO production. Therefore a screen was developed, allowing the quantitation of NO production in root tips of seedlings after INA (salicylic acid analog, known NO elicitor) treatment. The *COPPER AMINE OXIDASE 8* (*cuao8*) knockout line was selected for further research, displaying very low NO accumulation after INA treatment. The NO-deficient phenotype of *cuao8* was confirmed during salt stress. To analyze the connection between CuAO8 and NO production, a combination of biochemical, genetic and analytical techniques was applied. First, the activity of recombinant CuAO8 was characterized *in vitro*. Then, polyamine and amino acid levels were quantified by LC-MS-MS, to identify metabolic alterations in this mutant and to allow further assumptions about the molecular mechanism leading to altered NO production. Based on this analysis the activities of several enzymes involved in NO production (arginase, NR) were determined in the *cuao8* mutant. Finally, selected NO-related phenotypic traits were to be compared in *cuao8* and wild-type.

2. Results

The importance of NO production in plants specifically during the stress response, but also in developmental processes is unambiguous. However, the source of NO in plants is not as clear as in mammals. In mammals, NO can be formed by the oxidation of arginine catalyzed by three different NOS isoforms. In addition, several metalloproteins catalyze nitrite reduction thereby releasing NO (Maia et al., 2015). In plants, nitrate reductase is the only enzymatic source which has convincingly been demonstrated to produce NO (Dean and Harper, 1988; Rockel et al., 2002). In the last decades the question remained, if plants have additional proteins involved in NO formation similar to the mammalian NOS. Therefore the aim of this project was to identify new proteins or pathways participating in NO production in plants.

2.1 Identification of new genes involved in NO production

In order to identify new proteins or pathways involved in NO production, seedling root tips of 24 different *A. thaliana* T-DNA insertion lines were tested for disturbed NO production after 2,6-dichloro-isonicotinic acid (INA) treatment (Table 1, Figure 4). Seven tested T-DNA insertion lines were selected based on the function of mammalian homologs: Mammalian aldehyde oxidases (AAO) and xanthine dehydrogenases (XDH) were shown to be able to reduce nitrite to NO (Millar et al., 1998; Zhang et al., 1998; Li et al., 2009; Maia et al., 2015). Furthermore, rat NADPH-cytochrome P450 reductase was able to oxidize arginine to citrulline releasing NO (Boucher et al., 1992). Additionally, all knockout lines of annotated amine oxidases (AO) (polyamines oxidase (PAO) and copper amine oxidase (CuAO) family) were included because externally added polyamines (PA) were able to induce NO production and *cuaol* displayed disturbed NO formation (Tun et al., 2006; Wimalasekera et al., 2011). Moreover one representative member of the lysine specific demethylase 1 (LSD)-family was included (LDL3) which have an annotated but not functional AO domain.

To ensure the sensitivity of the chosen assay, several lines were included which have already been demonstrated to display reduced (*noa1*, GIB1-OX) or enhanced (nNOS, *Nox1/cue1*) NO production. *Noa1* (NO associated 1) has a mutation in a chloroplastic inverse GTPase leading to less NO production via an unknown mechanism (Guo et al., 2003; Moreau et al., 2008). GIB1-OX line has a higher hemoglobin type 1 content, which scavenges NO effectively (Hebelstrup and Jensen, 2008). The nNOS line is transformed with rat neuronal NOS (nNOS) and is described to have a higher constitutive NO production (Shi et al., 2012). *Nox1/cue1* has mutations in a plastidial phosphoenol-pyruvate/phosphate translocator resulting in enhanced NO formation presumably due to increased arginine levels (He et al., 2004).

To monitor NO production in the selected mutant lines, five day old seedlings were first stained with DAF-FM DA, which is an intracellular NO sensitive fluorescent dye and then stimulated with 2,6-dichloro-isonicotinic acid (INA, 2 mM). INA is a functional analogue of

the plant hormone salicylic acid (SA) which is well-established NO elicitor (Zottini et al., 2007). After 45 min, microscopy images were captured and the fluorescence intensity, which is proportional to NO production, was evaluated using ImageJ software. Therefore, two seedlings (Col-0 and mutant line) were placed on one microscope slide and the fluorescence in the root tip of the mutant line was relatively quantified to the respective Col-0 root tip. As expected, the nNOS and *cue1* line displayed significantly increased NO production in comparison to Col-0, whereas *noal* and GLB1-OX showed reduced NO accumulation (20 and 5% respectively; Fig. 4). Among all tested knockout lines, *cuao8* and *paob6* revealed a significant decrease in fluorescence intensity (around 30%), indicative of a severely disturbed NO production. Both proteins belong to the group of AOs, one to the copper binding (*cuao8*) and one to the FAD binding class (*paob6*). In this work *cuao8* was chosen for further characterization.

Table 1: *A. thaliana* T-DNA insertion lines which were screened for disturbed NO production after INA treatment. AAO: aldehyde oxidase, *atao1*: copper amine oxidase 1, CuAO: copper amine oxidase, *ldl3*: LSD1-like 3 protein, XDH: xanthine dehydrogenase, *p450 red*: NADPH- cytochrome P450 reductase

gene name	AGI code	SALK institute identifier	gene name	AGI code	SALK institute identifier
<i>LDL3</i>	AT4G16310	SALK_146733	<i>PAO1</i>	AT5G13700	SALK_013026
<i>CuAO1</i>	AT1G62810	SALK_206657	<i>PAO2</i>	AT2G43020	SALK_046281
<i>CuAO2</i>	AT1G31710	SALK_012167	<i>PAO4</i>	AT1G65840	SALK_133599
<i>CuAO3</i>	AT2G42490	SALK_095214	<i>PAO5</i>	AT4G29720	SALK_053110
<i>CuAO4</i>	AT1G31670	SALK_012213	<i>PAO6</i>	AT1G57770	SAIL_92_E04
<i>CuAO5</i>	AT3G43670	SALK_097684	<i>PAO7</i>	AT3G09580	SALK_058610
<i>CuAO6</i>	AT4G12270	SALK_124509	<i>AAO1</i>	AT5G20960	SALK_018100
<i>CuAO7</i>	AT4G12280	SALK_021559	<i>AAO2</i>	AT3G43600	SALK_104895
<i>CuAO8-1</i>	AT1G31690	SALK_037584	<i>AAO3</i>	AT2G27150	SALK_072361
<i>CuAO8-2</i>	AT1G31690	SALK_201804	<i>AAO4</i>	AT1G04580	SALK_037365
<i>CuAO9</i>	AT4G12290	SALK_039444	<i>XDH1</i>	AT4G34890	SALK_037365
<i>AtAO1</i>	AT4G14940	SALK_082394	<i>XDH 2</i>	AT4G34900	SALK_015081
<i>p450 red</i>	AT4G30210	SALK_152766			

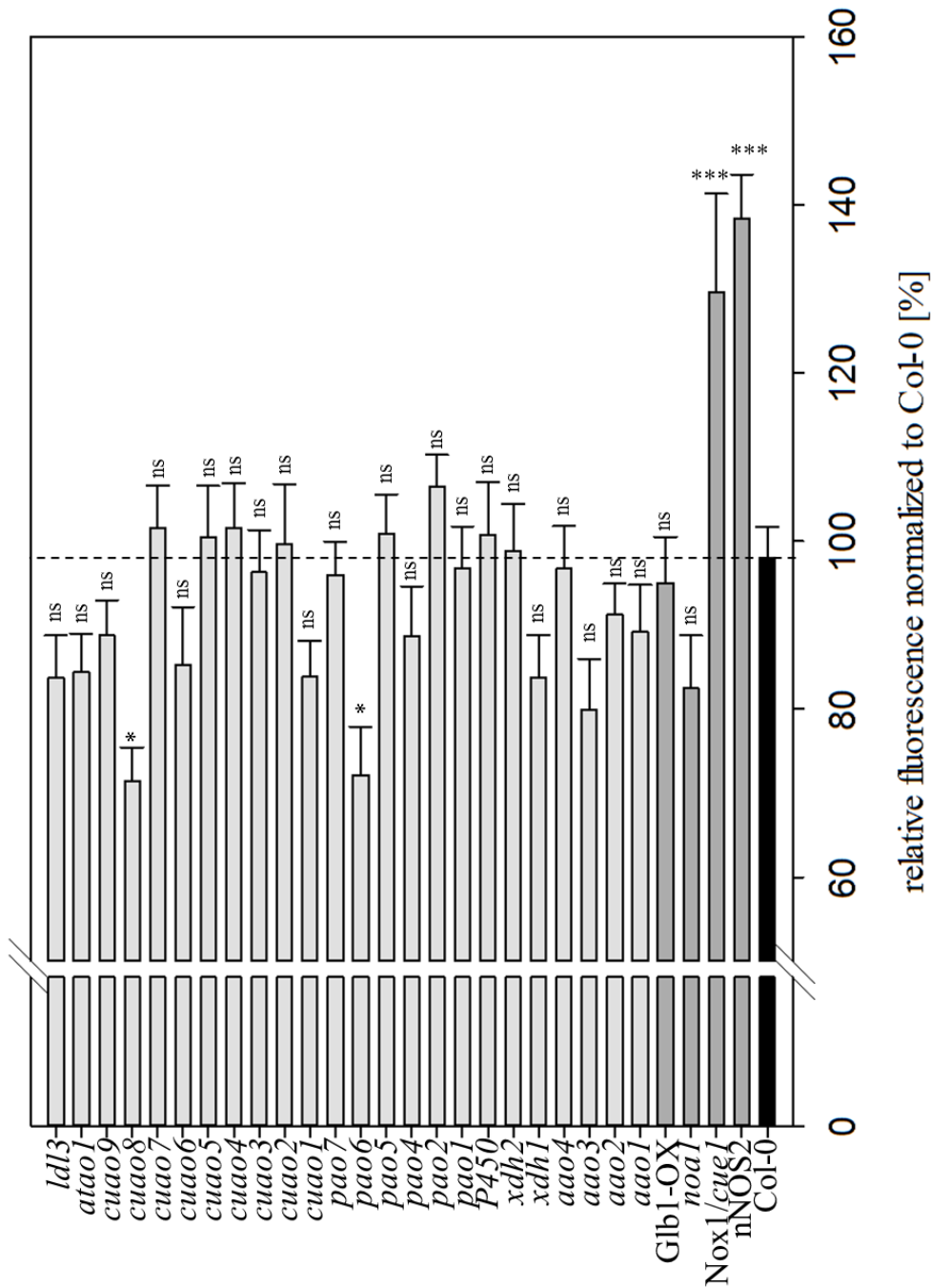


Figure 4: INA induced NO production in root tips of different *A. thaliana* mutant lines. Five day old seedlings were stained with DAF-FM DA (15 μ M, 15 min) and afterwards treated with INA (2 mM, 45 min), to induce NO production. The evolved fluorescent signal was observed by epifluorescence microscopy and quantified using ImageJ. The fluorescent signal of the mutant line was relatively normalized to Col-0 set as 100%. Means \pm SE of at least three individual experiments are shown (n=19-31). (***) Significant difference $P < 0.001$ based on ANOVA (Holm-Sidak test) with respect to Col-0. INA: 2,6-dichloro-isonicotinic acid, nNOS: neuronal NOS overexpression, Nox 1: NO overproducer, noal: NO-associated 1, GLB1-OX: hemoglobin 1 overexpression, aa0: aldehyde oxidase, xdh: xanthine dehydrogenase, P450: NADPH cytochrome P450 reductase, pao: polyamine oxidase, cuao: copper amine oxidase, atao: *A. thaliana* amine oxidase, ldl3: Lysine specific demethylase 1-like 3 protein. ns = not significant

2.2 Reduced NO production in root tips of *cuao8-1* and *cuao8-2* seedlings in response to INA

To verify the results of the screen, a second *CuAO8* T-DNA insertion line was tested for NO production in root tips after INA treatment. Here, the experimental setup used for the screen was modified. To account for possible differences in basal levels of NO between Col-0 and *cuao8-1* or *cuao8-2*, a normalization of the fluorescence intensity of INA treated roots to the fluorescence intensity of non-treated roots was performed. In Col-0, the fluorescence intensity after INA application increased approximately about five fold in comparison to non-treated control (Figure 5A and B). In contrast, *cuao8-1* and *cuao8-2* displayed only a two-fold increase after INA treatment. Hence, NO production in *cuao8-1* and *cuao8-2* was reduced around 50% compared to Col-0. Furthermore, fluorescence intensity after INA treatment of Col-0 could be significantly reduced by co-application of the NO scavenger cPTIO, demonstrating the specificity of the assay. However, DAF-FM DA does not only react with NO, it is also proposed that it forms fluorescent adducts with N_2O_3 , which is an oxidation product of NO (Wardman, 2007; Cortese-Krott et al., 2012). Therefore, the assay was repeated with $Cu_2(F12E)$. $Cu_2(F12E)$ is an intracellular dye, which specifically reacts with NO by trapping NO in a copper complex thereby emitting fluorescence. It does not react with oxidation products of NO therefore providing enhanced specificity as compared to DAF-FM DA (McQuade and Lippard, 2010). Using $Cu_2(F12E)$, a significant increase of fluorescence (1.4 fold) was observed after INA treatment of Col-0. As expected from the higher sensitivity of this dye, the increase was lower than for DAF-FM DA. In contrast, the knockout lines did not show any increase in fluorescence intensity after INA treatment. This indicates a total loss of NO production after INA treatment. However, cPTIO only slightly reduced fluorescence intensity after INA treatment in Col-0. Taking into account the results of both experiments, it can be concluded that loss of *CuAO8* severely affects NO production in root tips of seedlings after INA treatment.

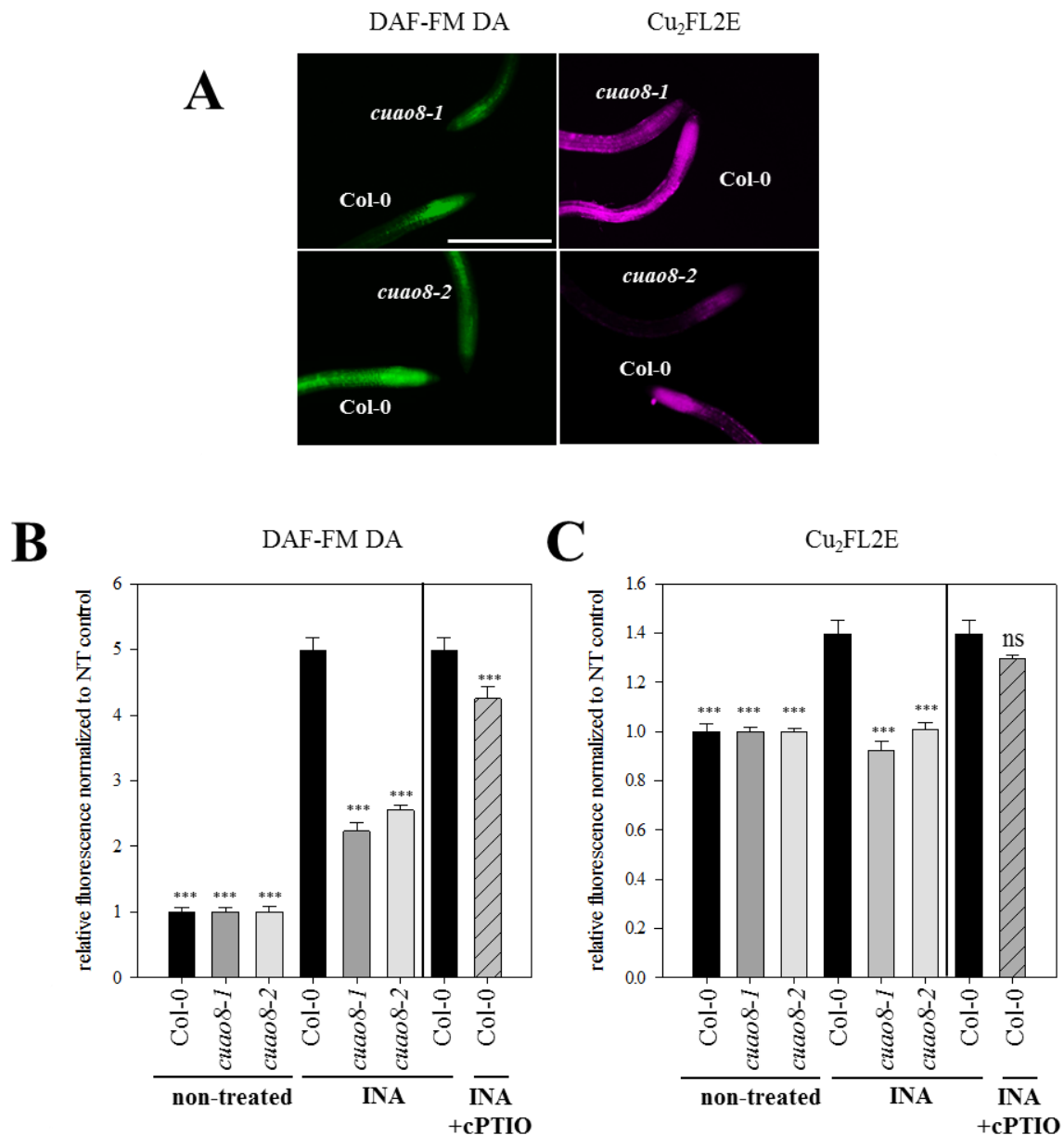


Figure 5: INA induced NO production in Col-0, *cuao8-1* and *cuao8-2* root tips. (A) Representative images of five day old root tips from Col-0, *cuao8-1* and *cuao8-2* stained with DAF-FM DA or Cu₂FL2E and treated with INA. Scale bar: 500 μ m. Fluorescence quantification analysis of five day old seedlings from Col-0, *cuao8-1* and *cuao8-2*, stained with (B) DAF-FM DA (15 μ M; 15 min) or (C) Cu₂FL2E (5 μ M, 45 min) and treated with INA (2 mM; 45 min) or buffer (control, non-treated). The fluorescent signal in the root tips was observed by epifluorescence microscopy. Shown is the relative fluorescence normalized to the non-treated control. A NO scavenger (cPTIO, 200 μ M) was added during staining and treatment. Means \pm SE of at least three individual experiments are shown (DAF-FM DA: n= 24-34; Cu₂(FL2E): n=21-29). (***) Significant difference $P < 0.001$ based on ANOVA (Holm-Sidak test) with respect to INA treated Col-0.

2.3 General characterization of *CuAO8* and CuAO8

Since *CuAO8* protein and knockout line has not yet been described, experiments were conducted to analyze the enzymatic activity and subcellular localization of CuAO8. Furthermore, some selected NO-associated phenotypic traits of *cuao8-1* and *cuao8-2* were examined.

2.3.1 Loss of *CuAO8* mRNA and CuAO8 protein in *cuao8-1* and *cuao8-2*

Subsequent experiments were conducted with two independent T-DNA insertion lines of *CuAO8* (*cuao8-1* and *cuao8-2*). RT-PCR with primers spanning the complete CDS revealed a complete knock-out of *CuAO8* mRNA in both mutant lines (Figure 6A). Furthermore, the absence of CuAO8 protein in both lines was demonstrated by western blot of total protein extracts using a CuAO8 specific primary antibody and wild-type as a control (Figure 6B). To note, the predicted MW from CuAO8 is 76 kDa (TAIR database). The detected larger size of around 90 kDa is presumably due to glycosylation events which have already been described in apple AOs or a human AO (Airenne et al., 2005; Zarei et al., 2015). In conclusion, a complete knockout of *CuAO8* in both T-DNA insertion lines can be assumed.

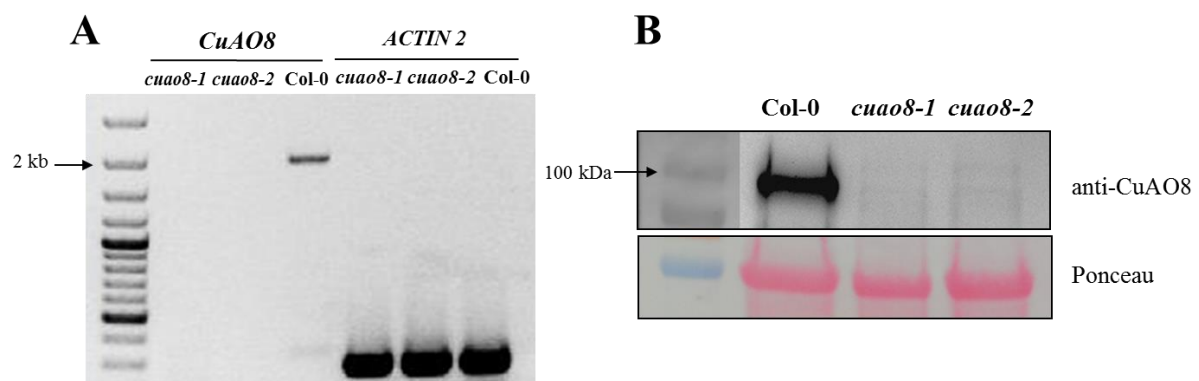


Figure 6: Verification of the complete knockout of *CAO8* in *cuao8-1* and *cuao8-2* T-DNA insertion lines on mRNA and protein level. (A) Transcriptional analysis of *CuAO8*: The expression of *CuAO8* CDS was tested in four week old leaves. As a positive control *ACTIN 2* was amplified. (B) Western-Blot analysis of protein extracts from Col-0, *cuao8-1* and *cuao8-2* to confirm entire knockout of CuAO8. Total protein extracts of four week old leaves were separated by SDS-PAGE and western blotted. The membrane was probed with anti-CuAO8 primary antibody and a secondary antibody coupled with HRP. Loading control: Ponceau staining

2.3.2 Copper amine oxidase activity of CuAO8

To analyze the enzymatic activity of CuAO8, first recombinant expression in different *E. coli* strains was performed. However, expression in the bacterial host resulted in mostly insoluble or inactive protein (data not shown). Therefore, the expression host was changed to tobacco (*N. benthamiana*) to circumvent folding problems and missing posttranslational modifications. In tobacco, CuAO8-His₆ was recombinantly expressed by applying the magnICON® system using the 5' module pICH17388, leading to cytosolic protein expression,

the 3' module pICH1159, containing CuAO8-His₆, and the integrase module pICH14011 (see Figure 7A). The transient expression of CuAO8-His₆ is achieved by *in planta* assembly of the viral provectors providing cell-to-cell movement of active replicons resulting in an better protein yield (Marillonnet et al., 2005; review: Peyret and Lomonosoff, 2015). CuAO8-His₆ was expressed for ten days and afterwards purified by Ni-NTA chromatography. The obtained protein fraction was analyzed by SDS-PAGE revealing one dominant band at the expected size of around 90 kDa (Figure 7B). Only minor impurities were detected indicating successful enrichment of CuAO8-His₆. The identity of CuAO8-His₆ was verified by western blotting using an anti-His and anti-CuAO8 primary antibody. An additional light band of approximately 180 kDa appeared in both SDS-PAGE and western blot analysis which could correspond to a non-reduced dimer of CuAO8 since anti-His and anti-CuAO8 antibody both give a positive signal and CuAOs act as homodimers.

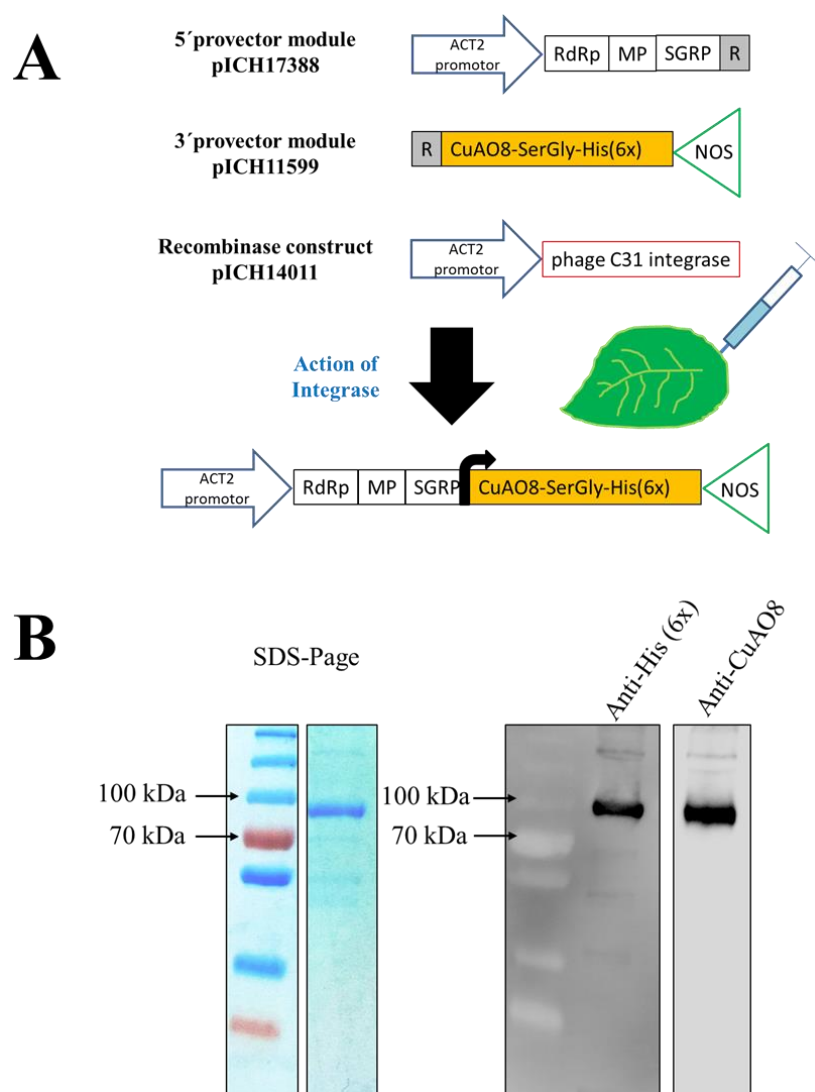


Figure 7: Expression system and purification of CuAO8-His₆. (A) magnICON system which consists out of three modules: The integrase module allows the recombination of the 3' and 5' module to form an active replicon (adapted from (Marillonnet et al., 2004; Peyret and Lomonosoff, 2015)). ACT2: actin2; RdRp RNA dependent RNA polymerase; MP: viral movement proteins; SGRP: subgenomic promoter initiating CuAO8-His₆ expression; R: recombination site; NOS: nos terminator (B) SDS-PAGE and western blot analysis of recombinant CuAO8-His₆, transiently expressed in *N. benthamiana*. Shown are representative SDS-PAGE (Coomassie-staining) and western-blot of the Ni-NTA elution fraction (200 mM Imidazol). The western blot was probed with primary anti-His or anti-CuAO8 antibody and a secondary antibody coupled with HRP.

CuAOs are described to produce H_2O_2 by deaminating polyamines. Therefore, enzymatic activity of CuAO8 was evaluated with Amplex Red which is an H_2O_2 reacting fluorescent dye. 100 ng of recombinant CuAO-His₆ were incubated with 1 mM of different PAs, including agmatine, putrescine, spermidine and spermine. CuAO8-His₆ produced H_2O_2 by oxidative deamination of all tested di-/polyamines. The highest activity was detected for putrescine as a substrate (0.36 $\mu M H_2O_2/min$) followed by spermidine (0.30 $\mu M H_2O_2/min$), spermine (0.22 $\mu M H_2O_2/min$) and agmatine (0.13 $\mu M H_2O_2/min$) (Figure 8). The specificity of the assay was demonstrated by a co-incubation with aminoguanidine, which is a general CuAO competitive inhibitor. Aminoguanidine efficiently blocked oxidative deamination of all tested di-/polyamines highlighting the specificity of the chosen assay. To note, arginine was also tested as a substrate but H_2O_2 production could not be detected (data not shown). Furthermore, Amplex Red was replaced by DAR-4M AM, to detect if NO was produced by recombinant CuAO8-His₆ using di-/polyamines or arginine as a substrate. However, no enhanced fluorescence was detected which implies that CuAO8-His₆ cannot produce NO from polyamines (data not shown). In summary, the heterologously expressed CuAO8 showed classical AO activity producing H_2O_2 by oxidative deamination of di-/polyamines.

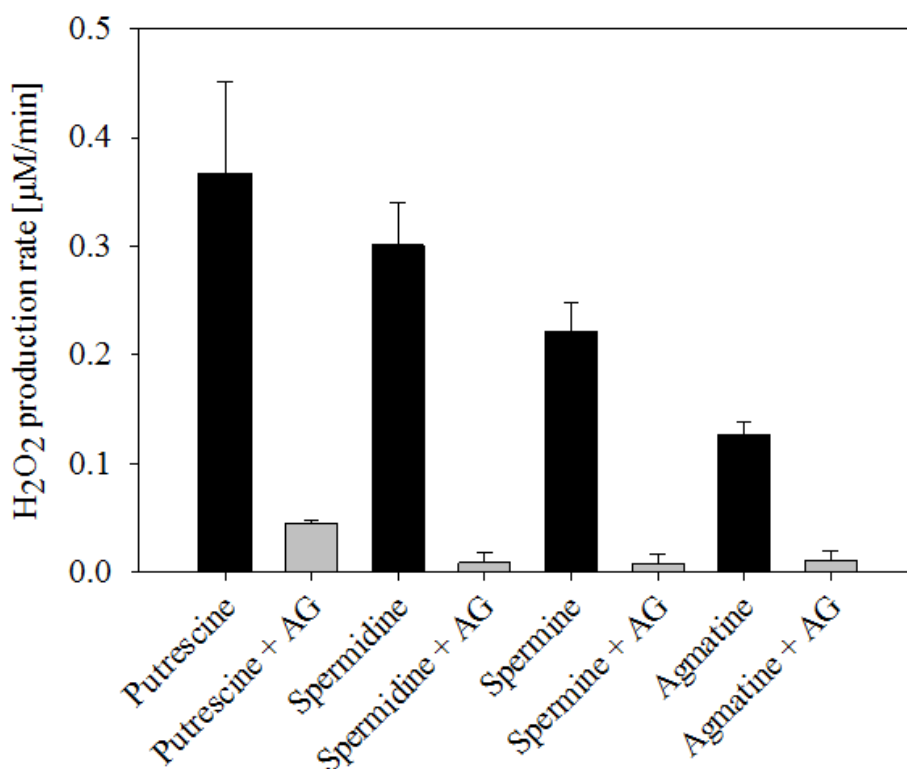


Figure 8: Amine oxidase activity test of recombinant CuAO8. Amine oxidase activity was tested with Amplex Red peroxidase test detecting produced H_2O_2 of CuAO8-His₆ over time. 100 ng of protein was incubated with 1 mM substrate alone or in combination with 0.5 mM amine oxidase inhibitor (AG: Aminoguanidine). Means \pm SE of three individual experiments are shown.

2.3.3 Cytosolic and plasma membrane localization of GFP-CuAO8

In literature, the subcellular localization of four *A. thaliana* CuAOs has been described. AtAO1 and CuAO1 are localized in the apoplast and CuAO2 and CuAO3 are primarily found in the peroxisome (Planas-Portell et al., 2013; Ghuge et al., 2015b). To analyze the subcellular localization of CuAO8, a GFP-CuAO8 fusion construct was transiently expressed in *N. benthamiana* leaves using agrobacterium mediated transformation. The cell wall and plasma membrane were visualized by co-staining with propidium iodid (cell wall, Figure 9) and FM4-64 respectively (plasma membrane, Figure 10). Confocal laser scanning microscopy of transformed leaf sections revealed a GFP signal mainly distributed within the cytosol. However, the GFP-CuAO8 signal partially overlapped with the plasma membrane staining both in epidermal and mesophyll cells (see enlargement in Figure 10, light blue color, (see red arrow) while being clearly distinct from the cell wall staining (Figure 9). To note, CuAO8 is predicted to possess a 20 amino acid long N-terminal signal peptide which is potentially masked by the N-terminal GFP (TargetP software, (Supplemental Figure 4) (Emanuelsson et al., 2007). This possibly prevents complete targeting of CuAO8 to the plasma membrane. However, despite a lot of effort, transient expression of CuAO8 with a C-terminal GFP-tag was not successful in *N. benthamiana* leaves, prohibiting a more detailed localization analysis.

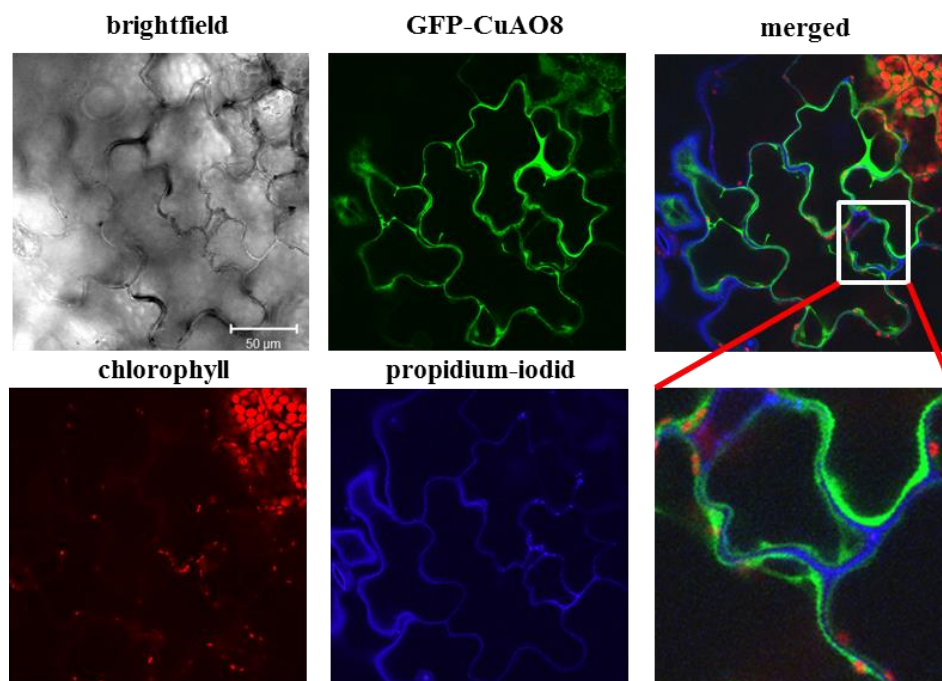


Figure 9: Subcellular localization of GFP-CuAO8 and PI in epidermal cells of *N. benthamiana*. GFP-CuAO8 was transiently expressed in five week old *N. benthamiana* cells for five days. The expression was observed with the cLSM Zeiss META 510 using a 40 x objective. Propidium-iodid (PI) staining was applied (10 µg / ml; 15 min) to visualize the cell wall. Scale: 50 µm

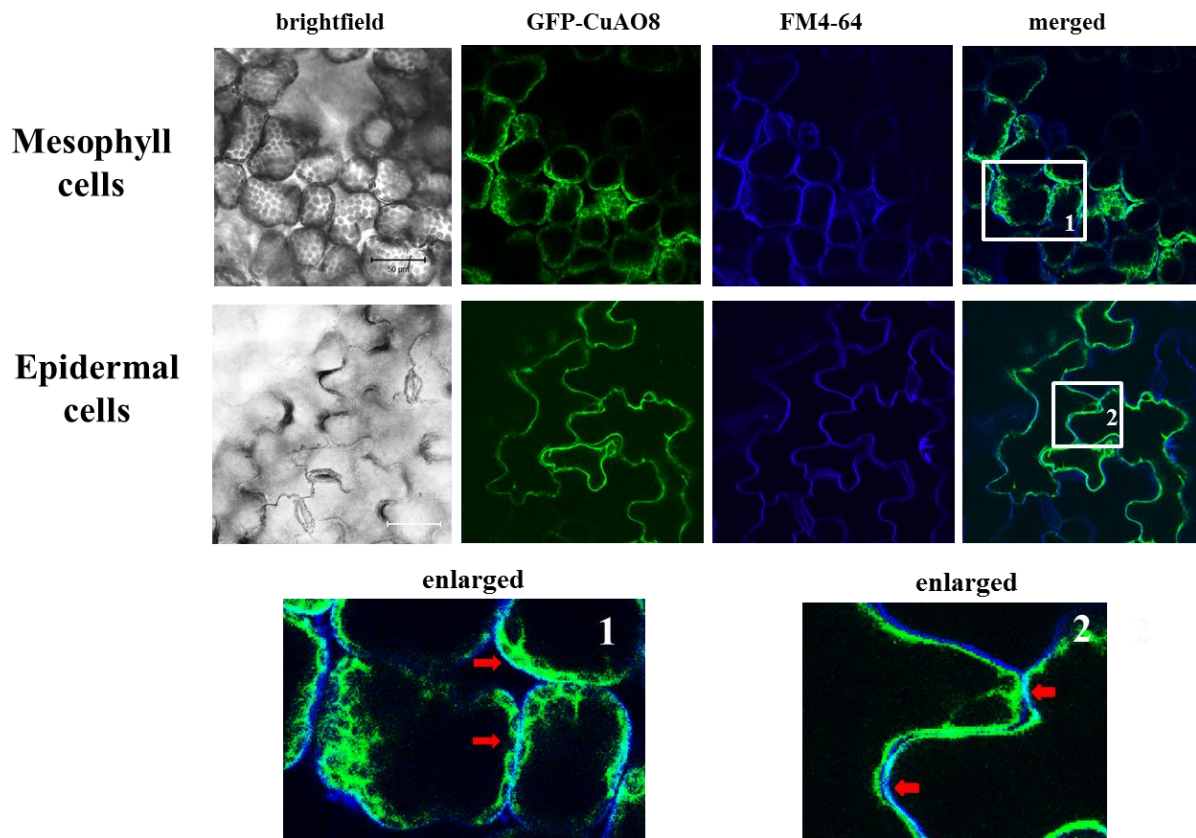


Figure 10: Subcellular localization of GFP-CuAO8 and FM4-64 in mesophyll and epidermal cells of *N. benthamiana*. GFP-CuAO8 was transiently expressed in five week old *N. benthamiana* cells for five days. The expression was observed with the cLSM Zeiss META 510 using a 40 x objective. FM4-64 (20 μ M; 15 min) staining was applied to visualize the plasma membrane. Light blue color represents overlap between GFP and FM4-64 signal. Scale: 50 μ m

2.3.4 Reduced primary root growth of *cuao8-1* and *cuao8-2*

NO is shown to be involved in several developmental and physiological processes. Since *cuao8-1* and *cuao8-2* displayed disturbed NO production several selected phenotypic traits associated with NO were analyzed in these mutants. As NO is described to represses the floral transition (He et al., 2004), the flowering time of Col-0, *cuao8-1* and *cuao8-2* was analyzed by counting the number of days until the stem height was 1 cm and when the first white flower appeared (Figure 11A). 1 cm stem height was in all three genotypes achieved after around 42 days (Col-0 = 41.8 days; *cuao8-1* = 41.8 days; *cuao8-2* = 43.1 days) and the first white flowers appeared after around 44 days (Col-0 = 43.7 days; *cuao8-1* = 43.4 days; *cuao8-2* = 45.9 days). The flowering time was therefore similar in Col-0 and mutant lines suggesting no involvement of CuAO8 in flowering time regulation.

Additionally, NO also plays a role in primary root growth. A bilateral character is proposed where low levels of NO promote primary root growth but high levels of NO inhibit primary root growth. High levels of NO was shown to decrease the number of auxin transporters (PIN1) which leads to reduced cell division in the root apical meristem and reorganization of the quiescent center (Fernandez-Marcos et al., 2011; Fernández-Marcos et al., 2012; Liu et al., 2015). Therefore, the primary root length of Col-0, *cuao8-1* and *cuao8-2* was measured after

eight, eleven and 15 days of growth ($1/2$ -MS medium). *Cuaos-1* and *cuaos-2* displayed significantly shorter primary roots (around 3-5 mm) compared to Col-0 (Figure 11B). Although only small differences were measured, it indicates a role of CuAO8 in primary root growth.

Furthermore, a faster chlorophyll breakdown was observed in the *noal* mutant line, which was correlated with its decreased NO content (Liu and Guo, 2013). Therefore, chlorophyll breakdown was monitored in detached leaves of Col-0 and *cuaos-1* (Figure 11C). Here, similar chlorophyll breakdown was observed in Col-0 and *cuaos-1* implicating no role of CuAO8 in NO formation during leaf senescence. In sum, CuAO8 is involved in primary root growth whereas flowering time and chlorophyll breakdown is independent of CuAO8.

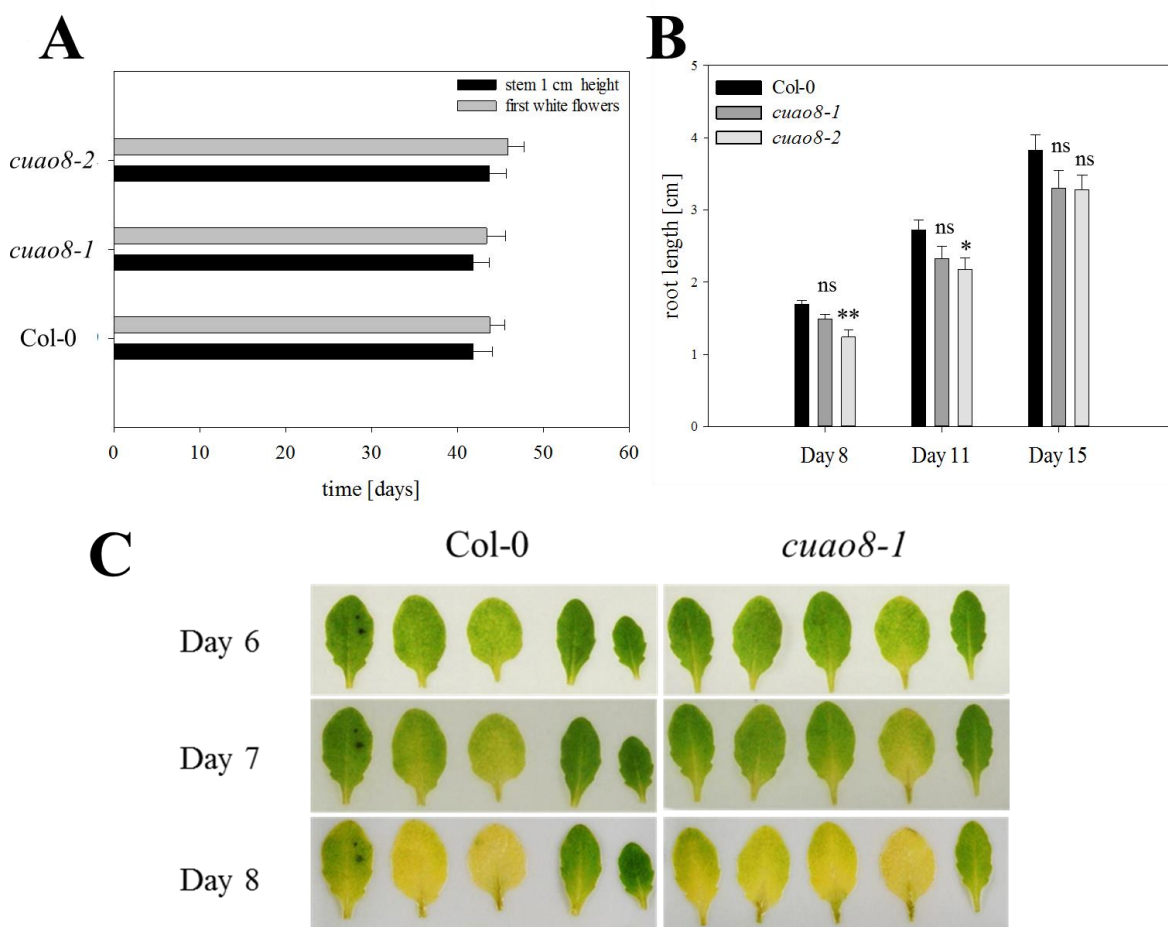


Figure 11: Flowering time, primary root length and senescing phenotype of detached leaves in the dark were observed in Col-0, *cuaos-1* and *cuaos-2*. (A) Number of days until the stem of Col-0, *cuaos-1* and *cuaos-2* reached 1 cm height and until the first flower was detected. Means \pm SDV of two individual experiments are shown (n= 12-16). (B) The primary root length of Col-0, *cuaos-1* and *cuaos-2* was measured with ImageJ after eight, eleven and fifteen days of growing in vertical $1/2$ MS plates. Means \pm SE of at least three individual experiments are shown (n= 14-17). (***) Significant difference $P < 0.001$ based on ANOVA (Holm-Sidak test) with respect to Col-0. ns = not significant (C) Representative picture of fully-expanded detached leaves from Col-0 and *cuaos-1* which were stored in the dark and the chlorophyll breakdown was observed. Three individual experiments were conducted.

2.4 Reduced NO production of *cuao8-1* and *cuao8-2* during salt stress

NO formation in response to INA treatment critically depends on CuAO8 as demonstrated in the previous results. For the screen a rather high concentration of INA (2 mM) was applied to provoke a fast and strong NO response. The treatment was substituted by sodium chloride (NaCl) to analyze NO production in Col-0, *cuao8-1* and *cuao8-2* seedlings in a more physiological context. NaCl was chosen since PAs and NO are clearly connected in promoting salt stress resistance in *A. thaliana* (Quinet et al., 2010; Tanou et al., 2014).

2.4.1 Reduced NO production in *cuao8-1* and *cuao8-2* root tips during salt stress

NaCl induced NO production in five day old seedlings was again analyzed by applying the intracellular NO sensitive fluorescent dyes DAF-FM DA and DAR-4M AM. Both dyes represent NO production by emitting fluorescence after NO binding, and especially DAR-4M AM is very pH- and photostable (Kojima and Nagano, 2000). NO production in root tips was monitored by epifluorescence microscopy after six hours of NaCl treatment and analyzed as described previously for the INA treatment. Both stainings revealed that NaCl treatment of Col-0 induced a 50% increase in fluorescence intensity compared to control conditions indicating a robust NO production during salt stress (Figure 12A and B). In contrast, the fluorescence intensity after NaCl treatment in *cuao8-1* and *cuao8-2* was similar to control conditions. This implies a lack of NO formation in both mutant lines during salt stress treatment. The specificity of both stainings was proven by applying the NO scavenger cPTIO which significantly reduced the NO production in Col-0 during NaCl stress. The results confirm the impaired NO production in *cuao8-1* and *cuao8-2* and demonstrate that salt induced NO production in seedling root tips is dependent on CuAO8.

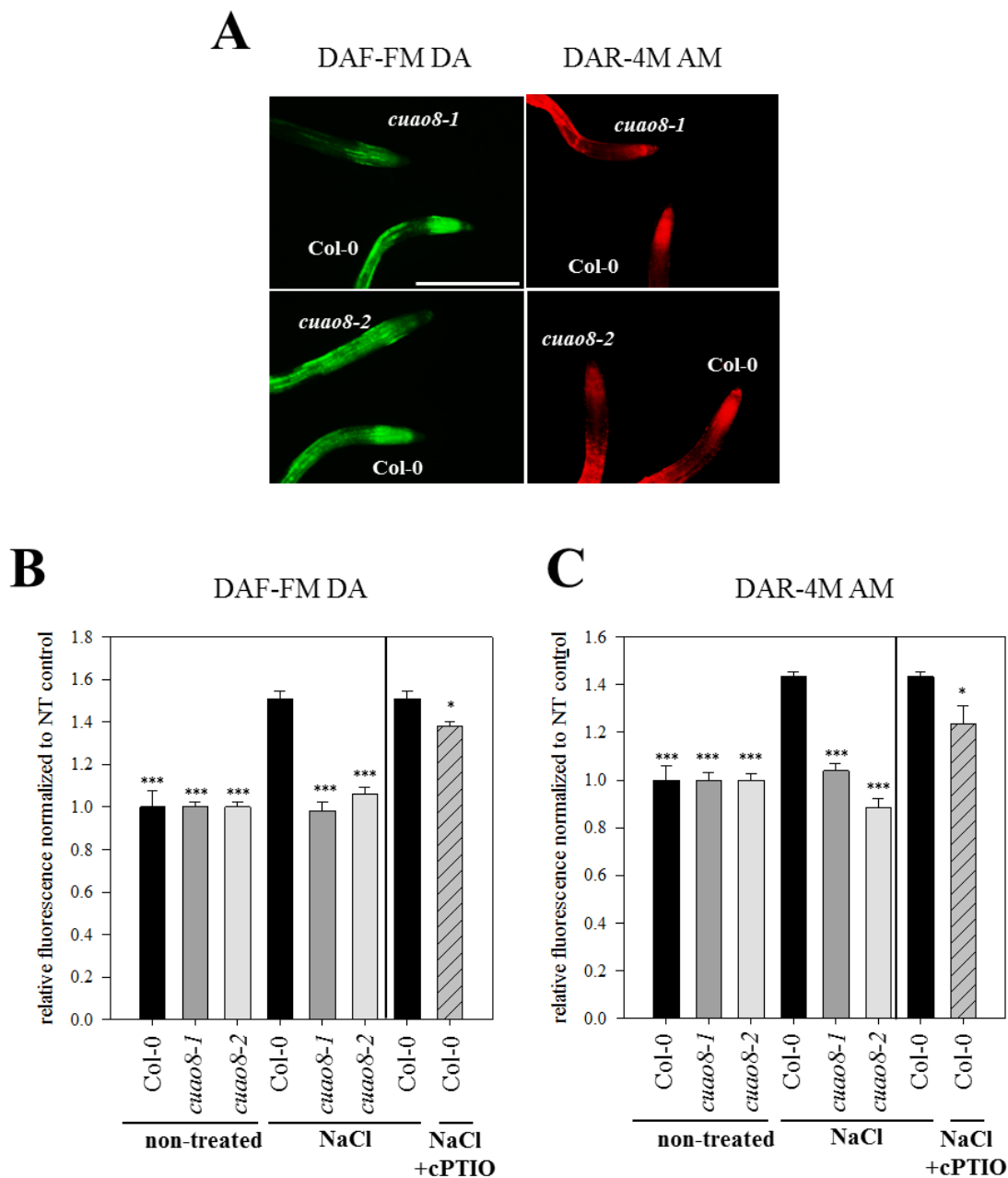


Figure 12: NaCl induced NO production in Col-0, *cuao8-1* and *cuao8-2* root tips. (A) Representative images of five day old root tips from Col-0, *cuao8-1* and *cuao8-2* stained with DAF-FM DA or DAR-4M AM and treated with NaCl. Scale bar: 500 μ m. Fluorescence quantification analysis of five day old seedlings from Col-0, *cuao8-1* and *cuao8-2* stained with (B) DAF-FM DA (15 μ M; 15 min) or (C) DAR-4M AM (5 μ M, 60 min) and treated with NaCl (DAF-FM DA staining: 150 mM, 5,5 h; DAR-4M AM staining: 200 mM, 6 h) or buffer (control, non-treated). The fluorescent signal in the root tips was observed by epifluorescence microscopy. Shown is the relative fluorescence normalized to the non-treated control. A NO scavenger (cPTIO, 200 μ M) was added during staining and treatment. Means \pm SE of at least three individual experiments are shown (DAF FM DA n= 22-27; DAR 4M AM n= 24-34). (***) Significant difference $P < 0.001$ based on ANOVA (Holm-Sidak test) with respect to NaCl treated Col-0.

2.4.2 Reduced NO production in *cuao8-1* and *cuao8-2* cotyledons during salt stress

Until now the work focused on the NO production in root tips. To investigate whether CuAO8 might also be involved in the NO formation in leaves, NO production in cotyledons of five day old seedling after salt stress was tested (Figure 13A, done by Paul Eckrich). The seedlings

were stained with DAF-FM DA and afterwards treated with NaCl for six hours. The fluorescence intensities were measured from a representative part of the leaf and relatively quantified to (separately measured) NaCl treated Col-0. Values were normalized to untreated cotyledons as described for root tip NO measurements. In cotyledons of Col-0, the fluorescence increased around 10% after salt stress treatment, which is weaker than in root tips (Figure 13B). Nevertheless, this increase was abolished in *cuaos-2* and slightly decreased in *cuaos-1*. Accordingly, CuAO8 appears to be involved in NO production in cotyledons as well although to a lesser extent than in roots.

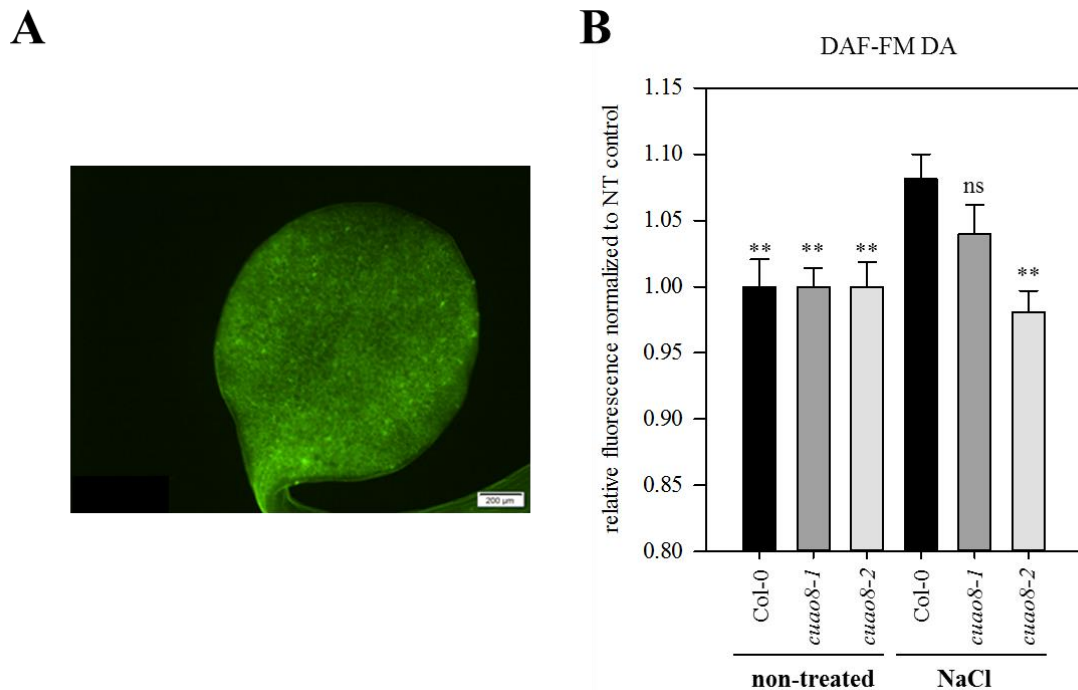


Figure 13: NaCl induced NO production in Col-0, *cuaos-1* and *cuaos-2* in cotyledons of five day old seedlings. (A) Representative image of a cotyledon from a five day old seedling of Col-0 stained with DAF-FM DA and treated with NaCl. Scale: 200 μ m. (B) Fluorescence quantification analyses of five day old seedlings from Col-0, *cuaos-1* and *cuaos-2* stained with DAF-FM DA (15 μ M; 15 min) and treated with NaCl (200 mM, 6h) or buffer (control, non-treated). The fluorescent signal in cotyledons was observed with an epifluorescence microscope. Shown is the relative fluorescence normalized to the non-treated control. Means \pm SE of at least three individual experiments are shown (n= 30-43). (***) Significant difference $P < 0.001$ based on ANOVA (Holm-Sidak test) with respect to NaCl treated Col-0. ns = not significant

2.5 Reduced H₂O₂ production in root tips of *cuaos-1* and *cuaos-2* during salt stress

H₂O₂ was demonstrated to induce NO production in *A. thaliana* seedlings roots or in stomata (Bright et al., 2006; Wang et al., 2010). Since CuAO8 produces H₂O₂ by oxidative deamination of di-/polyamines (Figure 8), we speculated whether the decreased NO production in *cuaos-1* and *cuaos-2* might be due to reduced H₂O₂ levels. Therefore, H₂O₂ production in root tips of five day old seedlings was analyzed after salt stress using the intracellular H₂O₂ sensing dyes DCF-DA and Amplex Red. The quantitative analysis of DCF-DA stained root tips revealed no significant differences in H₂O₂ production between

Col-0 and *cuao8-1* or *cuao8-2* after six hours salt stress (Figure 14A). Using Amplex Red, *cuao8-1* exhibited around 20% less fluorescence whereas *cuao8-2* displayed H₂O₂ levels comparable to Col-0 (Figure 14B). This indicated that H₂O₂ levels in *cuao8-1* and *cuao8-2* are only slightly reduced during salt stress, which is unlikely to account for the dramatic differences of NO formation observed in these mutants. CuAO8 seems to play only a minor role for H₂O₂ production in root tips during salt stress treatment.

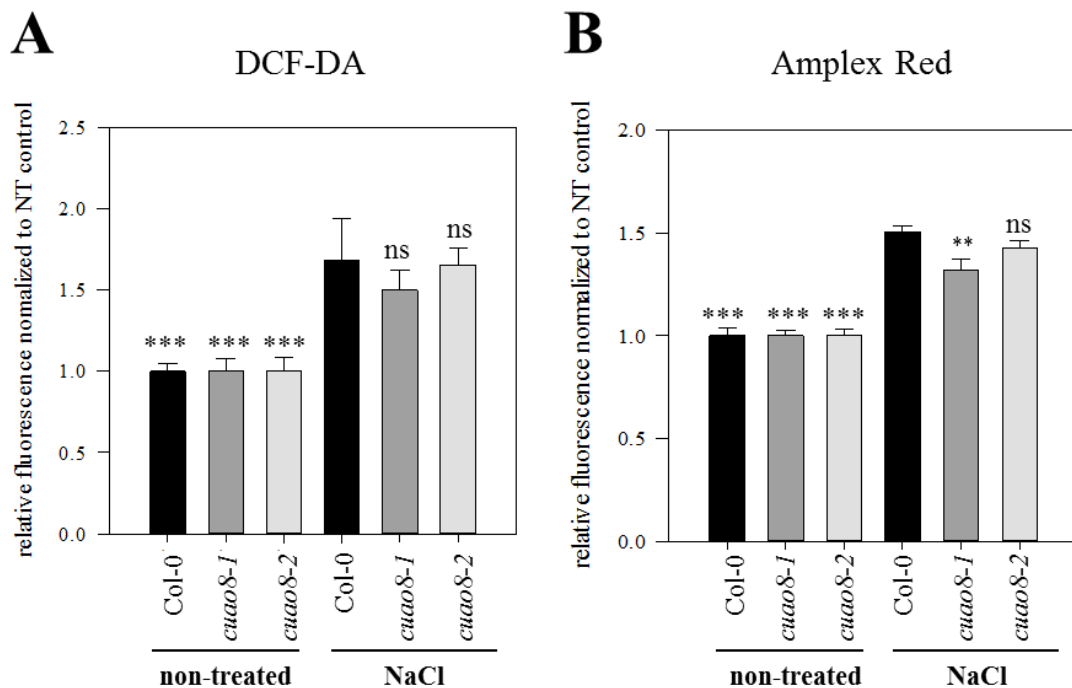


Figure 14: NaCl induced H₂O₂ production in Col-0, *cuao8-1* and *cuao8-2* root tips. Fluorescence quantification analysis of five day old seedlings from Col-0, *cuao8-1* and *cuao8-2* stained with (A) DCF-DA (20 μ M; 15 min) or (B) Amplex Red (100 μ M, 20 min) and treated with NaCl (200 mM, 6 h) or buffer (control, non-treated). The fluorescent signal was observed by epifluorescence microscopy. Shown is the relative fluorescence normalized to the non-treated control. Means \pm SE of at least three individual experiments are shown (DCF-DA n= 21-31, Amplex Red n= 22-30). (***) Significant difference P < 0.001 based on ANOVA (Holm-Sidak test) with respect to NaCl treated Col-0. ns = not significant

2.6 Increased amount of putrescine in *cuao8-1* and *cuao8-2* during salt stress

CuAO8 was previously shown to deaminate the three classical di-/polyamines putrescine, spermidine and spermine, and polyamines were also connected with NO production (Tun et al., 2006). Therefore, altered NO levels in *cuao8-1* and *cuao8-2* might be caused by changes in the polyamines levels. For this reason, free amounts of putrescine, spermidine and spermine were quantified (with HPLC) in five day old seedlings of Col-0, *cuao8-1* and *cuao8-2* before and after NaCl treatment. The measurements revealed that the amount of spermidine and spermine were similar in Col-0, *cuao8-1* and *cuao8-2* both before and after salt stress (Figure 15, Supplemental Figure 1). In contrast, putrescine levels appeared to be increased around 60% after NaCl treatment in *cuao8-1* and *cuao8-2* compared to Col-0. This increase was only measured after NaCl treatment and not after control treatment implying a specific CuAO8 dependent salt stress response. In conclusion, CuAO8 seems to deaminate

specifically putrescine during salt stress treatment. This goes in line with the *in vitro* activity measurements, where putrescine was the substrate with the highest deamination rate. Although that CuAO8-His₆ is also able to deaminate spermidine and spermine *in vitro*, this data suggests that *in vivo* putrescine is the main substrate for CuAO8 during salt stress.

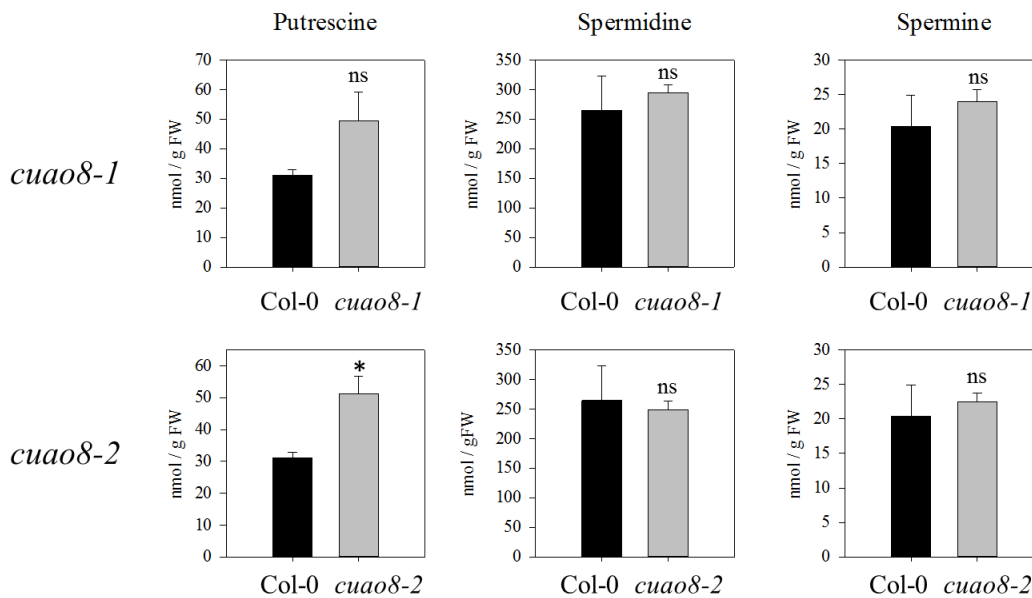


Figure 15: Effect of NaCl treatment on free polyamine levels in five day old seedlings of Col-0, *cuao8-1* and *cuao8-2*. The free levels of putrescine, spermidine and spermine were determined with HPLC after NaCl (200 mM, 6h) treatment. Means \pm SE of three individual experiments are shown. (***) Significant difference $P < 0.001$ based on t-test with respect to Col-0. ns = not significant

2.7 Decreased amount of free arginine in *cuao8-1* and *cuao8-2* during salt stress

PA and amino acid metabolism are tightly connected, and especially altered levels of the amino acids arginine, proline and also glutamate were linked with altered NO production (Li et al., 2001; Mori, 2007; Mohapatra et al., 2010; Shi et al., 2012; Filippou et al., 2013; Shi et al., 2013). Therefore, the proteinogenic amino acids were extracted from 100 mg of seedlings and the amounts was determined by LC-MS-MS (Björn Thiele, Forschungszentrum Jülich)

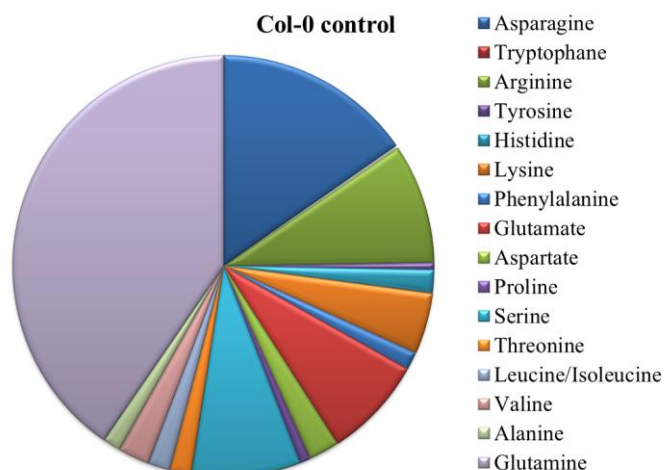


Figure 16: Representative distribution of amino acids in five day old seedlings. Representative distribution of all quantified amino acids in five day old seedlings (here: Col-0 after control treatment (buffer, 6h)).

before and after salt stress. The proportions (relative abundance) of all quantified amino acids were comparable in Col-0, *cuao8-1* and *cuao8-2* (Figure 16, Supplemental Table 1-3). Glutamines (41,%) showed the highest abundance followed by asparagine (14%), serine (8%) and arginine (8%). Among all proteinogenic amino acids, glutamate, glutamine, alanine, proline and arginine are closely connected to PA metabolism (Figure 17A). In general, the levels of these amino acids were higher in *cuao8-1* and *cuao8-2* than in Col-0 before and after salt stress treatment (Figure 17B). Specifically proline, glutamate and alanine were increased around 20% in the mutants. Nevertheless, one exception was obvious. The amount of arginine, which is the direct precursor of putrescine, was consistently decreased in all five biological replicates around 20% in *cuao8-1* and *cuao8-2* compared to Col-0 which is contrary to the other amino acids. Since arginine is a putative substrate for NO production, these measurements suggest, that the decreased NO levels in *cuao8-1* and *cuao8-2* might be caused by a lower arginine content.

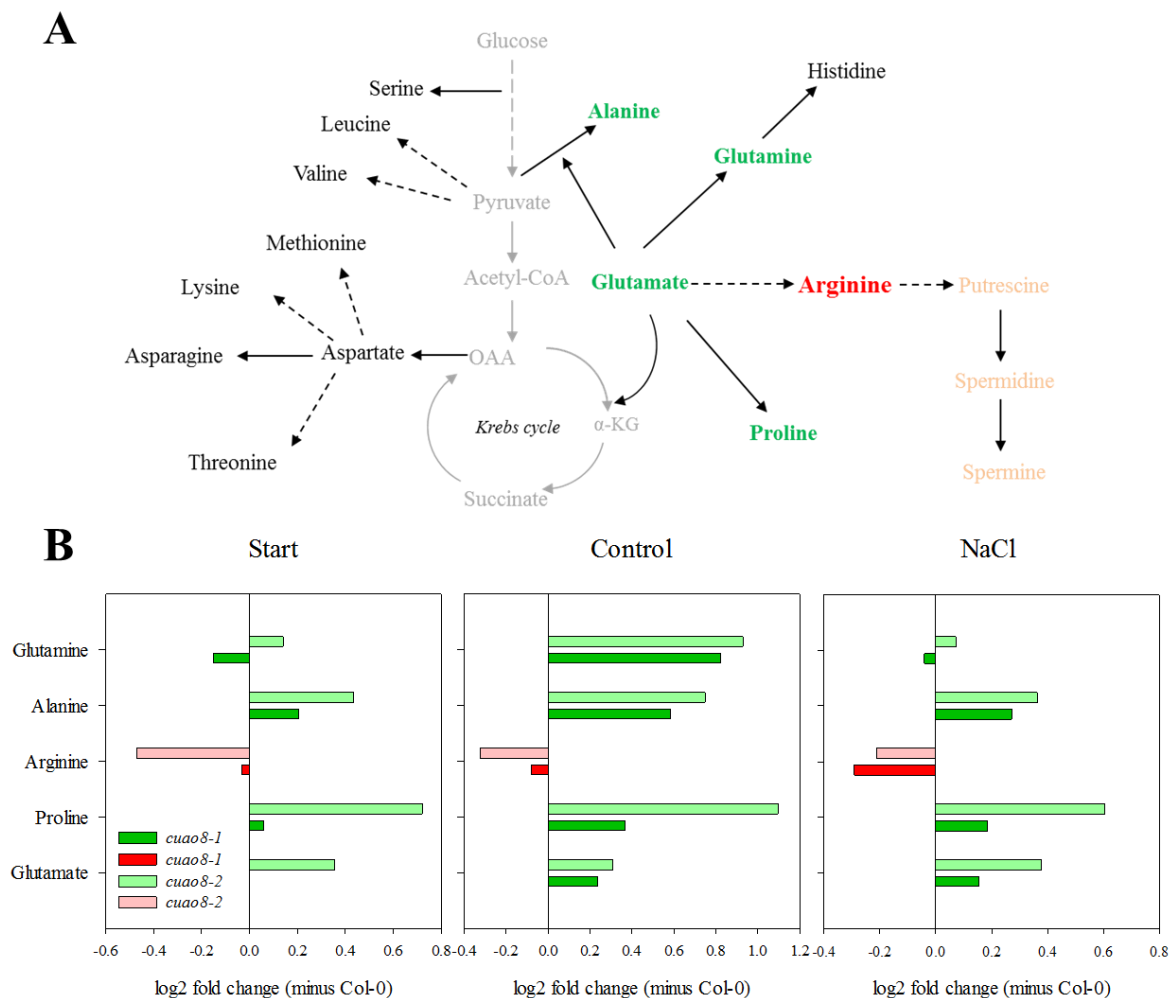


Figure 17: Overview of the metabolic network between PAs and amino acids and the influence of NaCl treatment on the amino acid levels in Col-0, *cuao8-1* and *cuao8-2*. (A) Schematic representation of the metabolic relationship among PAs and amino acids (modified from Mohapatra et al., 2009). The amino acids written in green/red color display the amino acids with the closest connection to the PA pathway. Dashed arrow: metabolic steps in between are left out. (B) The log₂ fold change of amino acids (shown in (A) in red/green) in five day old seedlings. Amino acids were measured with LC-MS-MS before (Start) and after NaCl (200 mM, 6h) respectively control treatment (buffer; 6h). Means of five individual experiments are presented.

2.8 Influence of Arginase activity on NO production in *cuao8-1* and *cuao8-2*

2.8.1 Increased arginase activity in *cuao8-1* and *cuao8-2* seedlings

The previous results revealed a decreased arginine amount in *cuao8-1* and *cuao8-2* seedlings. Arginine is consumed either by ADC for PA synthesis, arginase for urea production or it may serve as a substrate for the putative arginine dependent NO production. Arginase activity is already published to influence NO formation in mammals and plants (Gobert et al., 2000; Li et al., 2001; Flores et al., 2008; Shi et al., 2013; Meng et al., 2015). In mammals it is demonstrated that arginase depletes the arginine pool leaving less substrate for the NOS resulting in a decreased NO production (reviewed by: Boucher et al., 1999; Rabelo et al., 2015).

To analyze whether altered arginase activity might be responsible for lower arginine contents in *cuao8-1* and *cuao8-2*, arginase activity was measured in total protein extracts of five day old seedlings treated with salt (200 mM) or buffer (control) for six hours. Compared to Col-0, arginase activity was significantly enhanced in *cuao8-1* and *cuao8-2* (Figure 18A). Remarkably, arginase activity was similar after control and salt treatment in Col-0 (40 U/g protein) but increased from 51 U/g (*cuao8-1*) and 66 U/g (*cuao8-2*) to 75 U/g protein and 78 U/g protein respectively after salt treatment in *cuao8-1* and *cuao8-2*. Interestingly, the increased arginase activity in *cuao8-1* and *cuao8-2* is not caused by higher mRNA levels of both arginases (ARGH1, ARGH2, Supplemental Figure 2). These data suggest an aberrant activation of arginase during salt stress when CuAO8 is absent and thus imply a direct or indirect negative feedback regulation of CuAO8 on arginase.

To test whether higher arginase activity is responsible for the reduced NO production in *cuao8-1* and *cuao8-2*, NO formation was measured in the presence of an arginase inhibitor (*nor*-NOHA). Five day old seedlings were stained with DAR-4M AM, treated with salt or salt with *nor*-NOHA and root tip fluorescence was observed by epifluorescence microscopy. NO production could be partially (50%) but significantly restored upon addition of *nor*-NOHA in *cuao8-1* and *cuao8-2* (Figure 18B and C), demonstrating that enhanced arginase activity is to some extent responsible for the reduced NO production in *cuao8-1* and *cuao8-2* during salt stress.

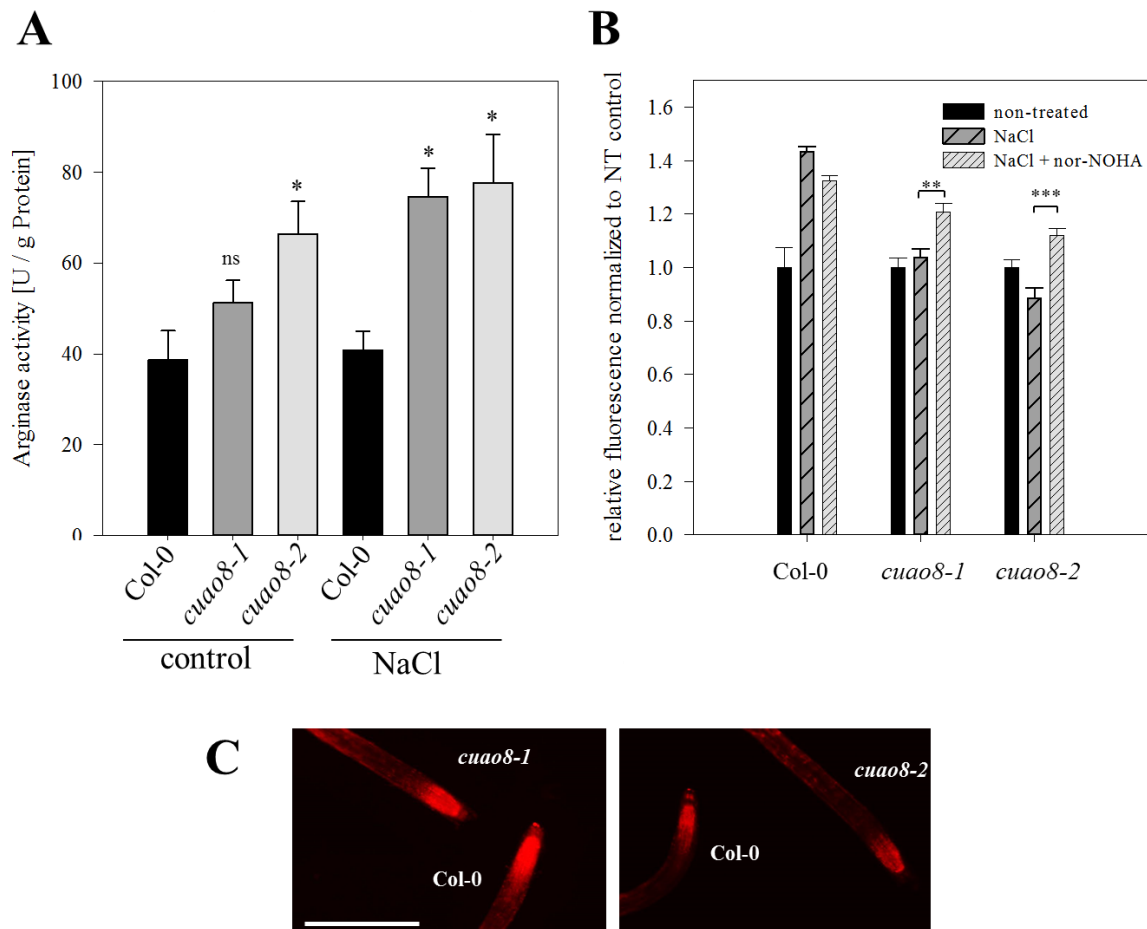


Figure 18: Arginase enzyme activity and the effect on the arginase inhibitor *nor*-NOHA on NO production in root tips during NaCl treatment. (A) Arginase enzyme activity was measured in total protein extracts of five day old seedlings from Col-0, *cuao8-1* and *cuao8-2* after NaCl (200 mM, 6h) respectively control (buffer, 6h) treatment. Means \pm SE of four individual experiments are shown. (***) Significant difference $P < 0.001$ based on ANOVA (Holm-Sidak test) with respect to Col-0. (B) Five day old seedlings of Col-0, *cuao8-1* and *cuao8-2* were stained with DAR-4M AM (5 μ M, 1h) and treated with buffer (control), NaCl (200 mM, 6h) or NaCl plus *nor*-NOHA (Arginase inhibitor, 100 μ M). The fluorescent signal in the root tips was observed by epifluorescence microscopy. Shown is the relative fluorescence normalized to the non-treated control. Means \pm SE of at least three individual experiments are shown ($n = 25-38$). (***) Significant difference $P < 0.001$ based on t-test with respect to the only NaCl treated genotype. (C) Representative images of DAR-4M AM stained five day old root tips from NaCl treated Col-0 and NaCl + *nor*-NOHA treated *cuao8-1* and *cuao8-2*. Scale: 500 μ m. ns = not significant

2.8.2 Arginine supplementation restored *cuao8-1* and *cuao8-2* phenotype

Previous experiments demonstrated that higher arginase activity is partially responsible for reduced the NO production in *cuao8-1* and *cuao8-2*. The question emerged, if the arginase activity itself is responsible for less NO production or, if the depletion of the substrate arginine, which was demonstrated by the amino acid content measurements, is the reason for reduced NO production. Therefore, NO formation in root tips of five day old seedlings was measured after co-application of NaCl and arginine. Strikingly, arginine addition (1 mM) significantly restored NO production in *cuao8-1* and *cuao8-2* to almost wild-type levels (Figure 19A), suggesting that the decreased arginine pool is responsible for the disturbed NO production in the mutants.

Next, it was tested if GSNO and arginine are able to restore the previous observed shorter root growth phenotype by complementing the NO or arginine deficiency in *cuao8-1* and *cuao8-2*. Moreover, GABA supplementation was also included because GABA is the deamination product of putrescine and has been demonstrated to be involved in root growth (Renault et al., 2010; Renault et al., 2011). Seedlings of Col-0, *cuao8-1* and *cuao8-2* were grown on ½-MS plates supplemented with either GSNO (50 µM), arginine (1 mM), or GABA (1 mM) and the primary root length was measured after eight days (Figure 19B). The measurement revealed that GSNO and arginine – in contrast to GABA - were able to partially restore root growth in *cuao8-1* and *cuao8-2* indicating that the shorter primary roots in *cuao8-1* and *cuao8-2* are founded in less NO production due to reduced arginine levels

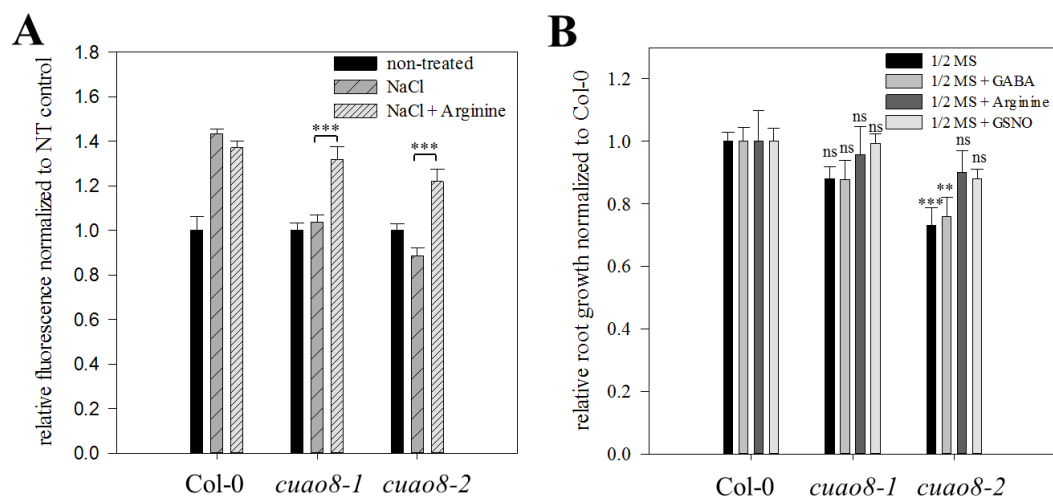


Figure 19: NO production of Col-0, *cuao8-1* and *cuao8-2* after co-application of NaCl stress and arginine as well as relative root growth of Col-0, *cuao8-1* and *cuao8-2* on only ½ MS plates or with GSNO, arginine and GABA supplementation. (A) Five day old seedlings of Col-0, *cuao8-1* and *cuao8-2* were stained with DAR-4M AM (5 µM, 1h) and treated with buffer (non-treated), NaCl (200 mM, 6 h) or NaCl plus arginine (1 mM). The fluorescent signal in the root tips was observed by epifluorescence microscopy. Shown is the relative fluorescence normalized to the non-treated control. Means ± SE of at least three individual experiments are shown (n= 22-34). (***) Significant difference $P < 0.001$ based on t-test with respect to the only NaCl treated genotype. **(B)** Relative root growth of Col-0, *cuao8-1* and *cuao8-2* after eight days on vertical ½-MS plates supplemented with GABA (1 mM; n = 13-17), arginine (1 mM; n = 14-18) or GSNO (50 µM; n = 25-30). Root growth was normalized to Col-0 and shown are the means ±SE of three individual experiments. (***) Significant difference $P < 0.001$ based on ANOVA (Holm-Sidak test) with respect to Col-0. GABA: γ -aminobutyric acid; GSNO: S-nitrosoglutathione; ns = not significant

2.9 Influence of NR activity on NO production in *cuao8-1* and *cuao8-2*

2.9.1 Increased nitrogen content in *cuao8-1* and *cuao8-2*

Arginine is a major nitrogen storage compound in plants. In Arabidopsis, arginase and urease activity are the only sources for endogenous nitrogen recycling by arginine breakdown to ammonia (Zonia et al., 1995; Goldraij et al., 1999) (Figure 20A). A higher arginase activity implicates a higher urea production followed by a higher ammonia concentration. Ammonium is also one product of nitrogen assimilation. Interestingly, Meng et al. (2015) found a higher nitrogen content in rice arginase overexpression plants. This could link higher arginase activity with nitrogen assimilation. To test whether higher arginase activity in *cuao8-1* and

cuao8-2 also affects the nitrogen assimilation in *A. thaliana*, the nitrite and nitrate contents were quantified in five day old seedlings after NaCl and control treatment. The nitrite measurements after NaCl stress revealed that the nitrite contents in *cuao8-1* and *cuao8-2* were higher than in Col-0 (Col-0: 84 pmol/mg protein, *cuao8-1*: 172 pmol/mg protein, *cuao8-2*: 168 pmol/mg protein) (Figure 20B). Similarly, *cuao8-1* and *cuao8-2* displayed enhanced nitrate levels compared to Col-0 (10 μ mol/mg protein. *cuao8-1*: 25 nmol/mg protein; *cuao8-2*: 21 nmol/mg protein). Our data suggest that CuAO8 also influences nitrogen assimilation presumably by regulating arginase activity.

Furthermore, nitrite amounts are also interesting in regard to NR dependent NO production. Since NR produces NO only in the presence of high nitrite concentrations, elevated nitrite levels in *cuao8-1* and *cuao8-2* should result in enhanced NO production by NR (Dean and Harper, 1988; Rockel et al., 2002; Planchet et al., 2005). Because NO production in *cuao8-1* and *cuao8-2* is severely disturbed despite of elevated nitrite levels, it seems likely that NR does not significantly contribute to NO production in seedling root tips during salt stress. This further supports the hypothesis that the disturbed NO production in *cuao8-1* and *cuao8-2* is caused by arginine deficiency and not by disturbed NR dependent NO production.

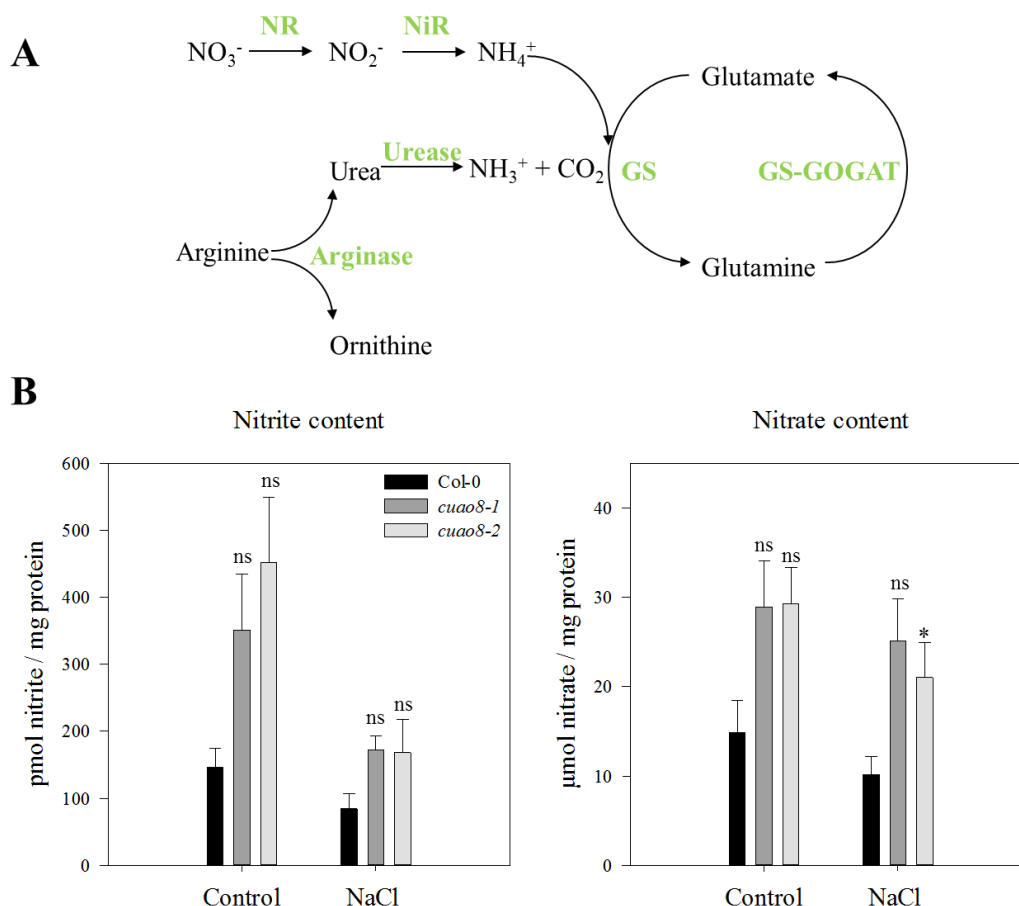


Figure 20: Nitrite and nitrate contents in five day old seedlings of Col-0, *cuao8-1* and *cuao8-2* after salt stress (A) Metabolic network of arginine and urea with nitrite and nitrate catabolism (modified from Mériçout et al., 2008) NR: Nitrate reductase, NiR: Nitrite reductase; GS: Glutamine synthetase; GOGAT: Glutamate synthase (B) Nitrite and nitrate contents in five day old seedlings after NaCl (200 mM, 6h) respectively control (buffer, 6h) treatment. Means \pm SE of four individual experiments are shown. (*) Significant difference $P < 0.001$ based on ANOVA (Holm-Sidak test) with respect to Col-0. ns = not significant**

2.9.2 NR activity is not altered in *cuao8-1* and *cuao8-2*

Besides the proposed arginine dependent NO production in *A. thaliana*, the well described nitrite reduction catalyzed by the cytosolic NR is also one source of NO formation (Dean and Harper, 1988; Yamasaki and Sakihama, 2000; Stöhr et al., 2001; Rockel et al., 2002). Therefore, the observed reduced NO production in *cuao8-1* and *cuao8-2* might possibly reflect altered NR activity. NR reductase activity is regulated by transcriptional and post-translational mechanisms (reviewed by: Kaiser and Huber, 2001; Kaiser et al., 2002). Posttranslational regulation includes phosphorylation of a serine, which allows the binding of a 14-3-3 protein. The 14-3-3 protein inhibits NR activity in the presence of cations like Mg^{2+} . The circumstance that 14-3-3 proteins only inhibit in the presence of cations allows to measure two different aspects of NR activity. Here, the NR activity was tested once in the presence of excess Mg^{2+} to measure the “real” *in vivo* NR activity (actual NR activity) and once in the presence of EDTA to determine the highest possible NR activity (total NR activity).

Total NR activity after NaCl stress was significantly decreased in *cuao8-1* and *cuao8-2* compared to Col-0 (Col-0: 131 nmol nitrite/mg protein, *cuao8-1*: 96 nmol nitrite/mg protein; *cuao8-2*: 91 nmol nitrite/mg protein) (Figure 21A). Surprisingly, the actual NR activity was similar between Col-0 and the mutants (Col-0: 110 nmol nitrite/mg protein; *cuao8-1*: 90 nmol nitrite/mg protein; *cuao8-2*: 101 nmol nitrite/mg protein). Accordingly, the reduced NO formation observed in *cuao8-1* and *cuao8-2* cannot be explained with decreased NR activity, which is also supported by the previous measured enhanced nitrite contents in the mutants. Moreover, these results suggest an effective posttranslational inhibition of NR in Col-0 (total activity > actual activity) which is missing in the mutants (total activity = actual activity).

In addition, mRNA levels of both cytosolic NR isoforms (*NIA1*, *NIA2*) were quantified in salt stressed seedlings of Col-0, *cuao8-1* and *cuao8-2*. The expression levels of both nitrate reductase isoforms were significantly decreased in *cuao8-1* and *cuao8-2* after NaCl treatment compared to Col-0 (Figure 21B). Accordingly, the measured higher total NR activity in Col-0 can be explained by increased transcription of *NIA1* and *NIA2*.

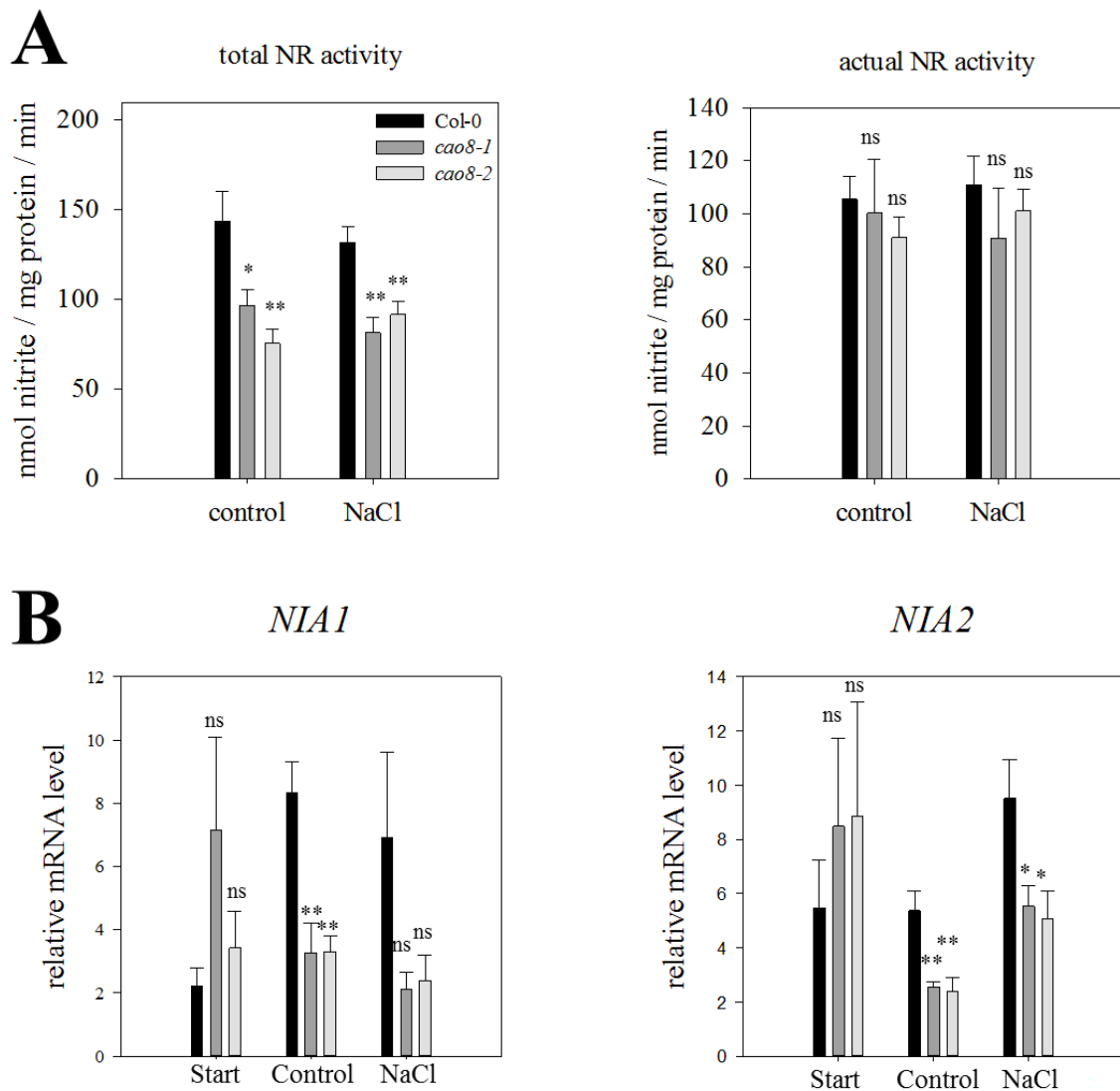


Figure 21: Nitrate reductase activity and mRNA level of *NIA1* and *NIA2* in five day old seedlings after NaCl stress. (A) Five day old seedlings were treated with NaCl (200 mM, 6h) or with buffer (control; 6h) and NR activity was measured in total protein extracts. Total NR activity was determined in the presence of EDTA and the actual NR activity in the presence of $MgCl_2$. Means \pm SE of at least three individual experiments are shown. (B) Relative expression of nitrate reductase 1 (*NIA1*) and 2 (*NIA2*) in five day old seedlings before (Start) and after NaCl (200 mM, 6h) respectively control (buffer, 6h) treatment. Means \pm SE of at least three individual experiments are shown (***) Significant difference $P < 0.001$ based on ANOVA (Holm-Sidak test) with respect to Col-0. NR: Nitrate reductase; ns = not significant

3. Discussion

3.1 CuAO8 - a classical copper amine oxidase

The genome of *Arabidopsis thaliana* contains 10 copper amine oxidase (CuAO) genes which were phylogenetically clustered into three clades based on their amino acid sequences (Tavladoraki et al., 2016). Clade I consists of CuAO 2, 4, 8 as well as AtAO1 and Clade II consists of CuAO 1, 5, and 9. Clade III is more distinct from clade I and II and comprises CuAO 3, 6 and 7 among which CuAO 6 and 7 are postulated as non-functional CuAOs being consecutive fragments of AtAO1 (Tavladoraki et al., 2016). Furthermore, gene sequence analysis revealed that CuAO3 (Clade III) displays remarkable differences to all other CuAO genes possessing different numbers and positions of introns which are rather similar within clade I and II (Tavladoraki et al., 2016). The high similarity of all CuAOs in clade I and II argues for a recent common ancestor (Tavladoraki et al., 2016) and may also indicate functional redundancy of some *A. thaliana* CuAOs. Despite the central role of polyamine metabolism during development and the stress response, it was found in this work that the deletion of CuAO8 did not cause a severe phenotype, suggesting a functional replacement of CuAO8 by other CuAOs presumably of the same phylogenetic clade. To reveal further physiological functions of CuAO8, it will be inevitable to analyze CuAO double mutants. In particular a double mutant of CuAO8 and CuAO2 would be of interest, due to their close relationship and high amino acid sequence identity of 80% (Supplemental Figure 4).

To define cellular compartments in which CuAO8 might operate, GFP-CuAO8 was transiently expressed in tobacco leaves. It was found that GFP-CuAO8 was mainly localized in the cytosol but also partially in the plasma membrane (Figure 10). Until now the localization of only three *A. thaliana* CuAOs was analyzed and these were distributed in the apoplast (CuAO1) or peroxisome (CuAO 2 and 3) although a peroxisomal targeting signal is missing in CuAO2 (Planas-Portell et al., 2013). The localization of CuAO8 is therefore clearly distinct from those of other published CuAOs. This might indicate a high degree of functional specification of CuAO family members, similar to other highly expanded protein families for instance the *Arabidopsis* aquaporin's (Quigley et al., 2002). However, since only N-terminally GFP-tagged CuAO8 could be analyzed in this work, it cannot be excluded that the GFP-tag might interfere with putative signal peptides, which are often positioned at the N-terminus. Still, apple amine oxidase (AO) 2 was also shown to be localized intra- and extracellularly supporting the result that CuAO8 could have different subcellular localizations (Zarei et al., 2015). Diverse cellular localizations might for instance be achieved by different interaction partners, which guide the distribution of CuAO8 (Wojtera-Kwiczor et al., 2013).

Similar to other CuAOs, western blot analysis revealed a monomer size of 90 kDa for CuAO8, although the molecular weight inferred from the primary sequence is considerably lower (77 kDa) (Planas-Portell et al., 2013; Zarei et al., 2015). This suggests that CuAO8 is extensively glycosylated *in vivo*, which has already been demonstrated for apple AO1 and

AO2 (Zarei et al., 2015). The presence of glycosylation strongly supports the plasma membrane localization of CuAO8 found in this study, since glycosylated proteins are usually found at the outer cell surface (Spiro, 2002). To verify that CuAO8 is a classical amine oxidase, the rate of oxidative deamination (measured by the formation of H₂O₂) for the putative substrates agmatine, putrescine, spermidine and spermine was analyzed (Figure 8). The highest turnover rate was observed for putrescine followed by spermidine, spermine and agmatine. CuAO3 and AtAO1 also preferred putrescine as substrate contrasting to CuAO1 and 2 which displayed the same H₂O₂ production rate for putrescine and spermidine (Møller and McPherson, 1998; Planas-Portell et al., 2013). Interestingly, CuAO8 is the first *A. thaliana* CuAO shown to be able to deaminate spermine and agmatine, indicating a rather low substrate specificity of this protein.

Since the *cuao8* knockout mutant displayed severely compromised arginine dependent NO production after INA treatment and during salt stress, the easiest conclusion would be that CuAO8 is able to directly produce NO, using arginine or derived metabolites as substrate. However, *in vitro* activity tests using DAR-4M AM as NO detecting probe revealed that CuAO8 cannot directly synthesize NO upon addition of putrescine, spermidine, spermine, agmatine or arginine. Although it cannot be excluded that CuAO8 might need certain interacting proteins to switch to NO synthesis, these results imply an indirect regulatory mechanism of CuAO8 on NO production. This conclusion is further supported by the fact, that NO production in *cuao8* could be rescued by arginine supplementation, which would not have been possible, if CuAO8 directly produces NO. Interestingly, *cuao1*, *cuao6* and *atao1* also showed decreased NO production after INA treatment, which was however not as pronounced as in *cuao8* (Figure 4). This suggests, that a central metabolite or substrate of CuAOs might be the cause of reduced NO formation in these mutants.

3.2 CuAO8 knockout affects NO production in *A. thaliana* by altering arginase activity

The present study revealed a pivotal influence of CuAO8 on NO production in *A. thaliana* seedlings. *CuAO8* knockout lines produced significantly less NO in response to salt stress, accompanied by increased arginase activity. The NO deficient phenotype of *cuao8* could be rescued by arginine supplementation or arginase inhibition (Figure 18 & 19). These data suggest a mechanism, in which enhanced arginase activity depletes the cellular arginine pool, thereby compromising the arginine dependent NO production. Our data thus strongly support the existence of an arginine dependent NO production pathway, which is still extensively debated in the plant NO community (Corpas et al., 2009; Fröhlich & Durner, 2011).

The main concern questioning arginine dependent NO production in higher plants is the lack of enzymes catalyzing the conversion of arginine to citrulline with concomitant release of NO, in a reaction similar to mammalian NOSes. An extensive study of 1087 higher plant and algae genomes did not reveal homologs of mammalian NOS genes in higher plants (Jeandroz et al., 2016). In contrast, NOS-like genes were identified in several algae species supporting another study in which the algae *Ostreococcus tauri* was demonstrated to possess NOS-like activity (Foresi et al., 2010). Furthermore, plants do not synthesize tetrahydrobiopterin (H₄B), which is a cofactor used by mammalian NOSes. However, it was suggested that H₄B can be

substituted by tetrahydrofolate (H_4F), since overexpression of rat NOS in Arabidopsis led to constitutively enhanced NO levels, demonstrating that – despite the lack of H_4B – a NOS-like reaction is principally possible in plants (Shi et al., 2012). On the other hand, many studies present evidences, which clearly support the existence of a NOS-like activity and NOS-like enzymes in higher plants. First, inhibitors of mammalian NOSes efficiently blocked/reduced NO production in various plant species (Delledonne et al., 1998; Durner et al., 1998; Desikan et al., 2002; Zhao et al., 2009). Second, the conversion of arginine to citrulline has been demonstrated in plant extracts, although the production of NO was not always proven in these experiments (Barroso et al., 1999). These results reinforce the existence of arginine dependent NO production in plants even though these studies do not allow to directly conclude on the presence of NOS-like enzymes.

The intracellular concentration of arginine critically influences NO production by NOS and NOS-like enzymes. The arginine pool is mainly regulated by two arginine-catabolizing enzyme families, namely arginine decarboxylases (ADCs) and arginases (Figure 22). ADCs are localized in the chloroplast and decarboxylate arginine to agmatine, which constitutes the first step of polyamine biosynthesis (Borrell et al., 1995) (see 1.3). There are two ADC isoforms in *A. thaliana*: ADC1 is constitutively expressed and ADC2 expression is enhanced during stress treatment (Urano et al., 2003; Sanchez-Rangel et al., 2016). Interestingly, the aldehyde of agmatine, inhibits iNOS thereby altering NO production during the inflammatory response (Satriano, 2004). However, ADC activity in regard to NO production is not well investigated in contrast to arginase activity. Both *A. thaliana* arginase isoforms (ARGH1 and 2) are localized in the mitochondria and hydrolyze arginine thereby producing ornithine and urea (see review: Winter et al., 2015). In mammals it is well known that arginase activity regulates NO production by decreasing the intracellular arginine pool (see review: Rabelo et al., 2015). Similarly, data from this work suggests that arginase is a crucial regulator of NO production in Arabidopsis. These data are supported by several studies demonstrating either enhanced NO formation in arginase deficient *A. thaliana* lines (Flores et al., 2008) or decreased NO production in arginase overexpressing plants (Shi et al., 2013; Meng et al., 2015). The arginase activity in mammals is a crucial factor regulating NO production by the NOSes. Both enzymes have comparable V_{max} and K_M values and therefore compete for arginine as substrate, resulting in an inverse correlation of arginase and NOS activity (Boucher et al., 1999; Mori, 2007). Moreover, an intermediate (L-NOHA) of the NOS catalyzed arginine to citrulline conversion efficiently inhibits arginase, which redirects the arginine flux towards NOS-based NO production (Berkowitz et al., 2003). Several cardiovascular and neuronal dysfunctions and diseases were connected with increased arginase activity (see review: Caldwell et al., 2015). For instance, patients with endothelial dysfunction displayed higher arginase activity which decreases the intracellular arginine availability leading to reduced NO production by the endothelial NOS (Berkowitz et al., 2003). Moreover, the uptake of insulin by endothelial cells is dependent on NO and type-2 diabetes patients possess reduced NO production and higher arginase activity in this tissue (Wang et al., 2013a; Ko vamees et al., 2016). The reciprocal relation of NO production and arginase activity is also important during neuroinflammation which is characterized by enhanced iNOS and decreased arginase activity (Ljubisavljevic et al., 2014). Interestingly,

Helicobacter pylori uses high arginase activity to prevent the execution of NO-based immune reactions (see review: Gobert et al., 2001).

In conclusion, the interplay between arginase and NOS(es) to control NO production is unambiguous in mammals. Our data in combination with other reports strongly suggests that a similar mechanism is also operative in plants. However, whether arginine is directly metabolized by a NOS-like enzyme or whether it is just the precursor for a substrate used by different enzymes to produce NO remains elusive.

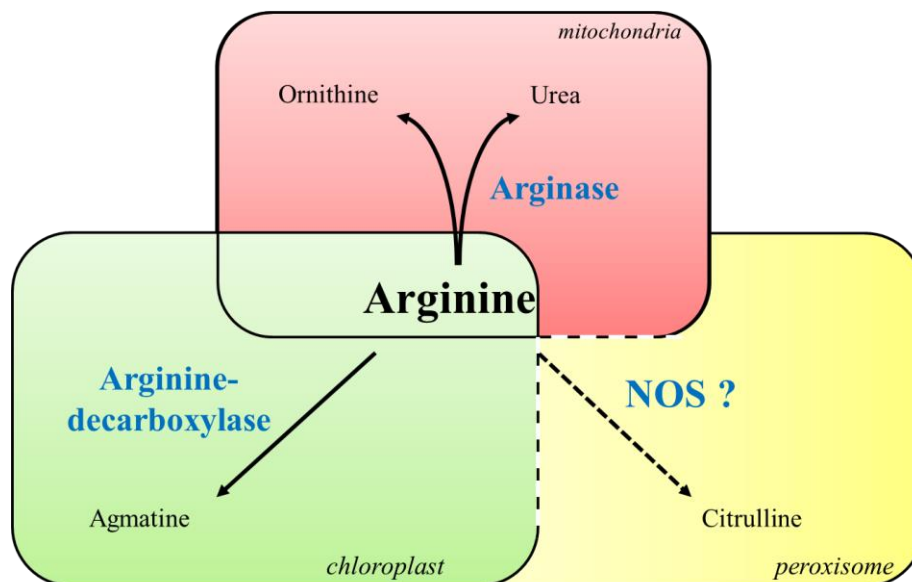


Figure 22: Catabolism of arginine in plants. Arginine can either be decarboxylated to agmatine by arginine-decarboxylase (ADC) or hydrolyzed to ornithine and urea by arginase. Another putative pathway of arginine breakdown involves NOS-like activity, which oxidizes arginine to citrulline thereby releasing NO. ADC is localized in the chloroplast whereas arginase was shown to be present in the mitochondria. NOS-like activity was detected in the chloroplast, mitochondria but also in the peroxisome.

3.3 Mammalian and plant arginine catabolism – a comparison

As outlined before, the existence of a plant arginine dependent NO production similar to that found in mammals has been questioned. Instead it was proposed that plants exclusively produce NO by the reduction of nitrite by nitrate reductase (NR) or non-enzymatically (Jeandroz et al., 2016). The main concern, arguing against arginine-based NO production is the lack of a NOS gene sequence homology/NOS-like enzyme in higher plants. However, closer inspection of plant enzymes involved in arginine metabolism in general reveals substantial differences compared to their mammalian counterparts. Arginine catabolizing enzymes in plants and mammals catalyze similar reactions but display high sequence divergence (Figure 23): These striking differences open the question whether it is an appropriate way to search for NOS-like enzymes in plants by sequence comparison with the mammalian NOS. This section will describe the differences between the enzymes involved in plant and animal arginine metabolism and will argue for alternative approaches to identify enzymes involved in arginine dependent NO production in plants.

Arginase

Arginase hydrolyzes arginine to ornithine and urea. Phylogenetic analysis of plant arginase revealed higher sequence similarity to vertebrate, fungi and bacteria agmatinase than to arginase (Chen et al., 2004). For instance, *Arabidopsis* arginase displayed 32-48% sequence identity with bacterial agmatinase and only 25-28% identity with arginases from other organisms (Yue et al., 2012). Furthermore, both isoforms of plant arginase are localized in the mitochondria whereas mammalian arginase 1 is found in the cytosol and only arginase 2 localizes to the mitochondria (Li et al., 2001; Flores et al., 2008).

Arginine decarboxylase (ADC)

ADC catalyzes the decarboxylation of arginine, thereby producing agmatine. Similar to arginase, the human and plant proteins show very low sequence homology (Zhu et al., 2004). Plant ADC is localized in the thylakoid membrane of chloroplasts and is insensitive to Ca^{2+} whereas mammalian ADC is activated by Ca^{2+} (Borrell et al., 1995; Zhu et al., 2004). Furthermore, a plant ADC inhibitor (DFMO) was not able to inhibit human ADC, but rather inhibited human ornithine decarboxylase (ODC) illustrating that plant ADC is closer related to human ODC than ADC (Zhu et al., 2004). In plants, the produced agmatine is then further metabolized to N-carbamoyl-putrescine and subsequently to putrescine by agmatine iminohydrolase (AIH) and N-carbamoylputrescine amidohydrolase (CPA), respectively (see Figure 23). In contrast, in mammals the enzyme agmatinase catalyzes the direct conversion of agmatine to putrescine, replacing the action of AIH and CPA (Wang et al., 2014).

Ornithine decarboxylase (ODC)

ODC catalyzes the conversion of ornithine to putrescine which constitutes the first step of an alternative way of putrescine biosynthesis (Figure 23). The ODC of plants and mammals display high sequence homology. Interestingly in some *Brassicaceae* species including *A. thaliana* and the moss *Physcometrella patens* the existence of an ODC is questioned since no homologous gene has been identified and ODC protein activity could not be detected (Hanfrey et al., 2001; Fuell et al., 2010; Illingworth and Michael, 2012). Therefore, in these species putrescine synthesis is completely dependent on the ADC pathway. Moreover, plant and mammalian ODC are differently regulated. In mammals, ODC activity is adjusted by the non-competitive inhibitor antizyme, which is not able to inhibit plant ODCs (Illingworth and Michael, 2012). Remarkably, since several photosynthetic organisms lost ODC independently, it was concluded that ODC dependent putrescine biosynthesis is not essential for plants (Fuell et al., 2010). This is in clear contrast to mammals in which putrescine synthesis occurs mainly via ODC (Kurian et al., 2011).

In summary, although arginine catabolism creates citrulline, ornithine and putrescine in plants and mammals, the enzymes catalyzing these processes display low sequence homology, different subcellular localizations and some of the mammalian enzymes are even absent in several plant species or *vice versa*. This suggests that arginine metabolism evolved differently in mammals and plants. Since principal modules are conserved in both kingdoms a functional NOS analogue is likely to be present in plants. However, it seems rather unlikely that a plant

NOS shows high sequence homology to its mammalian counterparts, challenging current approaches which are mainly based on gene sequence comparisons. At first glance, the fact that mammalian NOS inhibitors also suppress NO production in plants seems to contradict this hypothesis. However, most of these inhibitors are arginine derivatives or arginine based peptides (see review: Vítěček et al., 2012) and thus will likely influence any enzyme using arginine as substrate. Furthermore, the applied inhibitors are not specific, for instance, aminoguanidine, which is a widely used and accepted iNOS-inhibitor also suppresses CuAO activity (Griffiths et al., 1993; Bouchereau et al., 1999). Therefore, alternative approaches are suggested for the search of NOS-like enzymes in plants, for instance affinity chromatography based identification or arginine binding proteins or yeast complementation assays as it was done for the identification of arginase from *Arabidopsis* (Krumpelman et al., 1995).

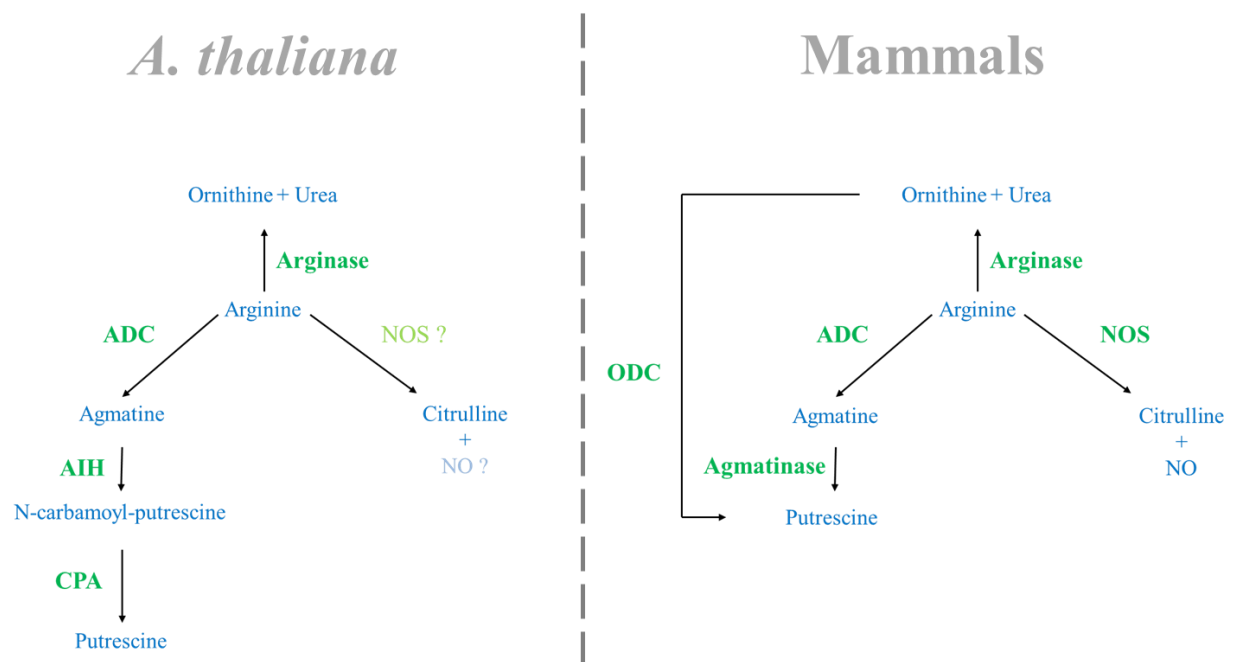


Figure 23: Arginine catabolism in *A. thaliana* and mammals. Arginine consumption in *A. thaliana* and mammals displays conspicuous differences concerning gene sequences of arginase and ADC and the absence of ODC and Agmatinase in *A. thaliana*. ADC: Arginine-decarboxylase, ODC: Ornithine-decarboxylase, AIH: agmatine iminohydrolase, CPA: N-carbamoylputrescine amidohydrolase, NOS: nitric oxide synthase, NO: nitric oxide

3.4 How could CuAO8 affect arginase activity?

In this study it was found that the absence of CuAO8 critically affects NO production by enhancing arginase activity. However, the molecular mechanism connecting CuAO8 and arginase activity could not be resolved. Since the transcript level of arginase was similar in Col-0, *cua08-1* and *cua08-2* it seems likely that CuAO8 influences arginase activity by posttranslational mechanisms (Supplemental Figure 2). Posttranslational control could be executed by direct interaction of arginase and CuAO8, resulting in the inhibition of arginase. Since CuAO8 is localized in the cytosol/plasma membrane (Figure 10) and both arginase isoforms reside in the mitochondria (Flores et al., 2008), this scenario would require the shuttling of one of the proteins. Supporting this hypothesis, human arginase was observed to

move from mitochondria to the cytosol upon the perception of lipoprotein signals (Caldwell et al., 2015).

Inhibition of arginase activity by CuAO8 could also be mediated indirectly either by CuAO8 related metabolites or CuAO8 dependent signaling cascades. An accumulation of putrescine was found in *cuao8-1* and *cuao8-2* (Figure 15). Interestingly, purified arginase from soybean, oakmoss and ginseng displayed increased activity upon addition of putrescine, spermidine or spermine from which putrescine had the highest activation capacity (Martín-Falquina and Legaz, 1984; Kang and Cho, 1990; Hwang et al., 2001). Furthermore, poplar cells possessing higher putrescine levels, exhibited increased urea amounts probably resulting from enhanced arginase activity (Page et al., 2016). These studies strongly support the idea that the increased putrescine level in *cuao8-1* and *cuao8-2* is involved in the stimulation of arginase activity. Again, this scenario would require the translocation of putrescine into the mitochondria via specific translocators. However, mitochondrial PA transporters have not yet been identified although several putrescine transporters are described in *A. thaliana* (plasma membrane, golgi apparatus, endoplasmic reticulum) and additional PA transporter families are likely to be present (Fujita and Shinozaki, 2014). Nevertheless, mitochondrial import of putrescine is possible in *A. thaliana* since externally added radioactively labelled putrescine was incorporated into mitochondrial proteins (Votyakova et al., 1999).

In conclusion the following model is suggested: due to the absence of CuAO8 in *cuao8-1* and *cuao8-2* the putrescine levels in these mutants increase during salt stress. A certain proportion of putrescine translocates into the mitochondria, where it binds to arginase and stimulates its activity. Enhanced arginase activity results in the depletion of the cellular arginine pool, resulting in reduced NO formation. For the future it will be interesting to validate this model by i) testing the effect of putrescine on recombinant arginase from Arabidopsis and ii) analyzing NO production in other mutants compromised in putrescine metabolism.

3.5 Regulation of nitrate reductase by CuAO8

Nitrite reduction by nitrate reductase (NR) is one major source of NO production in plants. It was therefore tested whether decreased NR activity is responsible for the reduced NO production in *cuao8-1* and *cuao8-2*. Since NR activity is tightly regulated on a posttranslational level, total and actual NR activities have to be distinguished. Total NR activity represents the total amount of NR protein, which is present in the tissue and could be principally active. Actual NR activity refers to the activity, which is present in the cell or tissue and is composed of the action of all NR proteins, which are not inhibited post-translationally. Since the actual NR activity was similar in Col-0, *cuao8-1* and *cuao8-2* (Figure 21B), it can be concluded that altered NR activity did not contribute to the reduced NO production in *cuao8-1* and *cuao8-2*, reinforcing the central claim, that alternative NO production routes must exist in Arabidopsis.

Interestingly, total NR activity was higher in Col-0 compared to *cuao8-1* and *cuao8-2*, which can be explained by increased transcript levels of both NR isoforms (*NIA1* and *NIA2*) in Col-0 (Figure 21A). This implies that CuAO8 positively regulates the transcription of *NIA1* and

NIA2. High levels of glutamine and asparagine inhibit transcription of NR, since these amino acids are the primary nitrogen-acceptors in the cell, and increased levels are therefore indicative of a saturated nitrogen state (Migge et al., 2000). The levels of both amino acids were slightly increased in *cuao8-1* and *cuao8-2*, possibly explaining the lower NR transcript abundance in these mutants (Figure 17, Supplemental table 2 & 3).

Although NR transcript levels were higher in Col-0 than in *cuao8-1* and *cuao8-2* the actual NR activity was similar in all three genotypes. Furthermore, in *cuao8-1* and *cuao8-2* the total and actual NR activities were identical. This leads to the unexpected conclusion, that CuAO8 controls NR activity by a yet unknown posttranslational mechanism. What could be the molecular mechanism of this inhibition?

Inhibition of NR is achieved by phosphorylation and subsequent binding of 14-3-3 proteins. This mechanism is strictly dependent on high concentrations of divalent cations like Mg^{2+} and Ca^{2+} . The initial phosphorylation is mediated by a calcium dependent protein kinase (CDPK) or alternatively by a sucrose non-fermenting 1 related kinase (SNF1) (Kaiser et al., 2002). Interestingly, inhibition of NR was initiated/potentiated by NO (Rosales et al., 2011; Sanz-Luque et al., 2013), possibly mediated via an NO dependent influx of Ca^{2+} . A similar mechanism was described for stomatal closure, in which the initial NO burst led to an increase of the intracellular Ca^{2+} concentration followed by activation of Ca^{2+} dependent protein kinases (Sokolovski et al., 2005). The inhibition of NR activity in Col-0 (total > actual NR activity), which is absent in *cuao8-1* and *cuao8-2* (total = actual NR activity) could therefore be explained by the higher NO production in Col-0 which possibly affects CDPK activity and consequently phosphorylation and inhibition of NR.

In conclusion, we can exclude reduced NR activity as the reason for the disturbed NO production in *cuao8*. Nevertheless, CuAO8 has a profound effect on the regulation of NR activity, both by controlling transcription and posttranslational inhibition of NR.

3.6 Is CuAO8 involved in the prevention of oxidative stress?

The oxidative burst, which is characterized by the temporally and spatially controlled production of ROS and NO, is an inherent characteristic of biotic and abiotic stresses, fulfilling important signaling functions mainly mediated by posttranslational modifications. The oxidative burst is essential to increase the activity of Na^+/H^+ antiporters and to initiate targeted degradation of proteins during salt stress (Zhang et al., 2006; Miller et al., 2010). To prevent oxidative and nitrosative damage of the cell (e.g. lipid peroxidation, oxidative DNA and protein damage), the production of ROS and NO has to be strictly controlled. Data from this study together with other reports suggest a role of CuAO8 in the downregulation of the oxidative burst and hence the prevention of oxidative stress during abiotic challenge (Figure 24).

It has been demonstrated that high levels of H_2O_2 are able to deactivate CuAOs, possibly by oxidation of a histidine and tryptophan close to the active site (Pietrangeli et al., 2004). This implies that CuAO8 activity negatively correlates with the progression of the oxidative burst (1). Data from this study demonstrate that decreased CuAO8 activity (mimicked by the

situation in the *cuao8* knockout mutant) results in enhanced putrescine levels since putrescine is a direct substrate of CuAO8 (2). Putrescine accumulation could then initiate different physiological reactions, which together limit/prevent the accumulation of ROS and NO:

1. Downregulation of NO production. This work demonstrates that the absence of CuAO8 increases arginase activity (3), resulting in the depletion of the intracellular arginine pool, thereby limiting the arginine dependent formation of NO (4). Activation of arginase is probably mediated by increased putrescine levels (Martín-Falquina and Legaz, 1984; Kang and Cho, 1990; Hwang et al., 2001).
2. Activation of the antioxidant system (5). Putrescine enhanced the activity of several antioxidant enzymes like superoxide dismutase, catalase and peroxidase in *Brassica juncea*, thereby increasing tolerance against salinity stress (Verma and Mishra, 2005). In citrus plants, putrescine not only stimulated the activity but also activated the expression of antioxidant enzymes resulting in reduced ROS and RNS formation during salt stress. (Tanou et al., 2014). Finally, the Arabidopsis ecotype Shahdara (Sha) contained higher concentrations of putrescine, accompanied by elevated SOD and catalase activity and reduced H₂O₂ contents (Wang et al., 2013b).
3. Enhancement of photochemical efficiency (6). The photosynthetic apparatus is a major source of ROS production during abiotic stress. To prevent water loss, stomata become closed, which results in the over-reduction of the electron transport chain. As a consequence, electrons are transferred to oxygen, resulting in the production of ROS (see review: Miller et al., 2010). Binding of putrescine to components of photosystem II was demonstrated to increase photochemical efficiency thereby reducing the production of ROS during salt stress (Shu et al., 2015).

This model implies that CuAO8 undergoes a functional switch from a prooxidant enzyme producing H₂O₂ by oxidative deamination of putrescine to an antioxidant enzyme as soon as H₂O₂ concentrations exceed a certain threshold. The proposed feedback loop would allow the plant to quickly react on increased ROS and NO levels, since no *de novo* synthesis of proteins is required. Furthermore, this mechanism would allow a subtle fine-tuning of the antioxidative response, which is necessary to balance beneficial and harmful effects of ROS and NO. Furthermore, putrescine might act as a mobile signal to indicate the presence of oxidative stress to neighboring cells, since putrescine membrane transporters were found (Fujita and Shinozaki, 2014). In sum, we propose that CuAO8 is critically involved in the maintenance of the ROS and RNS homeostasis in plants, thus reinforcing the link between CuAO activity, putrescine and ROS/NO production.

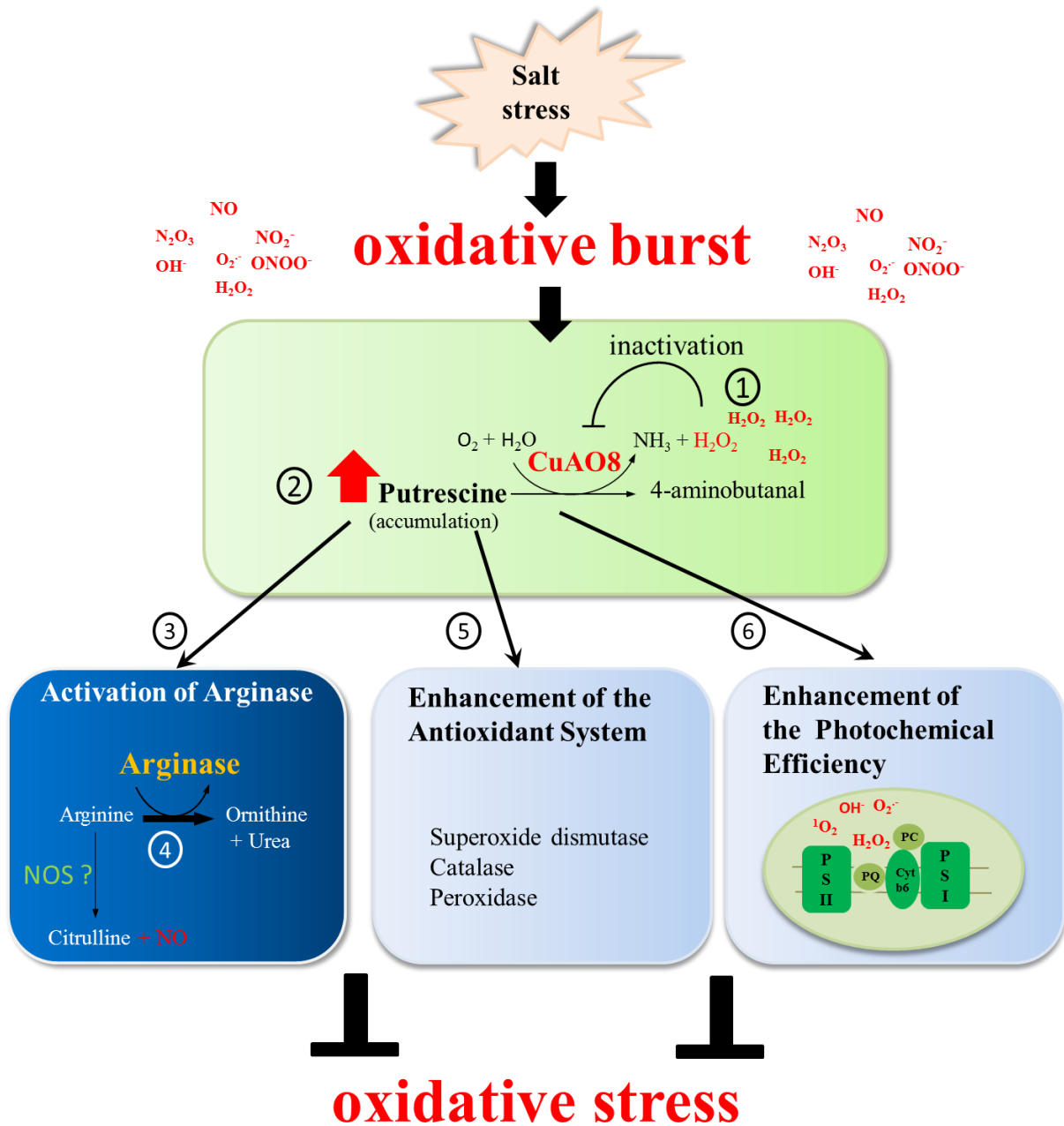


Figure 24: Hypothetical model how CuAO8 might limit the amplitude of the oxidative burst during salt stress. CuAO8 might be involved in the prevention of oxidative stress by several mechanisms: Inhibition of CuAO8 by high H₂O₂ levels (1) results in the accumulation of putrescine (2), which downregulates NO production (3) by enhancing arginase activity (4), activates the antioxidant machinery (5) or enhances photochemical efficiency (6). Together, these effects might prevent harmful overaccumulation of ROS and NO. Details see text. PS: Photosystem; PQ: Plastoquinone; PC: Plastocyanine; NO: Nitric oxide; NOS: Nitric oxide synthase

4. Outlook

Despite intense research during the last decades, one of the most important questions in the plant NO field has not yet been solved: is there a NO production route, which is based on the oxidation of arginine, similar to the catalytic reaction of NOSes in animals? The results from this study demonstrate that arginine availability critically influences NO production during salt stress, clearly arguing for the existence of arginine dependent NO production pathway in plants. Whether arginine is the direct substrate or a precursor for NO production cannot be decided at this stage and needs further research. Moreover, this work demonstrates for the first time a CuAO8-dependent regulatory mechanism for arginase, however the nature of this mechanism could not be completely solved.

Future research should address the following questions: is there a direct CuAO8-arginase interaction, affecting the activity of arginase? Recombinant expression of arginase and thorough biochemical characterization of this enzyme will be important to decide whether the effect of CuAO8 could be mediated indirectly, for instance by enhanced putrescine levels. In this context, analyzing different CuAO mutants will help to establish the molecular mechanism connecting CuAOs, arginase activity and NO production. We suggested a model of how CuAO8 might be involved in the downregulation of the oxidative burst, thereby preventing oxidative stress. To test this model, *in vitro* inactivation of CuAO8 should be tested first. Then, CuAO8 activity at different time points during salt stress could be correlated with putrescine- ROS- and RNS-levels, antioxidant activity and photochemical efficiency. In conclusion, this work establishes an unanticipated link between CuAOs, arginase activity and NO production and provides a new perspective on how NO production might be regulated during salt stress.

5. Material and Methods

5.1 Material

5.1.1 Plant Material

Table 2: Plant Material

Plant line	Plant species	Eco type	source	SALK-Institute identifier	description
Col-0/WT	<i>Arabidopsis thaliana</i>	Columbia			wild type line
25S:nNos2-OX	<i>Arabidopsis thaliana</i>	Columbia	(Shi et al., 2012)		rat neuronal NOS overexpression line 2
nox1/cue1	<i>Arabidopsis thaliana</i>	Columbia	(He et al., 2004)		NO overexpression line 1 /knock-out in a chloroplast phosphoenolpyruvate/phosphate translocator
noa1/nos1	<i>Arabidopsis thaliana</i>	Columbia	(Guo et al., 2003)		NO-associated 1 knock-out line
GLB1-OX	<i>Arabidopsis thaliana</i>	Columbia	Hebelstrup K, MBG, Aarhus Univ.		hemoglobin 1 overexpression line
aoa1	<i>Arabidopsis thaliana</i>	Columbia	SALK Institute	SALK_018100	knock-out of aldehyde oxidase 1
aoa2	<i>Arabidopsis thaliana</i>	Columbia	SALK Institute	SALK_104895	knock-out of aldehyde oxidase 2
aoa3	<i>Arabidopsis thaliana</i>	Columbia	SALK Institute	SALK_072361	knock-out of aldehyde oxidase 3
aoa4	<i>Arabidopsis thaliana</i>	Columbia	SALK Institute	SALK_037365	knock-out of aldehyde oxidase 4
xdh1	<i>Arabidopsis thaliana</i>	Columbia	SALK Institute	SALK_148366	knock-out of xanthine dehydrogenase 1
xdh2	<i>Arabidopsis thaliana</i>	Columbia	SALK Institute	SALK_015081	knock-out of xanthine dehydrogenase 2
cyt red p450	<i>Arabidopsis thaliana</i>	Columbia	SALK Institute	SALK_152766	knock-out of NADPH-cytochrome P450 reductase
pao1	<i>Arabidopsis thaliana</i>	Columbia	SALK Institute	SALK_013026	knock-out of polyamine-oxidase 1
pao2	<i>Arabidopsis thaliana</i>	Columbia	SALK Institute	SALK_046281	knock-out of polyamine-oxidase 2

<i>pao4</i>	<i>Arabidopsis thaliana</i>	Columbia	SALK Institute	SALK_133599	knock-out of polyamine-oxidase 4
<i>pao5</i>	<i>Arabidopsis thaliana</i>	Columbia	SALK Institute	SALK_053110	knock-out of polyamine-oxidase 5
<i>pao6</i>	<i>Arabidopsis thaliana</i>	Columbia	SALK Institute	SAIL_92_E04	knock-out of polyamine-oxidase 6
<i>pao7</i>	<i>Arabidopsis thaliana</i>	Columbia	SALK Institute	SALK_058610	knock-out of polyamine-oxidase 7
<i>cuao1</i>	<i>Arabidopsis thaliana</i>	Columbia	SALK Institute	SALK_206657	knock-out of copper amine oxidase 1
<i>cuao2</i>	<i>Arabidopsis thaliana</i>	Columbia	SALK Institute	SALK_012167	knock-out of copper amine oxidase 2
<i>cuao3</i>	<i>Arabidopsis thaliana</i>	Columbia	SALK Institute	SALK_095214	knock-out of copper amine oxidase 3
<i>cuao4</i>	<i>Arabidopsis thaliana</i>	Columbia	SALK Institute	SALK_012213	knock-out of copper amine oxidase 4
<i>cuao5</i>	<i>Arabidopsis thaliana</i>	Columbia	SALK Institute	SALK_097684	knock-out of copper amine oxidase 5
<i>cuao6</i>	<i>Arabidopsis thaliana</i>	Columbia	SALK Institute	SALK_124509	knock-out of copper amine oxidase 6
<i>cuao7</i>	<i>Arabidopsis thaliana</i>	Columbia	SALK Institute	SALK_021559	knock-out of copper amine oxidase 7
<i>cuao8-1</i>	<i>Arabidopsis thaliana</i>	Columbia	SALK Institute	SALK_037584	knock-out of copper amine oxidase 8
<i>cuao8-2</i>	<i>Arabidopsis thaliana</i>	Columbia	SALK Institute	SALK_201804	knock-out of copper amine oxidase 8
<i>cuao9</i>	<i>Arabidopsis thaliana</i>	Columbia	SALK Institute	SALK_039444	knock-out of copper amine oxidase 9
<i>atao1</i>	<i>Arabidopsis thaliana</i>	Columbia	SALK Institute	SALK_082394	knock-out in one copper amine oxidase
<i>ldl3</i>	<i>Arabidopsis thaliana</i>	Columbia	SALK Institute	SALK_146733	knock-out in LSD1-like 3 protein
WT	<i>Nicotiana bethamiana</i>				Tobacco wild type

5.1.2 Bacteria

Table 3: Bacteria strains

strain	Chromosomal genotype	source	purpose
<i>E. coli</i> DH5 α	<i>fhuA2 lac(del)U169 phoA glnV44 Φ80'</i> <i>lacZ(del)M15 gyrA96 recA1 relA1</i> <i>endA1 thi-1 hsdR17</i>	Lab	Cloning
<i>E.coli</i> DB3.1	<i>F- gyrA462 endA1 glnV44 Δ(sr1-recA)</i> <i>mcrB mrr hsdS20(r_B⁻, m_B⁻) ara14 galK2</i> <i>lacY1 proA2 rpsL20(Sm^r) xyl5 Δleu</i> <i>mtl1</i>	Lab	Maintaining gateway vectors
<i>Agrobacterium tumefaciens</i> GV3101 pMP90	chromosomal encoded resistance against rifampicin and PTi plasmid encoded resistance against gentamycin (pMP90)		Expression and plant transformation

5.1.3 Kits

Table 4: Applied Kits

Kit name	Company
Amplex Red Hydrogen Peroxide/Peroxidase Assay Kit, No. A22188	ThermoFisher Scientific, Waltham, USA
Arginase Activity Assay Kit, No. MAK112	SIGMA-ALDRICH, St. Louis, USA
Extract-N-Amp TM Plant PCR Kit, No. SLBH0328	SIGMA-ALDRICH, St. Louis, USA
Gateway pENTR TM /D-TOPO, No. K240020	Invitrogen, Karlsruhe, Germany
Gateway [®] LR Clonase TM Enzyme Mix, No.11791-019	Invitrogen, Karlsruhe, Germany
innuPREP Gel Extraction Kit, No. 845-KS-50300	Analytik Jena, Jena, Germany
Mini-PROTEAN [®] TGX TM Precast Gels, No. 4561044	Bio-Rad, Hercules, USA
Nitric oxide sensor (intracellular) Kit (FL2E), No. 96-0396	STREM Chemicals, Newburyport, USA
Plant Total Protein Extraction Kit, No. PE0230	SIGMA-ALDRICH, St. Louis, USA
Plant Cell Viability Assay Kit, No. PA0100	SIGMA-ALDRICH, St. Louis, USA
QIAprep [®] Spin Miniprep Kit, No. 27104	Qiagen GmbH, Hilden, Germany
QIAquick [®] Gel Extraction Kit, No. 28704	Qiagen GmbH, Hilden, Germany
QuantiTect [®] Reverse Transcription Kit, No. 205311	Qiagen GmbH, Hilden, Germany

REDExtract-N-Amp™ Plant PCR Kitm No. XNAP-1KT	SIGMA-ALDRICH, St. Louis, USA
RNeasy® Mini Kit, No. 74104	Quiagen GmbH, Hilden, Germany
RNeasy® Plant Mini Kit, No. 74904	Quiagen GmbH, Hilden, Germany
SensiMix SYBR Low Rox-Kit, No. QT625	Bioline, London, UK
Western Lightning Plus ECL Kit, No. NEL103001EA	Perkin Elmer, Waltham, USA

5.1.4 Buffers and solutions

Buffers and solutions which were included in Kits are not listed.

Table 5: Buffers and solutions

Buffer name	Composition
Amino acid extraction buffer	0.05 M aqueous HCl–ethanol (1:1, v/v) and 10 µl of 1.0 mM d2-Phe as an internal standard (Thiele et al., 2008)
Blocking Buffer	5% BSA in TBST-T
Blot Buffer	1:8 Dilution of 10 x SDS-PAGE running buffer
CuAO8 protein extraction buffer	1x PBS (pH 7.4), 150 mM NaCl, 10% Glycerin, 1% Triton, 1 mM DTT, 1x protease inhibitor cocktail (cOmplete, EDTA free, Roche)
Coomassie R-250 staining solution	0.25% (w/v) Coomassie Brilliant Blue R-250, 50% (v/v) methanol, 10% (v/v) glacial acetic acid
Coomassie R-250 destaining solution	30% (v/v) methanol, 10% (v/v) glacial acetic acid
CTAP buffer	1.4 M NaCl, 100 mM Tris-HCl pH 8, 20 mM EDTA pH 8, 25 (w/v) Cetyltrimethylammoniumbromid, 1% (w/v) Polyvinylpyrrolidone
Desalting buffer	1x PBS (pH 7.4), 150 mM NaCl, 10% Glycerin, 0.1% Triton, 1 mM DTT, 1x protease inhibitor cocktail (cOmplete, EDTA free, Roche), 30 mM Imidazole
Elution buffer Ni-NTA	1x PBS (pH 7.4), 300 mM NaCl, 10% Glycerin, 0.1% Triton, 1 mM DTT, 50-300 mM Imidazole, protease inhibitor cocktail
Infiltration buffer (<i>N. benthamiana</i>)	10 mM MES-KOH pH5.7, 10 mM MgCl ₂
Nitrate reductase extraction buffer	50 mM Hepes-KOH pH 7,5, 0,5 mM EDTA, 100 µM FAD, 5 mM Na ₂ MoO ₄ , 6mM MgCl ₂ , protease inhibitor cocktail (cOmplete, EDTA free, Roche)
Phosphate buffered saline (PBS)	10 mM Na ₂ HPO ₄ , 1.8 mM KH ₂ PO ₄ , 2.7 mM KCl, 137 mM NaCl, pH 7.4
Ponceau S solution	0.5% (w/v) Ponceau S, 1% acetic acid

STM buffer (standard MES puffer)	50 mM MES-KOH, pH 5.7, 0.25 mM KCl, 1 mM CaCl ₂
TBS	50 mM Tris-HCl pH 7.6, 150 mM NaCl
TBST-T	0.05% (w/v) Tween in TBS
Transfer buffer	80% (v/v) Blot buffer, 20% Methanol
Triiodide solution (NO Analyzer)	35 mL glacial acetic acid, 325 mg iodine, 500 mg KI, 10 mL ddH ₂ O

5.1.5 Antibiotics

Table 6: Antibiotics

Antibiotic	Stock concentration	Working concentration
Ampicillin (Amp)	100 mg/mL (in ddH ₂ O)	100 µg/mL
Gentamycin (Gent)	50 mg/mL (Carl-Roth)	25 µg/mL
Kanamycin (Kan)	50 mg/ml in ddH ₂ O	50 µg/mL
Rifampicin (Rif)	50 mg/ml (in Methanol)	50 µg/mL
Spectinomycin (Spec)	100 mg/ml in ddH ₂ O	100 µg/mL

5.1.6 Media

All media were prepared with ddH₂O and autoclaved before use. Plant tissue culture grade chemicals were used.

Table 7: Media

Medium	Composition
LB	1% (w/v) tryptone, 0.5% (w/v) yeast extract, 0.5% (w/v) NaCl, 1.5% (w/v) agar for solid media, <i>adjust to pH 7.0</i>
½ MS	2.2 g/L Murashige-Skoog salts incl. vitamins, 1% (w/v) sucrose, 0.5 g/L MES hydrate, 1.2% (w/v) phytoagar for solid media, <i>adjust to pH 5.7 (with KOH)</i>
RB media	1% (w/v) Tryptone, 0.5% (W/v) yeast extract, 0.5% (w/v) NaCl, 0.2% (w/v) 1 M NaOH
TFB1 (transformation buffer 1)	100 mM RbCl, 50 mM MnCl ₂ , 30 mM C ₂ H ₃ KO ₂ , 10 mM CaCl ₂ , 15% (v/v) Glycerin, <i>adjust to pH 5.8 (with acetic acid)</i>
TFB2 (transformation buffer 2)	10 mM MOPS, 75 mM CaCl ₂ , 10 mM RbCl, 15% (v/v) Glycerin, <i>adjust to pH 6.5 (with KOH)</i>

5.1.7 Chemicals

Common chemicals were purchased from SIGMA-Aldrich, Merck, Duchefa, or Carl-Roth.

Table 8: Chemicals

Chemicals	Company
Agmatine, No. A7127	SIGMA-ALDRICH, St. Louis, USA
Aminoguanidine, No. 396494	SIGMA-ALDRICH, St. Louis, USA
Amplex Red, No. 12222	ThermoFisher Scientific, Waltham, USA
L-Arginine, No. A0704	Duchefa Biochemie, Haarlem, Netherlands
Bradford Reagent, No. 500-0006	Biorad, Germany
Carboxy-PTIO potassium salt (cPTIO), No. C221	SIGMA-ALDRICH, St. Louis, USA
Di-amino-fluorescein diacetate (DAF-FM DA), No. D2321	SIGMA-ALDRICH, St. Louis, USA
1,2-Diaminoheptane, No. D17408	SIGMA-ALDRICH, St. Louis, USA
Diaminorhodamine-4M AM solution (DAR-4M AM), No. D9194	SIGMA-ALDRICH, St. Louis, USA
2',7'-Dichlorofluorescein diacetate (DCF-DA), No. D6886	SIGMA-ALDRICH, St. Louis, USA
2,6-Dichloropyridine-4-carboxylic acid (INA), No. 456543	SIGMA-ALDRICH, St. Louis, USA
Ethanol, Chromasolv®, No. 34852	SIGMA-ALDRICH, St. Louis, USA
9-Fluorenylmethoxycarbonyl chloride (FMOC-Cl), No. 23186	SIGMA-ALDRICH, St. Louis, USA
Hypochloric acid, No. 84415	SIGMA-ALDRICH, St. Louis, USA (Fluka Analytcs)
LiChrosolv® Methanol, No. 1.06007	Merck, Darmstadt, Germany
LiChrosolv® Water, No. 1.15333	Merck, Darmstadt, Germany
Perchloric acid, No. 30755	SIGMA-ALDRICH, St. Louis, USA
Phyto Agar, No. P.1003	Duchefa Biochemie, Haarlem, Netherlands

Propidium iodid, No. P3566	ThermoFisher Scientific, Waltham, USA
Putrescine dihydrochloride, No. P7505	SIGMA-ALDRICH, St. Louis, USA
S-nitrosoglutathione (GSNO), No. N4148	SIGMA-ALDRICH, St. Louis, USA
Spermidine, No. S2626	SIGMA-ALDRICH, St. Louis, USA
Spermine, No. S3256	SIGMA-ALDRICH, St. Louis, USA
Sulfanilamide, No. 8035	Merck, Darmstadt, Germany
N-(1-Naphthyl)ethylenediamine dihydrochloride, No. 222488	SIGMA-ALDRICH, St. Louis, USA
N^o-hydroxy-nor-Arginine (<i>nor</i>-NOHA), No. 10006861	Cayman chemicals, Ann Arbor, USA
N-(3-Triethylammoniumpropyl)-4-(6-(4-(Diethylamino) Phenyl) Hexatrienyl) Pyridinium Dibromide (FM4-64), No. 70021	Biotium, Hayward, USA
SuperBlock Blocking buffer (in TBS), No. 37535	ThermoFisher Scientific, Waltham, USA
2x SDS-loading buffer, No. S3401	SIGMA-ALDRICH, St. Louis, USA
γ-aminobutyric acid, No. A2129	SIGMA-ALDRICH, St. Louis, USA

5.1.8 Antibodies

Table 9: Antibodies

Antibody	species	Dilution	Company
Anti-rabbit-IgG HRP conjugate, No. W401B	mouse	1:2500	Promega, Fitchburg, USA
Anti-mouse2a-IgG-HRP	rat	1:1000	produced by Core Facility Monoclonal Antibody Development, Helmholtz-Zentrum München, Germany
Anti-His6-tagged protein, ab137839	rabbit	1:5000	Abcam, Cambridge, UK
Anti-CuAO8	mouse	1:10	produced by Core Facility Monoclonal Antibody Development, Helmholtz-Zentrum München, Germany

5.1.9 Resins, columns, membranes

Table 10: Resins, columns, membranes

Product	Company
ZebaSpin™ spin columns, No. 10280584	ThermoFisher Scientific, Waltham, USA
Ni-NTA Agarose, No. 30210	Quiagen, Hilden Germany
Amersham protran Nitrocellulose membrane, No. 10600007	GE Healthcare, Freiburg, Germany
Amicon ultra -0.5mL, UFC 501024	Merck, Darmstadt, Germany

5.1.10 Enzymes

Table 11: Enzymes

Enzyme	Company
iProof High-fidelity™ Phusion Polymerase, No. 1725300	Bio-Rad, Munich, Germany
NcoI Fast Digest, No. FD0573	ThermoFisher Scientific, Waltham, USA
PstI Fast Digest, No. FD0614	ThermoFisher Scientific, Waltham, USA

5.1.11 Vectors

Table 12: Vectors

Vector	Company/source
pENTR/D-TOPO	ThermoFisher Scientific, Freiburg, Germany
pK7WGF2	Helmholtz-Zentrum München, lab ware
3'-provector module pICH11599	magnICON®, Bayer Crop Science, Monheim, Germany
integrase vector pICH14011	magnICON®, Bayer Crop Science, Monheim, Germany
5'-provector module pICH17388	magnICON®, Bayer Crop Science, Monheim, Germany

5.1.12 Oligonucleotides

Primer used for cloning:

Table 13: Oligonucleotides

name	Primer forward 5' -> 3'	Primer reverse 5' -> 3'	purpose
<i>CuAO8</i>	caccATGGCTCAAGTTCACTT AACCATT	TTATTCGTTCTTCGTAGTACACT TTGG	Cloning of <i>CuAO8</i> in pENTR/D-Topo
<i>CuAO8-SerGly-His (6x)</i>	AAAAAaccATGGCTCAAGTTC ACTTAACCATT	AAAAAACTGCAGTTAATGGTG ATGGTGATGGTGGCCACTTCCG CTGCCTTCGTTCTTCGTAGTAC ACTTTGG	cloning of <i>CuAO8</i> in pICH11599 (magnICON®)

Primer used for quantitative PCR:

Designed with QuantPrime software, <http://www.quantprime.de> (Arvidsson et al., 2008):

name	Primer forward 5' -> 3'	Primer reverse 5' -> 3'	Amplicon size
<i>ARGH1</i>	TGAAGCTGGTGATGGAAGAG GAAC	TCCTCCAAGTTTCTCCGAAACAGC	104
<i>ARGH2</i>	CACGGGTTCTAACTGATGTTG GG	AACGGACGCAATGGTTCCTC	133
<i>CuAO1</i>	TTAGGGTCGAAGATGGGCAT TTG	ATCACACTTCTTGGTTCACCTGTC	133
<i>CuAO8</i>	CATTAGCCGTATGGTCCCAA AGAG	TTGGTTGGCCGAAGTTCAAAGC	148
<i>NIA1</i>	CTGAGCTGGCAAATCCGAA GC	TGCGTGACCAGGTGTTGTAATC	95
<i>NIA2</i>	AACTCGCCGACGAAGAAGGT TG	GGGTTGTGAAAGCGTTGATGGG	123
<i>UBIQUITIN 5</i>	GGTGCTAAGAAGAGGAAGAA G	CTCCTTCTTTCTGGTAAACGT	240
<i>S16</i>	TCTGGTAACGAGAACGAGCA C	TTTACGCCATCCGTCAGAGTAT	186
<i>TUBULIN 9</i>	GTACCTTGAAGCTTGCTAATC CTA	GTTCTGGACGTTTCATCATCTGTTC	184

Primer used for genotyping obtained from SALK-institute:

iSect Primers tool: <http://signal.salk.edu/tdnaprimers.2.html>

plant line	LP Primer	RP Primer
<i>aaol</i>	TGCTCACAGTGTGTTGTTTTGC	GCGCGAATTAAGGGTATAAAGG
<i>aaol2</i>	ACTGCATGGGAGTGTCTTTTTG	GAGGTTTTGGAGGGAAATCTG
<i>aaol3</i>	TTCTATTGGAAATGCATTGCC	TAAAACATCGGATGAACCTCG
<i>aaol4</i>	TCTTTGCAGCTTAAATGGGTG	GGAAGAAGCAATCCACCTAGG
<i>xdh1</i>	ATTCAAAGAATCGCAGCTGAG	GCGTTCCTTTTCCAGATATC
<i>xdh2</i>	ATTGGCATAACGCAGAGACAAC	GATTAAGGAAGGTGCTCCTGG
<i>cyt red p450</i>	ATTTGACATTGCTGGAAGTGG	TCAGTACCCAGCAAAAACACC
<i>pao1</i>	AAATGGCTGAGGAATTTCTCG	AAGCTTGAGAGGAGAGCAAGC
<i>pao2</i>	CACTTTTTGCAAGCTTGGTTTC	TCAATCCAGTTGAATAAGCGC
<i>pao4</i>	ATTCCCATGCATGTCAAAAAG	TCGTTTGCTCAATTATTTCCG
<i>pao5</i>	TGAGCCTTCCATTGTTGAATC	TGGGTTCTATGTGTTGCTTCC
<i>pao6</i>	CGGCACATCATTAGAAATTC	ATGCTGACCAGAATGTGGTTC
<i>pao7</i>	TACTCGAGGCTTCTTCAGGTG	ATGCTGACCAGAATGTGGTTC
<i>cuao1</i>	TTTTATCTGCTGTCTTTCCGG	CGAAAATCTCGGGTAGGAAAC
<i>cuao2</i>	CAACTGTTGGTTTGCTTTTTGC	CACGATTTACGTGATTCATG
<i>cuao3</i>	GTAGGATGGGAAAATCGAAGC	CAAGGAGCGATTCTGTTTCAC
<i>cuao4</i>	GCAATATGCTTTCTGTGTTTGTG	CCTAATGCTAAGGGAACCGAG
<i>cao5</i>	AAACAAAATCCCCCAAATG	TAGTTCCCAACAGAACATGCC
<i>cuao6</i>	TAAATAGTAGGGGGCATTGCC	TATACTTGTGCATTCCCTCCG
<i>cuao7</i>	ACCACTCATTGCTGGACAATC	TTTCGGTTTTTACAATGTTCC
<i>cuao8-1</i>	CCCTAAAACCCTCTTGGTGAC	TCGTCATTCTTCAATTGGTC
<i>cuao8-2</i>	AAACTAGGCTTGAGAGCGGAG	ATTCATCGAATGATGAGCTGG
<i>cuao9</i>	TCTCTATCCCTGCATCACACC	TATCTTTGAGAGTTACGCCGG
<i>ataol</i>	ACGTTTCATGGACATTGGAGAG	ATCACTATAAAAACCCACCGGC
<i>ldl3</i>	AGAAAGCCTTGCTCATTCTCC	CTCAGAACCCTACCAAGGAC

5.1.13 General Instruments

Table 14: General instruments

Instrument	Type	Company
Autoclave	D-150	Systec, Puchheim, Germany
Balance	CPA225D	Sartorius, Göttingen, Germany

Centrifuge	Mikro220R	Hettich, Tuttlingen, Germany
	RC26+	Sorvall, Freiburg, Germany
	Rotanta 460R	Hettich, Tuttlingen, Germany
Camera	Powershot G2	Canon, Tokyo, Japan
DNA Electrophoresis Unit		Peqlab, Erlangen, Germany
Gel Documentation	MegaCapt	Vilber, Eberhardzell, Germany
Homogenizer	Silamat S6	Ivoclar vivadent, Ellwangen, Germany
Incubator	Innova4340	New Brunswick Scientific, Nürtingen, Germany
	G25	New Brunswick Scientific, Nürtingen, Germany
NO-Analyzer	Sievers 280i	GE Healthcare, Freiburg, Germany
pH measurement	pH523	WTW, Weilheim, Germany
Protein Electrophoresis system	Mini-PROTEAN Tetra system	Bio-Rad, Munich, Germany
Protein Blotting system	SemiDry Electroblotter	Sartorius, Göttingen, Germany
Rotors (for RC26+)	GS-3	Sorvall, Freiburg, Germany
	SS34	Sorvall, Freiburg, Germany
Scanner	Image Scanner II	GE Healthcare, Freiburg, Germany
Shaker	Polymax 1040	Heidolph, Schwabach, Germany
Spectrophotometer	DU 640	Beckmann, Hamburg, Germany
	NanoDrop ND-1000	NanoDrop Technologies, Freiburg, Germany
	Infinite M1000 Pro	Tecan, Männedorf, Suisse
Thermal cycler	T100	Bio-Rad, Munich, Germany
	PTC-200	
Real time thermal cycler	ABI 7500 Fast	Applied biosystems, Freiburg, Germany
UltraPure water system	UltraClear	Siemens, Munich, Germany
Transilluminator	UV Transilluminator	UVP, Inc, Jena, Germany

5.1.14 Webtools and software

PCR-Miner <http://ewindup.info/miner/> (qPCR data management)

Quant prime <http://www.quantprime.de/?page=registration> (qPCR Primer design tool)

ImageJ 1.46r of the National Institutes of Health, USA (microscopy picture management)

Adobe Photoshop CS6 Extended (microscopy picture management)

iSect Primer tool <http://signal.salk.edu/tdnaprimers.2.html> (T-DNA primer selection)

SigmaPlot 12 (Graphs)

PubMed www.pubmed.com (Literatur)

Mendely Desktop, <https://www.mendeley.com/> (source management)

TargetP <http://www.cbs.dtu.dk/services/TargetP/>

UniProt server <http://www.uniprot.org/uniprot/>

5.2 Methods

5.2.1 Plan cultivation

5.2.1.1 *Cultivation on soil*

Seeds were sown on soil mixed with sand in a 5:1 ratio. After two days of stratification at 4°C, plants were grown under long-day (14 h light/10 h dark) or short-day (10 h light/ 14 h dark) conditions. Temperatures were 20°C during the day and 18°C during the night, with relative humidity's of 70 and 50 %, respectively. Plants were covered with plastic foil during the first week to ensure high humidity and proper growth. Plants were bottom-up watered three times a week.

5.2.1.2 *Cultivation under sterile conditions*

Seeds were sterilized with hypochloride gas for 3 h and distributed on ½ MS plates. After two days of stratification at 4°C in the dark the plates were placed in long-day (14 h light/10 h dark) or short-day (10 h light/ 14 h dark) conditions.

5.2.2 General NaCl treatment of five day old seedlings

Five days old seedlings, grown on ½ MS-plates under short-day, were harvested and washed twice with STM buffer (50 mM MES-KOH, pH 5.7, 0.25 mM KCl, 1 mM CaCl₂) to remove remaining solid media. Seedlings were then distributed and transferred to STM buffer (control) and STM buffer containing 200 mM NaCl (treatment) for 6 h in the dark. After the treatment the seedlings were washed once with STM buffer to remove remaining NaCl and then once with ddH₂O (to prevent a disturbance of the STM buffer on the follow up analysis). For a zero time point only the washing steps were performed. Finally, 100 or 200 mg of seedlings were frozen in liquid N₂ and stored at -80°C.

5.2.3 Molecular methods

5.2.3.1 *Genomic DNA isolation (CTAP method)*

Plant tissue was ground to a fine powder and 250 µl of 2% CTAB buffer (1.4 M NaCl, 100 mM Tris-HCl, 1% (w/v) Cetyltrimethylammoniumbromid, 20 mM EDTA pH 8.0, 1%

(w/v) polyvinylpyrrolidone) was added. After incubation for 15 to 30 min at 65°C, the sample was mixed with 200 µL Chloroform:Isoamylalcohol (24:1 ratio) by vortexing, followed by phase separation through centrifugation for 2 min at 14000 rpm and 4°C. 200 µL of the supernatant was transferred to a new E-cup with already provided 1% linear polyacrylamide. Then, 600 µL Ethanol (100%, p.A.) was added, mixed well and incubated for at least 20 min at -20°C. After centrifugation for 15 min at 13 000 rpm and 4°C the DNA pellet was washed with 70% Ethanol and after an additional centrifugation and washing step the pellet was dried at 37°C for 30 min. The DNA was dissolved in 100 µL ddH₂O at 37°C for 10 min and stored at -20°C for further use. For PCR an aliquot of 2 µL DNA was used.

5.2.3.2 RNA extraction and cDNA synthesis

RNA was extracted from 50–100 mg of seedlings using the RNeasy Plant Mini Kit (Quiagen) according to the manufacturer's instructions. 1 µg of total RNA was then used as input for reverse transcription using the QuantiTect® Reverse Transcription Kit (Quiagen). Concentration and purity of cDNA was estimated by spectrophotometry (NanoDrop, ND-1000).

5.2.3.3 Polymerase chain reaction

GOI were amplified from cDNA (50 ng) or plasmid (1 ng) using corresponding primer pairs and the suitable annealing temperatures and elongation times in a total volume of 25-50 µL. In most of the cases the iProof Polymerase (Bio-Rad) was used, which needs 15–30 seconds/kb. Sufficient amount of DNA was obtained after 25–35 cycles. PCR samples were purified by Gel-extraction and the concentration was measured by spectrophotometry (NanoDrop).

5.2.3.4 BP reaction Gateway system

150 ng of donor vector (pDONR221) were incubated with 50 fmol of attB-sites containing PCR product (ensuring a molar 1:1 ratio) together with 1 µL BP Clonase and 1 µL BP clonase buffer in a total reaction volume of 5 µL overnight at 25°C (in a thermomixer with heated lid). BP reaction was stopped by adding Proteinase K and incubating for 10 min at 37°C. 1 2 µL of the reaction was transformed into *E. coli* DH5α. A selection of grown colonies were picked and grown in 3 mL of LB medium with appropriate antibiotics at 37°C overnight. After plasmid purification the presence of the insert was verified by PCR.

5.2.3.5 LR reaction Gateway system

100 ng of entry clone was incubated with an equal molar amount of destination vector and 1 µL of LR clonase and 1 µL of LR clonase buffer in a total reaction volume of 5 µL. After 3-5 hours, LR reaction was stopped by incubating with Protease K (37°C, 10 min). 1-2 µL of the reaction was transformed into *E. coli* DH5α. Five colonies were picked and grown in 3 mL of LB medium with appropriate antibiotics at 37°C overnight. The plasmid was isolated and the concentration was determined by spectrophotometry. Plasmids were sequenced (Eurofins MWG) and stored at -20°C.

5.2.3.6 Restriction digest

Restriction sites were added at the 5' ends of the PCR primers to allow for subsequent conventional sticky end cloning. 1 µg of PCR product was incubated with 1 µL of each restriction enzyme (ThermoFisher Scientific, Fast Digest) in a total reaction volume of 30 µL using the appropriate buffer system. After 2 h typically at 37°C, the sample was subjected to 1% agarose gel electrophoresis to deactivate the enzymes and purify the DNA by gel extraction.

5.2.3.7 Ligation

Vector and insert (both cut with the same restriction enzymes) were incubated in a molar 1:4 ratio together with 1 µL T4 Ligase and 1 µL T4 ligase buffer (containing ATP) in a total reaction volume of 10 µL overnight at 16°C. 1-2 µL of the reaction was transformed into *E. coli* DH5α. Five colonies were picked and grown in two 3 mL of LB medium at 37°C overnight. The plasmid was isolated and the concentration was determined by spectrophotometry. Plasmids were sequenced (Eurofins MWG) and stored at -20°C.

5.2.3.8 Plasmid isolation

Plasmid isolation of transformed bacteria was performed with the QIAprep Spin Miniprep Kit (Quiagen). The manufactures instructions were followed and the plasmid DNA concentration was measured by spectrophotometry (NanoDrop).

5.2.3.9 Agarose-gel electrophoresis

DNA samples were separated by size using 1% agarose gels (1g of highly pure agarose in 100 mL of TAE buffer) supplemented with ethidium bromide. Gels were run at 120 V for 30–45 min. DNA was visualized on a UV transilluminator (BioRad).

5.2.3.10 Extraction of DNA from Agarose Gels

Gel extraction of DNA was performed using the QIAquick[®] Gel Extraction Kit (Quiagen) or with the innuPREP Gel Extraction Kit (Analytic Jena) according to the manufacturer's instructions.

5.2.3.11 Preparation of chemically competent *E. coli* DH5α cells

250 mL of RB media were inoculated with 2.5 mL overnight culture and grown at 37°C under continuous shaking (300 rpm) until an OD₆₀₀ 0.4-0.6. The cells were harvested by centrifugation at 3800 rpm at 4°C for 5 min and the pellet was resuspended in 100 mL ice cold TFB1 buffer (100 mM RbCl, 50 mM MnCl₂, 30 mM C₂H₃KO₂, 10 mM CaCl₂, 15% (v/v) Glycerin, pH 5.8 (with acetic acid)). After 5 min incubation on ice and a centrifugation step (3800 rpm, 4°C, 5 min), the pellet was resuspended in 10 mL TFB2 buffer (10 mM MOPS, 75 mM CaCl₂, 10 mM RbCl, 15% (v/v) Glycerin, pH 6.5 (with KOH)). The suspension was stored in ice for 60 min, aliquoted (50 µL), frozen in liquid N₂ and stored at -80°C.

5.2.3.12 Preparation of electro competent *A. tumefaciens* GV3101 pMP90

300 mL LB media were inoculated with a 2 mL overnight culture of *A. tumefaciens* and grown at 28°C under continuous shaking until an OD₆₀₀ 0.5-0.7. Afterwards the bacteria

culture was cooled for 30 min on ice, centrifuged at 4°C for 20 min at 4000 rpm and the pellet was resuspended in ice cold 125 mL ddH₂O. The suspension was stored on ice for 60 min and again centrifuged. Subsequently, the pellet was resuspended in 3 mL ice cold 15% (v/v) Glycerol, aliquoted (50µL), frozen in liquid N₂ and stored at -80°C

5.2.3.13 Transformation of chemical competent *E. coli* DH5α

1-2 µL of DNA sample (BP, LR, Ligation sample) were added to 50 µL of chemically competent cells. Mixing was achieved by gently tapping the reaction vessel. After 30 min incubation on ice, a heat-shock was performed (45 seconds at 42°C) and 500 µL of non-selective LB was added. After shaking for 1-1.5 h at 37°C, the bacteria solution was centrifuged (3 min, 8000 rpm) and the pellet was resuspended in 200 µL of LB media. The transformed *E. coli* DH5α sample was plated on selective media and grown overnight at 37°C.

5.2.3.14 Transformation of electro competent *A. tumefaciens* GV3101 pMP90

For electroporation, a 50 µL aliquot of competent *A. tumefaciens* was de-frozen on ice and 100 ng of the purified plasmid DNA was added. After 2 min on ice, the cell-DNA mixture was transferred to a pre-cooled electroporation cuvette (Bio-Rad, distance electrodes: 0.2 cm). The electroporation was performed with the Electroporator Gene Pulser (Bio-Rad) with 25 µFD capacitance, a volt impulse of 1,25 kV and a pulse of 400 Ω. Immediately afterwards 500 µL of LB media were added, the suspensions transferred to an E-cup and grown for 1-1.5 h at 28°C under continuous shaking (300 rpm). After centrifugation (3 min, 8000 rpm) the pellet was resuspended in 200 µL of LB medium, plated on selective LB media and grown for 2 days at 28°C.

5.2.3.15 Quantitative PCR

RNA und cDNA were prepared as described (see 4.2.3.2) and the cDNA was diluted 1:20. Because relative quantification was applied, three housekeeping genes were decided to use as reference: Ubiquitin5, S16 and Tubulin9. The corresponding primer as already been tested in the group of PD. Dr. Anton Schäffner (Helmholtz-Zentrum München).

Primer design

Primer pairs for detection of *ARGH1* and 2, *NIA1* and 2 mRNA were designed by using the QuantPrime software (Arvidsson et al., 2008) (<http://www.quantprime.de/>) based on the TAIR release 10. The primer pairs discriminated splice variants and span exon-exon borders to exclude amplification of genomic DNA.

qPCR performance

The qPCR was performed with Applied Biosystems 7500 and the Sequence Detection software 1.3.1 from Applied Biosystems. Analysis was done with PCR-Miner software: <http://ewindup.info/miner/> (Zhao and Fernald, 2005). Efficiency corrected CT values ((1+E)^{-CT}) were normalized against the geometric mean of the reference genes.

The PCR mixture contained the following:

component	volume [μ L]	final concentration
2x SensiMix® SYBR Low ROX Mastermix (Bioline)	12.5	1x
Primer forward	0.625	250 nM
Primer reverse	0.625	250 nM
H₂O	7.25	
cDNA	4	
	total 25	

Cycling conditions were:

Step	temperature	duration	cycles
Initial denaturation	95°C	15 min	1x
Denaturation	95°C	15 sec	} 40x
Annealing	60°C	30 sec	
Extension	72°C	45 sec	

5.2.4 Phenotyping methods

5.2.4.1 Flowering time

Flowering time was determined following the protocol found in the book: *Arabidopsis – A laboratory manual* (Weigel & Glazebrook, 2001). In brief: Each genotype was grown in a single pot and the pots with different genotypes were randomly placed in one tray. The tray was rotated every second day and the flowering time was characterized by counting the days when the stem height reached 1 cm and the day when the first white flower appeared.

5.2.4.2 Primary root growth

Plants were grown on vertical ½ MS plates (1% sucrose, 1,25% phytoagar) as well as ½ MS plates supplemented with either 1 mM Arginine, 1 mM GABA or 50 μ M GSNO. They were placed for two days in the dark at 4°C for stratification. Afterwards the plates were transferred to long day conditions and after 8, 11 and 15 days the plates were scanned with high resolution and the root length was measured using ImageJ software.

5.2.4.3 Chlorophyll breakdown

Chlorophyll breakdown was observed according to (Liu and Guo, 2013). Fully expanded rosette leaves of 5 week old plants (grown in short day) were detached and distributed in square petri dishes outlaid with two layers of whatman paper soaked with ddH₂O. Petri dishes

were wrapped with alufoil and kept in the dark at RT. Photos were made every second day controlling visible chlorophyll breakdown

5.2.5 Biochemical methods

5.2.5.1 SDS-Page

Proteins were separated by SDS-PAGE on precast 12% polyacrylamide gels (Mini-PROTEAN® TGX™ Precast Gels, Bio-Rad) in standard 1x SDS running buffer (Bio-Rad) on a Mini-PROTEAN Tetra cell system for 45 min at 200 V. Gels were stained with Coomassie (0.25% (w/v) Coomassie Brilliant Blue R-250, 50% (v/v) methanol, 10% (v/v) glacial acetic acid) for 1h and de-stained in (30% (v/v) methanol, 10% (v/v) glacial acetic acid).

5.2.5.2 Western Blot

Proteins were separated on 12% polyacrylamide gels and transferred to a nitrocellulose membrane (Amersham Protran, 0.45 µM NC, GE Healthcare) using a semi-dry western blot procedure. The membrane and the gel were sandwiched from the anode to the cathode: 6x whatman paper, nitrocellulose membrane, SDS-Gel, 3x whatman paper. Whatman paper and nitrocellulose membrane were pre-wetted in transfer buffer (80% (v/v) blot buffer, 20% methanol). Blotting was performed for 60 min (depending on the size of the protein of interest) at 2.5 x a x b mA, where a and b represent the dimensions of the membrane (blot buffer: 1:8 dilution 10x SDS-running buffer with ddH₂O). The membrane was stained by Ponceau Red solution to verify efficient transfer and blocked by incubation in blocking buffer (5% BSA in TBST, TBST: 0.05% (w/v) Tween-20 in TBS) for 1h at RT under moderate shaking. If tobacco protein samples were blotted, the membrane was blocked with SuperBlock Blocking buffer (ThermoFisher Scientific) for 1h at RT under moderate shaking. The primary antibody (diluted in 5% BSA in TBS-T) was added and incubated overnight at 4°C with continuous shaking. The membrane was washed 3x in 20 mL TBS-T and the secondary antibody (diluted in 5% BSA in TBS-T) was added. After 1 h the membrane was washed 3x for 5 min with 20 mL TBS-T and one time with 20 mL TBS. The signal was developed using the Western Lightning *Plus* ECL Kit (Perkin Elmer) according to the manufacturer's instructions.

5.2.5.3 Determination of protein concentration with Bradford

Protein concentration in extracts was estimated by Bradford Assay (Bradford, 1976). Briefly, 1 – 5 µL of protein extract were incubated with Bradford reagent (BioRad) in a total reaction volume of 1 mL. After 15 min, the absorption at 595 nm was measured in a spectrophotometer. Standard curves were recorded by measuring the absorbance for different amounts of BSA (1-10 µg).

5.2.5.4 Total protein extraction for CuAO8 knockout analysis

For extraction of total protein of plant tissue the Plant Total Protein Extraction Kit (Sigma-Aldrich) was applied. The protocol was performed after manufacturer's instructions. The protein samples were stored at -80°C until further analysis. This method was only used for testing the CuAO8 knockout in four week old *A. thaliana* leaves. For total protein extraction of *N. benthamiana* leaves see 5.2.5.10

5.2.5.5 *Determination of putrescine, spermidine and spermine contents by HPLC*

To quantify the levels of free putrescine, spermidine and spermine in five day old seedlings, a pre-column derivatization of polyamines (PA) was applied. Here, 9-fluorenylmethyl chloroformate (FMOC-Cl) reacts with the primary and secondary amine groups of the PAs, forming a stable fluorescent derivative detectable with UV light (Fellenberg et al., 2012).

Polyamine extraction:

Free putrescine, spermidine and spermine were extracted by grinding of 100 mg liquid nitrogen frozen plant material (five day old seedlings), addition of 1 mL of 5% PCA (Sigma-Aldrich) and vortexing for 15 sec. Afterwards, the samples were incubated in the dark at RT for 1 h, with periodic vortexing for 15 sec every 20 min. Then, the samples were centrifuged at 14 000 rpm for 10 min. The supernatant was transferred to a new E-cup and again centrifuged at 14 000 rpm for 10 min. The supernatant was then transferred in a fresh tube and stored at -80°C for further analysis.

Derivatization procedure:

For standard curve preparation, putrescine dihydrochloride, spermidine and spermine (Sigma-Aldrich) were serially diluted in 5% PCA from $51.2\ \mu\text{M}$ to $0.4\ \mu\text{M}$ ($51.2\ \mu\text{M}$, $25.6\ \mu\text{M}$, $12.8\ \mu\text{M}$, $6.4\ \mu\text{M}$, $3.2\ \mu\text{M}$, $1.6\ \mu\text{M}$, $0.8\ \mu\text{M}$, $0.4\ \mu\text{M}$). Then, $15\ \mu\text{L}$ of the tested plant extract or polyamine standard solution was processed in the following order: First, $360\ \mu\text{L}$ of $0.1\ \text{M}$ NaHCO_3 containing internal standard (1,7 Diaminoheptane; $10^{-7}\ \text{M}$, Sigma-Aldrich) was pipetted, second $100\ \mu\text{L}$ of acetone and afterwards $200\ \mu\text{L}$ of $6\ \text{mM}$ FMOC-Cl (in acetone) was added. The tube was inverted ten times, incubated for 5 min at RT followed by 10 min at 50°C in a water-bath and subsequently 5 min at -20°C . Then, $300\ \mu\text{L}$ of methanol was added and the sample was transferred in a HPLC vial (Carl Roth).

Detection with HPLC:

The HPLC measurement was conducted with a Beckman System Gold HPLC system equipped with a Shimadzu RF 10AxL fluorescence detector (excitation: 260 nm, emission: 313 nm; sensitivity x 32). The data was acquired and processed using Karat software 8.0. The reversed phase column (Luna $5\ \mu\text{m}$ $100\ \text{\AA}$ C18(2) $250 \times 4.6\ \text{mm}$ column, Phenomenex) was operated at 20°C with a flow rate of 1 ml/min. One cycle of the run included a water (solvent A) to methanol (solvent B, LiChrosolv®) solvent gradient from 80% to 100% methanol over 30 min. Then, 6 min 100% methanol followed by a re-equilibration of the column for 3 min to a 80% water to methanol solvent gradient (0-30 min 80-100% B, 30-36 min 100% B, 36-42 min 100-80% B, 42-45 min 80% B). The peaks were identified by comparison with the retention times of the applied standards (putrescine dihydrochloride: 16.5 min, 1,7 diaminoheptane: 19.8 min, spermidine: 26.8 min, spermine: 33.8 min)

5.2.5.6 *Amino acid analysis by LC-MS-MS*

Proteinogenic amino acids were measured by Dr. Björn Thiele (Institute of Bio- and Geosciences (IBG-2/BioSpec), Forschungszentrum Jülich) according to Thiele et al., 2008.

The extraction was conducted from 100 mg of five day old seedlings homogenized with an aqueous HCl-ethanol mixture containing an internal standard (d_5 -Phe, kindly provided by Dr. Björn Thiele). After incubation on ice and subsequent centrifugation, the supernatant transferred to a new E-cup, centrifuged again and the supernatant was analyzed with liquid chromatography electro spray ionization tandem mass spectrometry technique (LC-ESI-MS-MS) in the positive mode.

5.2.5.7 *Measurement of nitrite and nitrate contents*

The nitrite (NO_2^-) and nitrate (NO_3^-) content in five day old seedlings was determined with the Nitric Oxide Analyzer Sievers 280i from GE Healthcare (liquid program), which detects nitric oxide gas by oxidizing NO with internally produced ozone to NO_2 (excited state) and O_2 . During relaxation to its ground state, NO_2 emits a photon which is detected by a photomultiplier. For nitrite detection, NO_2^- was reduced to NO by I_3^- (Triiodide, 30°C vessel temperature) whose reducing power is not sufficient to reduce NO_3^- . For nitrate detection, NO_3^- was reduced using VCl_3 (Vanadium chloride, 90°C vessel temperature) and the previously measured amount of NO_2^- was subtracted. The areas of the resulting chemoluminescence peaks were measured and the contents were quantified using previously prepared calibration curves with sodium nitrite and sodium nitrate.

To quantify the nitrogen content in seedlings, 200 mg of five day old seedlings were ground to a fine powder, 500 μL of 1x PBS was added and then incubated on ice for 10 min with periodic vortexing. After centrifugation at 4°C for 10 min with maximum speed in a tabletop centrifuge, the supernatant was used for further analysis. The $\text{NO}_2^-/\text{NO}_3^-$ content was normalized to the protein content in the supernatant measured with Bradford reagent.

5.2.5.8 *Nitrate reductase activity measurement*

The nitrate reductase (NR) activity was measured as the rate of NO_2^- production determined with a spectrophotometric assay. Nitrite was detected using sulfanilamide and N(-)1-(naphthyl)-ethylene-diamine-dihydrochloride, resulting in the formation of a complex which displays an absorption maximum at 540 nm (Foyer et al., 1998; Frungillo et al., 2014). All samples were protected from light during the assay. To measure the NR activity, 100 mg of five day old seedlings were ground to a fine powder, 400 μL of extraction buffer was added (50 mM HEPES-KOH pH 7.5, 0.5 mM EDTA, 100 μM FAD, 5 mM Na_2MoO_4 , 6 mM MgCl_2 , protease inhibitor cocktail (cOmplete, EDTA free, Roche)) and the homogenate was kept on ice for 10-15 min with periodic vortexing. After centrifugation at full speed with a tabletop centrifuge for 10 min at 4°C, the supernatant was transferred to a new E-cup and centrifuged again. This supernatant was rebuffered using 10K Amicon Ultra 0.5 centrifugal filter units (Millipore). The protein extracts were aliquoted and frozen at -80°C after measuring the protein concentration with Bradford reagent. The protein activity assay was performed in a clear 96-well plate (Greiner) in a total reaction volume of 200 μL . First, 20 μL of the protein extracts were incubated with 80 μL extraction buffer supplemented with 1 mM KNO_3 , 1 mM NADH and either 2 mM EDTA or 6 mM MgCl_2 for 55 min at RT with gentle shaking. Then, 100 μL of a 1:1 mixture of 1% sulfanilamide ([w/v], in 1.5 M HCl) and 0.02% N(-)1-naphthyl)-ethylene-diamine-dihydrochloride ([w/v], in 1.5 M HCl) was added. After incubation for 15 min at RT with gentle shaking, the absorbance at 540 nm was measured and the

activity was calculated. The activity measured in the presence of EDTA represents the total NR activity and the activity measured in the presence of MgCl₂ represents the actual NR activity.

5.2.5.9 *Transient protein expression of CuAO8-His₆ in N. benthamiana*

The transient expression and subsequent purification of CuAO8-His (6x) was achieved with the modular transfection system magnICON® (Bayer CropScience GmbH, formerly ICON Genetics). It is a vector system based on the tobacco mosaic virus (TMV) and delivered by *A. tumefaciens* to the host plant. This system provides vectors which are optimized for cell to cell movement of the formed active replicons for efficient plant infection in *N. benthamiana* (Marillonnet et al., 2005). The system consists of three modules: the 3'-provector module for the GOI, the 5'-provector module e.g. for targeting signals of the protein, and the third vector carrying the phage C31 integrase. Here, the 3'-provector module pICH11599 carrying CuAO8-His (SerinGlycine-Linker and 6x His) was used together with the integrase module pICH14011 and the 5'-provector pICH17388 (without targeting signal -> cytosolic expression). Detailed information about the principle of magnICON® can be found in Marillonnet et al., 2005 (or review: Peyret and Lomonosoff, 2015). All three vectors were separately transformed in *A. tumefaciens* GV3101 pMP90. The agrobacteria were grown in LB media with the appropriate antibiotics at 28°C for around 24 h. The bacteria were harvested by centrifugation at 4000 rpm for 10 min, washed with infiltration buffer (10 mM MES-KOH pH 5.7, 10 mM MgCl₂) and centrifuged again. Each pellet was resuspended in infiltration buffer to an OD₆₀₀ of 0.3. After incubation for three hours at RT the three different agrobacterium cultures were mixed in a 1:1:1 ratio. This mixture of pICH11599-CuAO8-His₆, pICH14011 and pICH17388 containing agrobacteria was infiltrated with a syringe in the abaxial site of 6 week old *N. benthamiana* leaves. After infiltration, the plants were kept under standard growth conditions and 10 days post infection (dpi) the leaves were harvested, immediately frozen in liquid N₂ and stored at -80°C until further processing.

5.2.5.10 *Protein purification of CuAO8*

The harvested *N. benthamiana* leaves were ground to a fine powder with mortar and pestle. A small amount of sand was added for improved cell disruption. Two volumes of extraction buffer was added (1x PBS, 150 mM NaCl, 10% Glycerin, 1% Triton X-100, 1 mM DTT, 1x protease inhibitor cocktail (cOmplete, EDTA free, Roche)) and the suspension was kept on ice for 15 min, with regular vortexing in between. After centrifugation at 14 000 rpm for 25 min at 4°C the supernatant was filtered through a 45 µM filter and rebuffed using ZebaSpin desalting columns (1x PBS, 150 mM NaCl, 10% Glycerin, 0.1% Triton X-100, 1 mM DTT, 1x protease inhibitor cocktail (cOmplete, EDTA free, Roche)). The rebuffed extract was loaded on a pre-equilibrated Ni-NTA column (Ni-NTA Agarose, Qiagen). The column was washed using 30 column volumes (CV) of desalting buffer followed by 8 CV of desalting buffer containing 50 mM of imidazole. Elution was performed with 4 CV of desalting buffer containing 100 mM, 200 mM or 300 mM imidazole. The elution fractions were concentrated and rebuffed in 1x PBS with 10K Amicon Ultra-4 (Merck, Germany) filter units. The protein concentration was measured with Bradford reagent and the presence

of CuAO8 was verified by western blotting with anti-His-tag antibody and/or anti-CuAO8 antibody. The protein was stored at -80°C in 50% glycerin.

5.2.5.11 *CuAO8 activity measurement*

The H₂O₂ production by CuAO8 was measured with the Amplex® Red Hydrogen Peroxide/Peroxidase Assay Kit (ThermoFisher Scientific, No. A22118) according to the manufacturer's instructions. Briefly, 100 ng of CuAO8 were incubated with 1 mM substrate (agmatine, putrescine dihydrochloride, spermidine, spermine (Sigma-Aldrich)) in a total reaction volume of 100 µL. H₂O₂ production was detected using resorufin (detecting in 1:1 ratio) and the specific excitation and emission wavelength (Ex: 571 nm; Em: 585 nm) with the TECAN Reader Infinite M1000pro spectrophotometer using a black 96-well plate. The amine oxidase inhibitor Aminoguanidine (AG) was used in a concentration of 0.1 mM in combination with the provided substrates.

5.2.5.12 *Arginase activity measurement*

To measure arginase activity in total protein extracts of five day old seedlings the Arginase Activity Assay Kit (Sigma-Aldrich, No. MAK112) was used. The conversion of arginine to ornithine and urea is catalyzed by arginase. The used kit provides a reagent which reacts with urea producing a colored substance which has an absorbance maximum at 430 nm (see manual). Total protein extracts were prepared by grinding 100 mg of five day old seedlings to a fine powder, adding 500 µL of 50 mM Tris-HCl pH 9, vortexing for 10 sec and keeping the homogenate on ice for 15 min. After centrifugation at full speed with a table top centrifuge for 10 min at 4°C, the supernatant was transferred to a new E-cup and centrifuged again. The supernatant was rebuffered to 50 mM Tris-HCl pH 9.0 using 10K Amicon Ultra 0.5 centrifugal filter (Millipore). The protein extracts were aliquoted and frozen at -80°C after measuring the protein concentration with Bradford reagent. The assay was performed according to manufacturer's instructions. In brief: Urea content was measured in 20 µL of protein extract supplemented with arginine and manganese after 0 and 2 h of incubation at 37°C. Specific arginase activity was calculated in U/L according to this formula (see manual):

$$\frac{(A_{430})_{\text{sample}} - (A_{430})_{\text{blank}}}{(A_{430})_{\text{standard}} - (A_{430})_{\text{water}}} * \frac{1 \text{ mM} * 50 * 10^3}{(V * T)}$$

A = Absorbance

V = sample volume

T = reaction time

The U/L was then converted to U/g protein to account for different protein concentrations in the different samples.

5.2.5.13 Quantification of NO and H₂O₂ production in seedling root tips

Five day old seedlings, grown on vertical ½ MS plates, were harvested to monitor the NO and H₂O₂ production in root tips during stress application. Therefore, the whole seedling was stained with a dye which can react with NO/H₂O₂ thereby producing fluorescence. This fluorescence development was afterwards relatively quantified reflecting the NO/H₂O₂ production during the stress treatment. Different dyes were used in different concentrations and incubation times:

Table 15: Applied fluorescent dyes for the visualization of NO and H₂O₂.

Dye	concentration [µM]	time [min]	purpose	Microscope filter set
Amplex Red	100	20	H ₂ O ₂ detection	Red
DAF-FM DA	15	15	NO detection	eGFP
DAR-4M AM	5	60	NO detection	Red
DCF-DA	20	15	H ₂ O ₂ detection	eGFP
Cu₂FL2E	5	60	NO detection	eGFP

All staining's and treatments were performed in STM buffer (50 mM MES-KOH pH 5.7, 0.25 mM KCl, 1 mM CaCl₂) and in a 24-well plate (ThermoScientific). After the staining procedure the seedlings were washed 3x in STM buffer and then treated with 2 mM Dichloroisonicotinic acid (INA) for 45 min or 200/150 mM NaCl for 6 h. The usage of cPTIO (200 µM), a nitric oxide scavenger or the inhibitor *nor*-NOHA (100µM, Arginase inhibitor (Rabelo et al., 2015)) included a pre-treatment of the seedlings during the staining and a co-treatment during stress application. The solutions of the stress treatment including cPTIO/*nor*-NOHA were replaced with fresh ones after half of the incubation time (INA: 25 min; NaCl: 3 h).

The root tips were observed under the epifluorescence microscope (Olympus BX61, 4x UPlanSApo objective) with eGFP (Excitation filter: 474/23, Absorption filter: 525/45) or Red (Excitation filter: 585/20, Absorption filter: 647/57) filter settings. The microscope software (cellP/cellSens, Olympus Soft Imaging) was set on optimized histogram and flexible exposure time for single optimized images. The pictures were further processed with ImageJ software (version 1.46) for fluorescence intensity quantification. The microscope image included each time a stress treated Col-0 as reference and the tested genotype after stress or control treatment. The fluorescence intensities were each time quantified relative to Col-0 treated with INA/NaCl as an internal control. Afterwards, the values of the relative quantification were normalized to the non-treated control.

5.2.5.14 Quantification of NO production in cotyledons

Five day old seedlings, grown on vertical ½ MS plates, were harvested to monitor the NO production in the cotyledon of five day old seedlings. The experiment was conducted as

described in 5.2.5.13. Staining was performed with DAF-FM DA (15 μ M, 15 min) and NaCl treatment (200 mM, 6h) was applied. The fluorescence intensity of each cotyledon of each genotype was observed with the epifluorescence microscope (Olympus, see 5.2.5.13). Here, the microscope settings were fixed for each image accounting for subsequent fluorescence intensity quantification instead of including a stress treated Col-0 leaf on each picture. The fluorescence was quantified from a representative part of the leaf being in focus. Due to strong stomata auto-fluorescence, no stomata were included in the quantified representative part of the leaf. The intensities were afterwards normalized to the fluorescence of Col-0 NaCl treated.

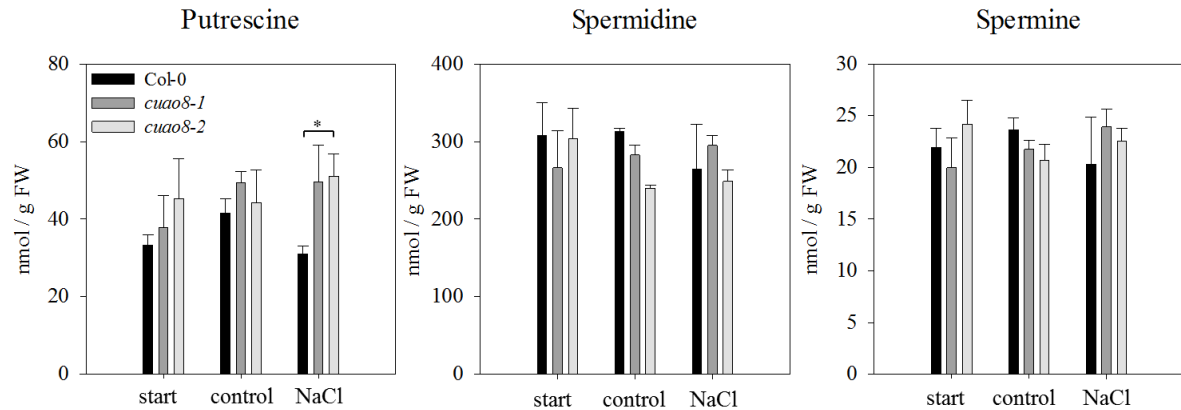
5.2.5.15 Transient expression and localization of GFP-CuAO8 in *N. benthamiana*

A. tumefaciens GV3101 pmP90 was transformed either with pK7WGF2-CuAO8, adding an N-terminal eGFP to CuAO8 or p19 RNA silencing suppressor vector (from *tomato bushy stunt virus*-kindly provided by Prof. Dr. Erich Glawischnig). The agrobacteria were grown in LB media with the appropriate antibiotics at 28°C until an OD₆₀₀ of 1.7-2.2. After harvesting by centrifugation at 4500 rpm for 10 min, the pellet was resuspended in infiltration buffer (10 mM MES-KOH pH5.7, 10 mM MgCl₂) centrifuged again and then resuspended to an OD₆₀₀ of 1.3-1.4. The agrobacterium solutions were kept at RT for at least 3 h, mixed in a 1:1 ratio and then infiltrated with a syringe in the abaxial site of 5 to 6 week old *N. benthamiana* leaves. After infiltration, the plants were kept under standard growth conditions and 5-7 dpi the GFP expression was monitored in leaf discs under the confocal laser scanning microscope (cLSM, Zeiss 510 META, C-Apochromat 40x/1.2 Water correction). To identify the localization of GFP-CuAO8 co-staining's carried out. Visualization of the cell wall was achieved with propidium iodide (PI) and of the plasma membrane with FM4-64. PI and FM4-64 staining was carried out with leaf discs, 3 x vacuum infiltrated in the PI/FM4-64 solution (PI: 10 μ g/ml, FM4-64: 20 μ M; in infiltration buffer) and followed by 15 min incubation in the dark. The following microscopy settings were used:

Table 16: Applied microscope settings (Zeiss, cLSM 510 META).

fluophore	laser line and excitation wavelength	primary dichroic mirror (HFT)	secondary dichroic mirror 1 (NFT)	secondary dichroic mirror 2 (NFT)	filter set
GFP	Argon 458 & 488	UV/488/543/633 Mirror		490	BP505-530 (Ch3)
Chlorophyll	Argon 458 & 488			545	LP650 (Ch3)
FM4-64	He/Ne 514 nm & 543 nm			545	BP565-615 IR (Ch3)/ LP560 (Ch3)
PI	He/Ne 514 nm & 543 nm			490	BP565-615 IR (Ch3)

6. Supplement



Supplemental Figure 1: Effect of NaCl treatment on free polyamine levels in five day old seedlings of Col-0, *cuao8-1* and *cuao8-2*. The free levels of putrescine, spermidine and spermine were determined with HPLC after before and after NaCl (200 mM, 6h) respectively control (buffer, 6h) treatment. Means \pm SE of three individual experiments are shown. (***) Significant difference $P < 0.001$ based on t-test with respect to Col-0. ns = not significant

Supplemental table 1: Amount of proteinogenic amino acids in five day old seedlings. Seedlings of Col-0, *cuao8-1* and *cuao8-2* were grown for five days on $\frac{1}{2}$ MS agar plates then harvested and the amino acids were extracted and measured with LC-MS-MS. Means \pm StDev of five individual experiments are shown.

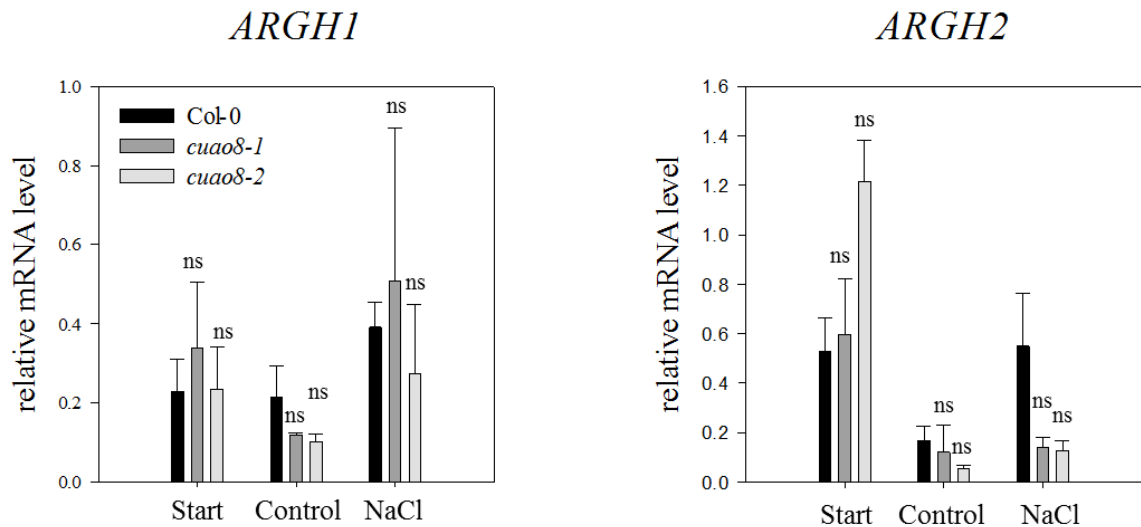
Compound	Col-0	<i>cuao8-1</i>	<i>cuao8-2</i>
[nmol / g FW]			
Asparagine	1265.4 \pm 140.4	1327.9 \pm 370.2	1030.8 \pm 474.6
Tryptophane	6.5 \pm 6.1	6.3 \pm 5.9	6.3 \pm 5.9
Arginine	1008.4 \pm 356.7	986.2 \pm 406.2	727.3 \pm 290.2
Tyrosine	0.3 \pm 0.7	0.6 \pm 1.4	1.1 \pm 1.5
Histidine	153.5 \pm 52.2	166.4 \pm 67.3	190.6 \pm 69.2
Lysine	241.1 \pm 36.4	233.1 \pm 51.9	200.9 \pm 61.7
Phenylalanine	27.7 \pm 2.0	29.9 \pm 6.2	30.5 \pm 3.3
Glutamate	927.4 \pm 366.2	927.2 \pm 334.5	1187.9 \pm 348.2
Aspartate	368.1 \pm 141.7	360.8 \pm 85.9	466.4 \pm 58.7
Proline	131.2 \pm 32.0	136.8 \pm 38.6	216.2 \pm 87.1
Serine	1357.4 \pm 484.3	1102.9 \pm 328.0	1209.8 \pm 436.6
Threonine	152.0 \pm 35.8	161.1 \pm 68.9	165.1 \pm 57.2
Leucin/Isoleucin	65.9 \pm 9.9	64.0 \pm 15.0	64.7 \pm 13.7
Valine	105.5 \pm 24.3	109.1 \pm 22.9	121.7 \pm 27.9
Alanine	225.6 \pm 107.2	260.2 \pm 82.5	304.8 \pm 78.1
Glutamine	5608.8 \pm 3306.0	5051.5 \pm 2558.0	6179.4 \pm 3284.1

Supplemental table 2: Amount of proteinogenic amino acids in five day old seedlings after 6h control treatment (buffer). Seedlings of Col-0, *cuao8-1* and *cuao8-2* were grown for five days on ½ MS agar plates and treated for 6h with buffer (control treatment). The amino acids were extracted and measured with LC-MS-MS. Means ± StDev of five individual experiments are shown.

Compound	Col-0	<i>cuao8-1</i>	<i>cuao8-2</i>
[nmol / g FW]			
Asparagine	2021.5 ± 214.7	2059.0 ± 169.4	2160.3 ± 219.0
Tryptophane	30.7 ± 8.1	31.2 ± 10.1	24.3 ± 7.7
Arginine	1213.8 ± 520.4	1147.8 ± 237.0	970.9 ± 302.0
Tyrosine	74.0 ± 8.2	83.5 ± 16.8	63.2 ± 11.2
Histidine	237.8 ± 80.3	246.6 ± 43.1	242.2 ± 62.3
Lysine	612.8 ± 172.5	645.0 ± 87.9	524.0 ± 76.5
Phenylalanine	182.7 ± 18.4	198.3 ± 42.5	157.8 ± 22.7
Glutamate	1030.2 ± 346.9	1215.0 ± 378.2	1276.3 ± 341.0
Aspartate	307.6 ± 55.7	378.7 ± 56.2	394.7 ± 79.6
Proline	110.0 ± 28.1	142.1 ± 28.9	235.4 ± 172.0
Serine	1111.6 ± 588.8	1147.4 ± 363.8	1055.6 ± 517.5
Threonine	215.1 ± 50.7	244.0 ± 62.6	237.4 ± 75.0
Leucin/Isoleucin	224.8 ± 45.5	258.5 ± 34.6	208.2 ± 19.9
Valine	316.7 ± 65.4	367.3 ± 42.5	315.4 ± 18.9
Alanine	183.8 ± 58.8	275.3 ± 75.0	308.8 ± 63.3
Glutamine	5338.7 ± 3039.0	5608.5 ± 2906.6	6036.5 ± 2859.5

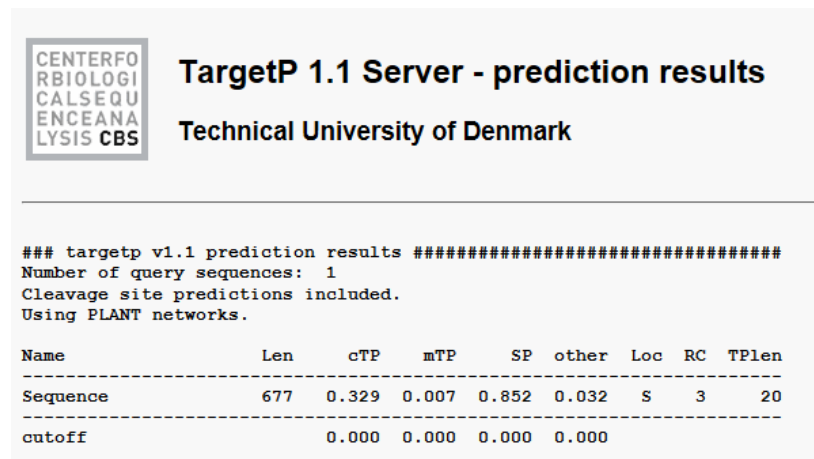
Supplemental table 3: Amount of proteinogenic amino acids in five day old seedlings after NaCl treatment. Seedlings of Col-0, *cuao8-1* and *cuao8-2* were grown for five days on ½ MS agar plates and treated for 6h with NaCl (200 mM). The amino acids were extracted and measured with LC-MS-MS. Means ± StDev of five individual experiments are shown.

Compound	Col-0	<i>cuao8-1</i>	<i>cuao8-2</i>
[nmol / g FW]			
Asparagine	1813.5 ± 449.0	1633.3 ± 487.5	1868.7 ± 522.1
Tryptophane	28.4 ± 8.1	29.3 ± 8.6	33.1 ± 4.8
Arginine	978.9 ± 465.0	799.8 ± 299.4	844.6 ± 404.2
Tyrosine	110.6 ± 49.7	119.6 ± 55.3	116.2 ± 35.8
Histidine	178.2 ± 68.6	165.2 ± 56.7	208.4 ± 72.7
Lysine	684.1 ± 276.6	694.4 ± 299.4	646.0 ± 176.2
Phenylalanine	192.5 ± 69.4	207.7 ± 86.0	203.1 ± 57.5
Glutamate	866.4 ± 514.9	963.9 ± 600.5	1125.1 ± 474.9
Aspartate	379.2 ± 246.1	421.1 ± 280.6	440.1 ± 196.9
Proline	223.1 ± 77.8	253.7 ± 89.4	339.3 ± 96.7
Serine	1089.3 ± 623.5	1038.2 ± 593.9	1080.1 ± 485.1
Threonine	190.0 ± 52.7	205.8 ± 34.4	222.0 ± 60.7
Leucin/Isoleucin	277.6 ± 123.8	309.3 ± 142.6	306.8 ± 92.7
Valine	290.9 ± 130.8	320.8 ± 152.1	333.2 ± 96.6
Alanine	289.9 ± 231.8	350.0 ± 237.1	372.8 ± 155.4
Glutamine	5268.7 ± 2965.2	5123.0 ± 2916.5	5540.3 ± 2553.1



Supplemental Figure 2: Relative mRNA level of arginase 1 and 2 in five day old seedlings. Relative expression of arginase 1 (*ARGH1*) and 2 (*ARGH2*) in five day old seedlings before (Start) and after NaCl (200 mM, 6h) respectively control (buffer, 6h) treatment. Means \pm SE of at least three individual experiments are shown. (***) Significant difference $P < 0.001$ based on ANOVA (Holm-Sidak test) with respect to Col-0. ns = not significant

Target P



Supplemental Figure 3: Results of the TargetP software predicting for possible localization of CuAO8 based on N-terminal pre-sequences. <http://www.cbs.dtu.dk/services/TargetP/> (Emanuelsson et al., 2007). Len: Sequence length; cTP: chloroplast transit sequence, mTP: mitochondrial transit sequence, SP/S: secretory pathway (= highest score the more likely is located); LOC: localization based on the scores; RC: reliability class: from 1 to 5 where 1 indicates the strongest prediction; TPlen: predicted presequence length

```

CuA08 MAQVHLTIF-IFSSIFVISSSSFIPPPFPDPLTETELKLVRNIIINKSYPIGHNHKFTFQ 59
CuA02 MAPLHFTILILFSFVIVVSSSFTPPRHPFDPLTETELKLVRTIINKSYVPGPNHKFTFQ 60
** :*: **: * * :*: ***** * ***** :* *****

CuA08 YVGLNEPEKSLVLSWHSSPDRNVKPPRQAFVIARDKGMREIVDFSTRAIVSNKIHVG 119
CuA02 YVGLNEPNKSLVLSWYSSPNHTIKPPRQAFVIARDNGKTRREIVLDFSSRAIVSDKIHVG 120
*****:*****:***: :*: *****: * :*: *: *****: *****

CuA08 NGNPMLTIDEQQAATAVQKYKPFCDSEIKRGLNLSEVVVTSSTMGWFGETKT--KRFIR 177
CuA02 NGYPMLSNDQEAEASTELVVKPFIDSVAKRGLNVSEIVFTTSTIGWYGETKAEAEVRIR 180
** ***: * *: * * : * * * * * : * * * * * : * * * * * : * * * * * : * * * * *

CuA08 TIPFFYLNGSVNTYLRPIEGMTIIVNLDQMKTGFKDRFTGPMKANGREYRISKLPKPPFG 237
CuA02 LMPFFYLDGTVMNMYLRPIEGMTIIVNLDQMKVSEFKDRSVVTMPIANGTEYRISKLPKPPFG 240
.: *****: * * * * * : * * * * * : * * * * * : * * * * * : * * * * *

CuA08 PSLRSVAVFQPDGPGFKIDGHVVRWANWEFHMSFDVRAGLVISLASIFDMDMNRVYQVLY 297
CuA02 PTLHNAVLLQPDGPGFKVDGHIWRWANWEFHISFDVRAGIVISLASLFDTDVVKYRQVLY 300
* * : * * : * * : * * : * * : * * : * * : * * : * * : * * : * * : * *

CuA08 KGHLSMFVPMYDNDWYFISYLDGCGEGQTAVSLEPYTDCPPNAAFMDGIFPGQDG 357
CuA02 KGHLSMFIPYMDPSDDWYFITYLDCGDFGCGQCAVSLQPYTDCPAGAVFMDGIFAGQDG 360
*****:*****:*****:*****:***** *****:***** * *****

CuA08 TPTKISNVMCIFEKYAGDIMWRHTEAEVPLKITEVVRPDVSLVARMVTVGNVDYIIEYE 417
CuA02 TPAKIPKVMCIFEKYAGDIMWRHTEAEIPNLEITEVVRPDVSLVARIVTVGNVDYIVDYE 420
* * : * * : * * : * * : * * : * * : * * : * * : * * : * * : * * : * *

CuA08 FKPSGSIKMGVGLTGVLEVKPVEYVHTSEIKE-DDIYGTIVADNTVGVNHDHFVTFRLDL 476
CuA02 FKPSGSIKMGVGLTGVLEVKPVEYIHTSEIKLGEDIHGTIVADNTVGVNHDHFVTFRLHL 480
*****:*****:*****:*****:***** *****:***** * *****

CuA08 DIDGTENSFVRTELVTTRKTPKSVNTPRKS YWTTKRNTAKTEADARVKLGLRAEELVVVNP 536
CuA02 DIDGTENSFVRNELVTTTRSPKSVNTPRKYWTTKPKTAKTEAEARVKLGLKAEELVVVNP 540
*****:*****:*****:*****:***** *****:*****:*****:*****

CuA08 TKKTKHGNEVGYRLLPGPASSPLLVQDDYPQIRAAFTNYNVWITPYNKSEVWASGLYADR 596
CuA02 NRKTKHGNEVGYRLLHGSAGPLLAQDDFPQIRAAFTNYNVWITPYNRSEVWAGGLYADR 600
.: ***** * * : * * : * * : * * : * * : * * : * * : * * : * * : * *

CuA08 SQGDDTLAVWSQRDREIENKDIVMWTYVGFHHVPCQEDFPTMPTMFGGFELRPTNFFEQN 656
CuA02 SQGDDTLAVWSQRNRKIEKEDIVMWTYVGFHHVPSQEDYPTMPTLSSGGFELRPTNFFERN 660
*****:*****:*****:*****:***** *****:*****:*****:*****

CuA08 PVLKAKPFNLTTIPKCTTKNE 677
CuA02 PVLKTKPKVTTARKCTPKND 681
*****: * * : * * * * * :

```

Supplemental Figure 4: Multiple sequence alignment of CuA08 and CuA02. Sequence Identity 79.736%; Similar positions: 99. Uni-Prot Server, CuA08: F4IAX0; CuA02: F4IAX1, Clustal Omega (1.2.2) software. Default parameters; HHalgin algorithm (Söding, 2005).

7. Literature

- Airenne TT, Nymalm Y, Kidron H, Smith DJ, Pihlavisto M, Salmi M, Jalkanen S, Johnson MS, Salminen T a.** (2005) Crystal structure of the human vascular adhesion protein 1: Unique structural features with functional implications. *Protein Sci* **14**: 1964–1974
- Albertos P, Romero-Puertas MC, Tatematsu K, Mateos I, Sánchez-Vicente I, Nambara E, Lorenzo O** (2015) S-nitrosylation triggers ABI5 degradation to promote seed germination and seedling growth. *Nat Commun* **6**: 8669
- Arvidsson S, Kwasniewski M, Riaño-Pachón DM, Mueller-Roeber B** (2008) QuantPrime—a flexible tool for reliable high-throughput primer design for quantitative PCR. *BMC Bioinformatics* **9**: 465
- Barber MJ, Kay CJ** (1996) Superoxide production during reduction of molecular oxygen by assimilatory nitrate reductase. *Arch Biochem Biophys* **326**: 227–32
- Barroso JB, Corpas FJ, Carreras A, Sandalio LM, Valderrama R, Palma JM, Lupiáñez JA, Del Río LA** (1999) Localization of nitric-oxide synthase in plant peroxisomes. *J Biol Chem* **274**: 36729–36733
- Berkowitz DE, White R, Li D, Minhas KM, Cernetich A, Kim S, Burke S, Shoukas AA, Nyhan D, Champion HC, et al** (2003) Arginase Reciprocally Regulates Nitric Oxide Synthase Activity and Contributes to Endothelial Dysfunction in Aging Blood Vessels. *Circulation* **108**: 2000–2006
- Bethke PC, Badger MR, Jones RL** (2004) Apoplastic synthesis of nitric oxide by plant tissues. *Plant Cell* **16**: 332–341
- Bogdan C** (2015) Nitric oxide synthase in innate and adaptive immunity: An update. *Trends Immunol* **36**: 161–178
- Borrell A, Culiánez-Macia FA, Altabella T, Besford RT, Flores D, Tiburcio AF** (1995) Arginine Decarboxylase Is Localized in Chloroplasts. *Plant Physiol* **109**: 771–776
- Boucher JL, Moali C, Tenu JP** (1999) Nitric oxide biosynthesis, nitric oxide synthase inhibitors and arginase competition for L-arginine utilization. *Cell Mol Life Sci* **55**: 1015–1028
- Bouchera J-L, Geneta A, Vadona S, Delaforgea M, Hen Y, Mansuya D** (1992) Cytochrome P450 catalyzes the oxidation of N omega-hydroxy-L-arginine by NADPH and O₂ to nitric oxide and citrulline. *Biochem Biophys Res Commun* **187**: 880–886
- Bouchereau A, Aziz A, Larher F, Martin-Tanguy J** (1999) Polyamines and environmental challenges: recent development. *Plant Sci* **140**: 103–125
- Bradford MM** (1976) Rapid and Sensitive Method for Quantitation of Microgram Quantities of Protein Utilizing Principle of Protein-Dye Binding. *Anal Biochem* **72**: 248–254

- Bright J, Desikan R, Hancock JT, Weir IS, Neill SJ** (2006) ABA-induced NO generation and stomatal closure in Arabidopsis are dependent on H₂O₂ synthesis. *Plant J* **45**: 113–122
- Butt YKC, Lum JHK, Lo SCL** (2003) Proteomic identification of plant proteins probed by mammalian nitric oxide synthase antibodies. *Planta* **216**: 762–71
- Cai D, Klinman JP** (1994) Evidence for a Self-catalytic Mechanism of. *J Biol Chem* **269**, No.51: 32039–32042
- Caldwell RB, Toque HA, Narayanan SP, Caldwell RW** (2015) Arginase: an old enzyme with new tricks. *Trends Pharmacol Sci* **36**: 395–405
- Campbell MG, Smith BC, Potter CS, Carragher B, Marletta M** (2014) Molecular architecture of mammalian nitric oxide synthases. *Proc Natl Acad Sci U S A* **111**: E3614-23
- Campbell WH** (1999) NITRATE REDUCTASE STRUCTURE, FUNCTION AND REGULATION: Bridging the Gap between Biochemistry and Physiology. *Annu Rev Plant Physiol Plant Mol Biol* **50**: 277–303
- Cervelli M, Cona A, Angelini R, Polticelli F, Federico R, Mariottini P** (2001) A barley polyamine oxidase isoform with distinct structural features and subcellular localization. *Eur J Biochem* **268**: 3816–3830
- Cervelli M, Tavladoraki P, Di Agostino S, Angelini R, Federico R, Mariottini P** (2000) Isolation and characterization of three polyamine oxidase genes from *Zea mays*. *Plant Physiol Biochem* **38**: 667–677
- Chen H, McCaig BC, Melotto M, He SY, Howe GA** (2004) Regulation of plant arginase by wounding, jasmonate, and the phytotoxin coronatine. *J Biol Chem* **279**: 45998–46007
- Corpas FJ, Palma JM, Del Río LA, Barroso JB** (2009) Evidence supporting the existence of L-arginine-dependent nitric oxide synthase activity in plants. *New Phytol* **184**: 1–3
- Corpas FJ, Palma JM, Sandalio LM, Valderrama R, Barroso JB, del Río LA** (2008) Peroxisomal xanthine oxidoreductase: Characterization of the enzyme from pea (*Pisum sativum* L.) leaves. *J Plant Physiol* **165**: 1319–1330
- Cortese-Krott MM, Rodriguez-Mateos A, Kuhnle GGC, Brown G, Feelisch M, Kelm M** (2012) A multilevel analytical approach for detection and visualization of intracellular NO production and nitrosation events using diaminofluoresceins. *Free Radic Biol Med* **53**: 2146–2158
- Daff S** (2010) NO synthase: Structures and mechanisms. *Nitric Oxide - Biol Chem* **23**: 1–11
- Dean J V., Harper JE** (1988) The Conversion of Nitrite to Nitrogen Oxide(s) by the Constitutive NAD(P)H-Nitrate Reductase Enzyme from Soybean. *Plant Physiol* **88**: 389–395
- Delledonne M, Xia Y, Dixon RA, Lamb C** (1998) Nitric oxide functions as a signal in plant disease resistance. *Nature* **394**: 585–588

- Desikan R, Griffiths R, Hancock J, Neill S** (2002) A new role for an old enzyme: nitrate reductase-mediated nitric oxide generation is required for abscisic acid-induced stomatal closure in *Arabidopsis thaliana*. *Proc Natl Acad Sci U S A* **99**: 16314–8
- Durner J, Wendehenne D, Klessig DF** (1998) Defense gene induction in tobacco by nitric oxide, cyclic GMP, and cyclic ADP-ribose. *Proc Natl Acad Sci U S A* **95**: 10328–33
- Eick M, Stöhr C** (2012) Denitrification by plant roots? New aspects of plant plasma membrane-bound nitrate reductase. *Protoplasma* **249**: 909–918
- Emanuelsson O, Brunak S, von Heijne G, Nielsen H** (2007) Locating proteins in the cell using TargetP, SignalP and related tools. *Nat Protoc* **2**: 953–971
- Feelisch M, Martin JF** (1995) The early role of nitric oxide in evolution. *Trends Ecol Evol* **10**: 496–499
- Fellenberg C, Ziegler J, Handrick V, Vogt T** (2012) Polyamine Homeostasis in Wild Type and Phenolamide Deficient *Arabidopsis thaliana* Stamens. *Front Plant Sci* **3**: 1–11
- Fernandez-Marcos M, Sanz L, Lewis DR, Muday GK, Lorenzo O** (2011) Nitric oxide causes root apical meristem defects and growth inhibition while reducing PIN-FORMED 1 (PIN1)-dependent acropetal auxin transport. *Proc Natl Acad Sci* **108**: 18506–18511
- Fernández-Marcos M, Sanz L, Lorenzo Ó** (2012) Nitric oxide: An emerging regulator of cell elongation during primary root growth. *Plant Signal Behav* **7**: 196–200
- Filippou P, Antoniou C, Fotopoulos V** (2013) The nitric oxide donor sodium nitroprusside regulates polyamine and proline metabolism in leaves of *Medicago truncatula* plants. *Free Radic Biol Med* **56**: 172–183
- Fincato P, Moschou PN, Ahou A, Angelini R, Roubelakis-Angelakis KA, Federico R, Tavladoraki P** (2012) The members of *Arabidopsis thaliana* PAO gene family exhibit distinct tissue- and organ-specific expression pattern during seedling growth and flower development. *Amino Acids* **42**: 831–841
- Flores HE, A.W. G** (1982) Polyamines and Plant Stress : Activation of Putrescine Biosynthesis by Osmotic Shock. *Science* (80-) **217**: 1259–1261
- Flores T, Todd CD, Tovar-Mendez A, Dhanoa PK, Correa-Aragunde N, Hoyos ME, Brownfield DL, Mullen RT, Lamattina L, Polacco JC** (2008) Arginase-Negative Mutants of *Arabidopsis* Exhibit Increased Nitric Oxide Signaling in Root Development. *Plant Physiol* **147**: 1936–1946
- Foresi N, Correa-Aragunde N, Parisi G, Caló G, Salerno G, Lamattina L** (2010) Characterization of a nitric oxide synthase from the plant kingdom: NO generation from the green alga *Ostreococcus tauri* is light irradiance and growth phase dependent. *Plant Cell* **22**: 3816–3830
- Forneris F, Binda C, Vanoni MA, Mattevi A, Battaglioli E** (2005) Histone demethylation catalysed by LSD1 is a flavin-dependent oxidative process. *FEBS Lett* **579**: 2203–2207
- Foyer CH, Valadier M-H, Migge A, Becker TW** (1998) Drought-Induced Effects on Nitrate Reductase Activity and mRNA and on the Coordination of Nitrogen and Carbon Metabolism in Maize Leaves 1. *Plant Physiol* **117**: 283–292

- Fröhlich A, Durner J** (2011) The hunt for plant nitric oxide synthase (NOS): Is one really needed? *Plant Sci* **181**: 401–404
- Frungillo L, Skelly MJ, Loake GJ, Spoel SH, Salgado I** (2014) S-nitrosothiols regulate nitric oxide production and storage in plants through the nitrogen assimilation pathway. *Nat Commun* **5**: 5401
- Fuell C, Elliott KA, Hanfrey CC, Franceschetti M, Michael AJ** (2010) Polyamine biosynthetic diversity in plants and algae. *Plant Physiol Biochem* **48**: 513–520
- Fujita M, Shinozaki K** (2014) Identification of polyamine transporters in plants: Paraquat transport provides crucial clues. *Plant Cell Physiol* **55**: 855–861
- Garcia-Mata C, Gay R, Sokolovski S, Hills A, Lamattina L, Blatt MR** (2003) Nitric oxide regulates K⁺ and Cl⁻ channels in guard cells through a subset of abscisic acid-evoked signaling pathways. *Proc Natl Acad Sci U S A* **100**: 11116–11121
- Ghuge SA, Carucci A, Rodrigues-Pousada RA, Tisi A, Franchi S, Tavladoraki P, Angelini R, Cona A** (2015a) The Apoplastic Copper AMINE OXIDASE1 Mediates Jasmonic Acid-Induced Protoxylem Differentiation in Arabidopsis Roots. *Plant Physiol* **168**: 690–707
- Ghuge S, Tisi A, Carucci A, Rodrigues-Pousada R, Franchi S, Tavladoraki P, Angelini R, Cona A** (2015b) Cell Wall Amine Oxidases: New Players in Root Xylem Differentiation under Stress Conditions. *Plants* **4**: 489–504
- Gibbs DJ, MdIsa N, Movahedi M, Lozano-Juste J, Mendiondo GM, Berckhan S, Mar??n-de la Rosa N, Vicente Conde J, Sousa Correia C, Pearce SP, et al** (2014) Nitric Oxide Sensing in Plants Is Mediated by Proteolytic Control of Group VII ERF Transcription Factors. *Mol Cell* **53**: 369–379
- Gobert AP, Daulouede S, Lepoivre M, Boucher JL, Bouteille B, Buguet A, Cespuglio R, Veyret B, Vincendeau P** (2000) L-arginine availability modulates local nitric oxide production and parasite killing in experimental trypanosomiasis. *Infect Immun* **68**: 4653–4657
- Gobert AP, McGee DJ, Akhtar M, Mendz GL, Newton JC, Cheng Y, Mobley HLT, Wilson KT** (2001) *Helicobacter pylori* arginase inhibits nitric oxide production by eukaryotic cells: A strategy for bacterial survival. *Proc Natl Acad Sci* **98**: 13844–13849
- Godber BLJ, Doel JJ, Sapkota GP, Blake DR, Stevens CR, Eisenthal R, Harrison R** (2000) Reduction of nitrite to nitric oxide catalyzed by xanthine oxidoreductase. *J Biol Chem* **275**: 7757–7763
- Goldraj A, Polacco JC** (1999) Arginase Is Inoperative in Developing Soybean Embryos. *Plant Physiol* **119**: 297–303
- Griffiths MJD, Messent M, Macallister RJ, Evans TW** (1993) Aminoguanidine selectively inhibits inducible nitric-oxide synthase. *Br J Pharmacol* **110**: 963–968
- Gross I, Durner J** (2016) In Search of Enzymes with a Role in 3', 5'-Cyclic Guanosine Monophosphate Metabolism in Plants. *Front Plant Sci* **7**: 576
- Guo F-Q, Okamoto M, Crawford NM** (2003) Identification of a Plant Nitric Oxide Synthase Gene Involved in Hormonal Signaling. *Science* (80-) **302**: 100–103

- Gupta KJ, Fernie AR, Kaiser WM, Dongen JT Van** (2011) On the origins of nitric oxide. *Trends Plant Sci* **16**: 160–8
- Gupta KJ, Kaiser WM** (2010) Production and scavenging of nitric oxide by barley root mitochondria. *Plant Cell Physiol* **51**: 576–584
- Hanfrey C, Sommer S, Mayer MJ, Burtin D, Michael AJ** (2001) Arabidopsis polyamine biosynthesis: Absence of ornithine decarboxylase and the mechanism of arginine decarboxylase activity. *Plant J* **27**: 551–560
- He Y, D MS, Amasino RM** (2003) Regulation of Flowering Time by Histone Acetylation in Arabidopsis. *Science* (80-) **302**: 1751–1754
- He Y, Tang R-H, Hao Y, Stevens RD, Cook CW, Ahn SM, Jing L, Yang Z, Chen L, Guo F, et al** (2004) Nitric oxide represses the Arabidopsis floral transition. *Science* **305**: 1968–71
- Hebelstrup KH, Jensen EØ** (2008) Expression of NO scavenging hemoglobin is involved in the timing of bolting in Arabidopsis thaliana. *Planta* **227**: 917–927
- Holtgreffe S, Gohlke J, Starmann J, Druce S, Klocke S, Altmann B, Wojtera J, Lindermayr C, Scheibe R** (2008) Regulation of plant cytosolic glyceraldehyde 3-phosphate dehydrogenase isoforms by thiol modifications. *Physiol Plant* **133**: 211–228
- Hwang HJ, Kim EH, Cho YD** (2001) Isolation and properties of arginase from a shade plant, ginseng (*Panax ginseng* C.A. Meyer) roots. *Phytochemistry* **58**: 1015–1024
- Illingworth C, Michael AJ** (2012) Plant ornithine decarboxylase is not post-transcriptionally feedback regulated by polyamines but can interact with a cytosolic ribosomal protein S15 polypeptide. *Amino Acids* **42**: 519–527
- Jasid S, Simontacchi M, Bartoli CG, Puntarulo S** (2006) Chloroplasts as a nitric oxide cellular source. Effect of reactive nitrogen species on chloroplastic lipids and proteins. *Plant Physiol* **142**: 1246–1255
- Jeandroz S, Wipf D, Stuehr DJ, Lamattina L, Melkonian M, Tian Z, Zhu Y, Carpenter EJ, Wong GK, Wendehenne D, et al** (2016) Occurrence, structure, and evolution of nitric oxide synthase-like proteins in the plant kingdom. *Sci Signal* **9**: re2
- Jiang D, Yang W, He Y, Amasino RM** (2007) *Arabidopsis* Relatives of the Human Lysine-Specific Demethylase1 Repress the Expression of *FWA* and *FLOWERING LOCUS C* and Thus Promote the Floral Transition. *Plant Cell* **19**: 2975–2987
- Kaiser WM, Huber SC** (2001) Post-translational regulation of nitrate reductase : mechanism , physiological relevance and environmental triggers. **52**: 1981–1989
- Kaiser WM, Weiner H, Kandlbinder A, Tsai C, Rockel P, Sonoda M, Planchet E** (2002) Modulation of nitrate reductase: some new insights, an unusual case and a potentially important side reaction. *J Exp Bot* **53**: 875–882
- Kamada-Nobusada T, Hayashi M, Fukazawa M, Sakakibara H, Nishimura M** (2008) A putative peroxisomal polyamine oxidase, AtPAO4, is involved in polyamine catabolism in Arabidopsis thaliana. *Plant Cell Physiol* **49**: 1272–1282

- Kang JH, Cho YD** (1990) Purification and Properties of Arginase from Soybean , Glycine max, Axes. *Plant Physiol* **93**: 1230–1234
- Kaur-Sawhney R, Flores HE, Galston a W** (1980) Polyamine-induced DNA Synthesis and Mitosis in Oat Leaf Protoplasts. *Plant Physiol* **65**: 368–71
- Kim DW, Watanabe K, Murayama C, Izawa S, Niitsu M, Michael AJ, Berberich T, Kusano T** (2014) Polyamine Oxidase 5 Regulates Arabidopsis thaliana Growth Through A Thermospermine Oxidase Activity. *Plant Physiol* **165**: 1575–1590
- Klema VJ, Wilmot CM** (2012) The role of protein crystallography in defining the mechanisms of biogenesis and catalysis in copper amine oxidase. *Int J Mol Sci* **13**: 5375–5405
- Klepper L** (1979) NITRIC OXIDE (NO) AND NITROGEN DIOXIDE (NO₂) EMISSIONS FROM HERBICIDE-TREATED SOYBEAN PLANTS *. *Atmos Enviroment* **13**: 537–542
- Ko vamees O, Shemyakin A, Pernow J** (2016) Amino acid metabolism reflecting arginase activity is increased in patients with type 2 diabetes and associated with endothelial dysfunction. *Diabetes Vasc Dis Res* **13**: 354–360
- Kojima H, Nagano T** (2000) Fluorescent indicators for nitric oxide. *Adv Mater* **12**: 763–765
- Kolbert Z, Bartha B, Erdei L** (2008) Exogenous auxin-induced NO synthesis is nitrate reductase-associated in Arabidopsis thaliana root primordia. *J Plant Physiol* **165**: 967–975
- Konishi M, Yanagisawa S** (2011) The regulatory region controlling the nitrate-responsive expression of a nitrate reductase gene, NIA1, in Arabidopsis. *Plant Cell Physiol* **52**: 824–836
- Koyanagi T, Matsumura K, Kuroda S, Tanizawa K** (2000) Molecular cloning and heterologous expression of pea seedling copper amine oxidase. *Biosci Biotechnol Biochem* **64**: 717–722
- Kozlova V, Staniek K, Nohl H** (1999) Nitrite reductase activity is a novel function of mammalian mitochondria. *FEBS Lett* **454**: 127–130
- Krumpelman PM, Freyermuth SK, Cannon JF, Fink GR, Polacco JC** (1995) Nucleotide sequence of Arabidopsis thaliana arginase expressed in yeast. *Plant Physiol* **107**: 1479–1480
- Kurian L, Palanimurugan R, Gödderz D, Dohmen RJ** (2011) Polyamine sensing by nascent ornithine decarboxylase antizyme stimulates decoding of its mRNA. *Nature* **477**: 490–494
- Kusano T, Berberich T, Tateda C, Takahashi Y** (2008) Polyamines: Essential factors for growth and survival. *Planta* **228**: 367–381
- Li H, Kundu TK, Zweier JL** (2009) Characterization of the magnitude and mechanism of aldehyde oxidase-mediated nitric oxide production from nitrite. *J Biol Chem* **284**: 33850–33858

- Li H, Meininger CJ, Hawker JR, Haynes TE, Kepka-Lenhart D, Mistry SK, Morris SM, Wu G** (2001) Regulatory role of arginase I and II in nitric oxide, polyamine, and proline syntheses in endothelial cells. *Am J Physiol Endocrinol Metab* **280**: E75-82
- Liu F, Guo FQ** (2013) Nitric Oxide Deficiency Accelerates Chlorophyll Breakdown and Stability Loss of Thylakoid Membranes during Dark-Induced Leaf Senescence in Arabidopsis. *PLoS One*. doi: 10.1371/journal.pone.0056345
- Liu JH, Nada K, Honda C, Kitashiba H, Wen XP, Pang XM, Moriguchi T** (2006) Polyamine biosynthesis of apple callus under salt stress: Importance of the arginine decarboxylase pathway in stress response. *J Exp Bot* **57**: 2589–2599
- Liu W, Li R-J, Han T-T, Cai W, Fu Z-W, Lu Y-T** (2015) Salt stress reduces root meristem size by nitric oxide-mediated modulation of auxin accumulation and signaling in Arabidopsis. *Plant Physiol* **168**: 343–356
- Ljubisavljevic S, Stojanovic I, Pavlovic R, Pavlovic D** (2014) The Importance of Nitric Oxide and Arginase in the Pathogenesis of Acute Neuroinflammation: Are Those Contra Players with the Same Direction? *Neurotox Res* **26**: 392–399
- Maia LB, Pereira V, Mira L, Moura JJG** (2015) Nitrite Reductase Activity of Rat and Human Xanthine Oxidase, Xanthine Dehydrogenase, and Aldehyde Oxidase: Evaluation of Their Contribution to NO Formation in Vivo. *Biochemistry* **54**: 685–710
- Marietta MA, Hurshmant AR, Rusche KM** (1998) Catalysis by nitric oxide synthase. *Curr Opin Chem Biol* **2**: 656–663
- Marillonnet S, Giritch A, Gils M, Kandzia R, Klimyuk V, Gleba Y** (2004) In planta engineering of viral RNA replicons: Efficient assembly by recombination of DNA modules delivered by Agrobacterium. *Proc Natl Acad Sci* **101**: 6852–6857
- Marillonnet S, Thoeringer C, Kandzia R, Klimyuk V, Gleba Y** (2005) Systemic Agrobacterium tumefaciens-mediated transfection of viral replicons for efficient transient expression in plants. *Nat Biotechnol* **23**: 718–723
- Martín-Falquina a, Legaz ME** (1984) Purification and Properties of the Constitutive Arginase of *Evernia prunastri*. *Plant Physiol* **76**: 1065–9
- McQuade LE, Lippard SJ** (2010) Fluorescence-based nitric oxide sensing by Cu(II) complexes that can be trapped in living cells. *Inorg Chem* **49**: 7464–7471
- Meng Z, Meng Z, Zhang R, Liang C, Wan J, Wang Y, Zhai H, Guo S** (2015) Expression of the rice arginase gene OsARG in cotton influences the morphology and nitrogen transition of seedlings. *PLoS One* **10**: 1–19
- Mérigout P, Lelandais M, Bitton F, Renou J-P, Briand X, Meyer C, Daniel-Vedele F** (2008) Physiological and transcriptomic aspects of urea uptake and assimilation in Arabidopsis plants. *Plant Physiol* **147**: 1225–1238
- Miggea, Bork C, Hell R, Becker TW** (2000a) Negative regulation of nitrate reductase gene expression by glutamine or asparagine accumulating in leaves of sulfur-deprived tobacco. *Planta* **211**: 587–95

- Migge A, Bork C, Hell R, Becker TW** (2000b) Negative regulation of nitrate reductase gene expression by glutamine or asparagine accumulating in leaves of sulfur-deprived tobacco. *Planta* **211**: 587–95
- Millar TM, Stevens CR, Benjamin N, Eisenthal R, Harrison R, Blake DR** (1998) Xanthine oxidoreductase catalyses the reduction of nitrates and nitrite to nitric oxide under hypoxic conditions. *FEBS Lett* **427**: 225–228
- Miller G, Suzuki N, Ciftci-Yilmaz S, Mittler R** (2010) Reactive oxygen species homeostasis and signalling during drought and salinity stresses. *Plant, Cell Environ* **33**: 453–467
- Miller-Fleming L, Olin-Sandoval V, Campbell K, Ralser M** (2015) Remaining Mysteries of Molecular Biology: The Role of Polyamines in the Cell. *J Mol Biol* **427**: 3389–3406
- Modolo L V., Augusto O, Almeida IMG, Pinto-Maglio CAF, Oliveira HC, Seligman K, Salgado I** (2006) Decreased arginine and nitrite levels in nitrate reductase-deficient *Arabidopsis thaliana* plants impair nitric oxide synthesis and the hypersensitive response to *Pseudomonas syringae*. *Plant Sci* **171**: 34–40
- Mohapatra S, Minocha R, Long S, Minocha SC** (2010) Transgenic manipulation of a single polyamine in poplar cells affects the accumulation of all amino acids. *Amino Acids* **38**: 1117–1129
- Mohapatra S, Minocha R, Long S, Minocha SC** (2009) Putrescine overproduction negatively impacts the oxidative state of poplar cells in culture. *Plant Physiol Biochem* **47**: 262–271
- Møller SG, McPherson MJ** (1998) Developmental expression and biochemical analysis of the *Arabidopsis atao1* gene encoding an H₂O₂-generating diamine oxidase. *Plant J* **13**: 781–91
- Moreau M, Gyu IL, Wang Y, Crane BR, Klessig DF** (2008) AtNOS/AtNOA1 is a functional *Arabidopsis thaliana* cGTPase and not a nitric-oxide synthase. *J Biol Chem* **283**: 32957–32967
- Mori M** (2007) Regulation of nitric oxide synthesis and apoptosis by arginase and arginine recycling. *J Nutr* **137**: 1616S–1620S
- Moschou PN, Sanmartin M, Andriopoulou AH, Rojo E, Sanchez-Serrano JJ, Roubelakis-Angelakis KA** (2008) Bridging the gap between plant and mammalian polyamine catabolism: a novel peroxisomal polyamine oxidase responsible for a full back-conversion pathway in *Arabidopsis*. *Plant Physiol* **147**: 1845–57
- Moschou PN, Wu J, Cona A, Tavladoraki P, Angelini R, Roubelakis-Angelakis KA** (2012) The polyamines and their catabolic products are significant players in the turnover of nitrogenous molecules in plants. *J Exp Bot* **63**: 5003–5015
- Navakoudis E, Lütz C, Langebartels C, Lütz-Meindl U, Kotzabasis K** (2003) Ozone impact on the photosynthetic apparatus and the protective role of polyamines. *Biochim Biophys Acta - Gen Subj* **1621**: 160–169

- Page AF, Cseke LJ, Minocha R, Turlapati SA, Podila GK, Ulanov A, Li Z, Minocha SC** (2016) Genetic manipulation of putrescine biosynthesis reprograms the cellular transcriptome and the metabolome. *BMC Plant Biol* **16**: 113
- Pagnussat GC, Lanteri ML, Lamattina L** (2003) Nitric Oxide and Cyclic GMP Are Messengers in the Indole Acetic Acid-Induced Adventitious Rooting Process. *PLANT Physiol* **132**: 1241–1248
- Peyret H, Lomonossoff GP** (2015) When plant virology met Agrobacterium: The rise of the deconstructed clones. *Plant Biotechnol J* **13**: 1121–1135
- Pietrangeli P, Nocera S, Federico R, Mondovì B, Morpurgo L** (2004) Inactivation of copper-containing amine oxidases by turnover products. *Eur J Biochem* **271**: 146–152
- Planas-Portell J, Gallart M, Tiburcio AF, Altabella T** (2013) Copper-containing amine oxidases contribute to terminal polyamine oxidation in peroxisomes and apoplast of *Arabidopsis thaliana*. *BMC Plant Biol* **13**: 109 (1-13)
- Planchet E, Gupta KJ, Sonoda M, Kaiser WM** (2005) Nitric oxide emission from tobacco leaves and cell suspensions : rate limiting factors and evidence for the involvement of mitochondrial electron transport. 732–743
- Pollard KJ, Samuels ML, Crowley KA, Hansen JC, Peterson CL** (1999) Functional interaction between GCN5 and polyamines: A new role for core histone acetylation. *EMBO J* **18**: 5622–5633
- Quigley F, Rosenberg JM, Shachar-Hill Y, Bohnert HJ** (2002) From genome to function: the *Arabidopsis* aquaporins. *Genome Biol.* doi: 10.1186/gb-2001-3-1-research0001
- Quinet M, Ndayiragije A, Lefèvre I, Lambillotte B, Dupont-Gillain CC, Lutts S** (2010) Putrescine differently influences the effect of salt stress on polyamine metabolism and ethylene synthesis in rice cultivars differing in salt resistance. *J Exp Bot* **61**: 2719–2733
- Rabelo LA, Ferreira FO, Nunes-Souza V, Fonseca LJS da, Goulart MOF** (2015) Arginase as a Critical Prooxidant Mediator in the Binomial Endothelial Dysfunction-Atherosclerosis. *Oxid Med Cell Longev* **2015**: 1–12
- Renault H, El Amrani A, Palanivelu R, Updegraff EP, Yu A, Renou JP, Preuss D, Bouchereau A, Deleu C** (2011) GABA accumulation causes cell elongation defects and a decrease in expression of genes encoding secreted and cell wall-related proteins in *Arabidopsis thaliana*. *Plant Cell Physiol* **52**: 894–908
- Renault H, Roussel V, El Amrani A, Arzel M, Renault D, Bouchereau A, Deleu C** (2010) The *Arabidopsis* pop2-1 mutant reveals the involvement of GABA transaminase in salt stress tolerance. *BMC Plant Biol* **10**: 20
- Roach T, Colville L, Beckett RP, Minibayeva F V., Havaux M, Kranner I** (2015) A proposed interplay between peroxidase, amine oxidase and lipoxygenase in the wounding-induced oxidative burst in *Pisum sativum* seedlings. *Phytochemistry* **112**: 130–138
- Rockel P, Strube F, Rockel A, Wildt J, Kaiser WM** (2002) Regulation of nitric oxide (NO) production by plant nitrate reductase in vivo and in vitro. **53**: 103–110

- Rosales EP, Iannone MF, Groppa MD, Benavides MP** (2011) Nitric oxide inhibits nitrate reductase activity in wheat leaves. *Plant Physiol Biochem* **49**: 124–130
- Sanchez-Rangel D, Chavez-Martinez AI, Rodriguez-Hernandez AA, Maruri-Lopez I, Urano K, Shinozaki K, Jimenez-Bremont JF** (2016) Simultaneous Silencing of Two Arginine Decarboxylase Genes Alters Development in *Arabidopsis*. *Front Plant Sci* **7**: 300
- Sanz-Luque E, Ocaña-Calahorra F, Llamas A, Galvan A, Fernandez E** (2013) Nitric oxide controls nitrate and ammonium assimilation in *Chlamydomonas reinhardtii*. *J Exp Bot* **64**: 3373–3383
- Satriano J** (2004) Arginine pathways and the inflammatory response: interregulation of nitric oxide and polyamines: review article. *Amino Acids* **26**: 321–329
- Seligman K, Saviani EE, Oliveira HC, Pinto-Maglio CAF, Salgado I** (2008) Floral transition and nitric oxide emission during flower development in *Arabidopsis thaliana* is affected in nitrate reductase-deficient plants. *Plant Cell Physiol* **49**: 1112–1121
- Shepard EM, Dooley DM** (2015) Inhibition and oxygen activation in copper amine oxidases. *Acc Chem Res* **48**: 1218–1226
- Shi H, Ye T, Chen F, Cheng Z, Wang Y, Yang P, Zhang Y, Chan Z** (2013) Manipulation of arginase expression modulates abiotic stress tolerance in *Arabidopsis*: Effect on arginine metabolism and ROS accumulation. *J Exp Bot* **64**: 1367–1379
- Shi HT, Li RJ, Cai W, Liu W, Wang CL, Lu YT** (2012) Increasing nitric oxide content in *Arabidopsis thaliana* by expressing rat neuronal nitric oxide synthase resulted in enhanced stress tolerance. *Plant Cell Physiol* **53**: 344–357
- Shi Y, Lan F, Matson C, Mulligan P, Whetstine JR, Cole PA, Casero RA, Shi Y** (2004) Histone demethylation mediated by the nuclear amine oxidase homolog LSD1. *Cell* **119**: 941–953
- Shu S, Yuan Y, Chen J, Sun J, Zhang W, Tang Y, Zhong M, Guo S** (2015) The role of putrescine in the regulation of proteins and fatty acids of thylakoid membranes under salt stress. *Sci Rep* **5**: 14390
- Söding J** (2005) Protein homology detection by HMM-HMM comparison. *Bioinformatics* **21**: 951–960
- Sokolovski S, Hills A, Gay R, Garcia-Mata C, Lamattina L, Blatt MR** (2005) Protein phosphorylation is a prerequisite for intracellular Ca²⁺ release and ion channel control by nitric oxide and abscisic acid in guard cells. *Plant J* **43**: 520–529
- Spiro RG** (2002) Protein glycosylation: nature, distribution, enzymatic formation, and disease implications of glycopeptide bonds. *Glycobiology* **12**: 43R–56R
- Stöhr C, Strube F, Marx G, Ullrich WR, Rockel P** (2001) A plasma membrane-bound enzyme of tobacco roots catalyses the formation of nitric oxide from nitrite. *Planta* **212**: 835–841
- Stoimenova M, Igamberdiev AU, Gupta KJ, Hill RD** (2007) Nitrite-driven anaerobic ATP synthesis in barley and rice root mitochondria. *Planta* **226**: 465–474

- Takahashi Y, Cong R, Sagor GHM, Niitsu M, Berberich T, Kusano T** (2010) Characterization of five polyamine oxidase isoforms in *Arabidopsis thaliana*. *Plant Cell Rep* **29**: 955–965
- Tanou G, Ziogas V, Belghazi M, Christou A, Filippou P, Job D, Fotopoulos V, Molassiotis A** (2014) Polyamines reprogram oxidative and nitrosative status and the proteome of citrus plants exposed to salinity stress. *Plant, Cell Environ* **37**: 864–885
- Tavladoraki P, Cona A, Angelini R** (2016) Copper-Containing Amine Oxidases and FAD-Dependent Polyamine Oxidases Are Key Players in Plant Tissue Differentiation and Organ Development. *Front Plant Sci*. doi: 10.3389/fpls.2016.00824
- Tavladoraki P, Rossi MN, Saccuti G, Perez-Amador MA, Polticelli F, Angelini R, Federico R** (2006) Heterologous expression and biochemical characterization of a polyamine oxidase from *Arabidopsis* involved in polyamine back conversion. *Plant Physiol* **141**: 1519–32
- Thiele B, Füllner K, Stein N, Oldiges M, Kuhn AJ, Hofmann D** (2008) Analysis of amino acids without derivatization in barley extracts by LC-MS-MS. *Anal Bioanal Chem* **391**: 2663–2672
- Tiburcio AF, Altabella T, Bitrián M, Alcázar R** (2014) The roles of polyamines during the lifespan of plants: from development to stress. *Planta* **240**: 1–18
- Tischner R, Planchet E, Kaiser WM** (2004) Mitochondrial electron transport as a source for nitric oxide in the unicellular green alga *Chlorella sorokiniana*. *FEBS Lett* **576**: 151–155
- Tun NN, Livaja M, Kieber JJ, Scherer GFE** (2008) Zeatin-induced nitric oxide (NO) biosynthesis in *Arabidopsis thaliana* mutants of NO biosynthesis and of two-component signaling genes. *New Phytol* **178**: 515–531
- Tun NN, Santa-Catarina C, Begum T, Silveira V, Handro W, Segal Floh EI, Scherer GFE** (2006) Polyamines induce rapid biosynthesis of nitric oxide (NO) in *Arabidopsis thaliana* seedlings. *Plant Cell Physiol* **47**: 346–354
- Urano K, Yoshiba Y, Nanjo T, Igarashi Y, Seki M, Sekiguchi F** (2003) Characterization of *Arabidopsis* genes involved in biosynthesis of polyamines in abiotic stress responses and. 1917–1926
- Verma S, Mishra SN** (2005) Putrescine alleviation of growth in salt stressed *Brassica juncea* by inducing antioxidative defense system. *J Plant Physiol* **162**: 669–677
- Víteček J, Lojek A, Valacchi G, Kubala L** (2012) Arginine-based inhibitors of nitric oxide synthase: Therapeutic potential and challenges. *Mediators Inflamm*. doi: 10.1155/2012/318087
- Votyakova T V, Wallace HM, Dunbar B, Wilson SB** (1999) The covalent attachment of polyamines to proteins in plant mitochondria. *Eur J Biochem* **260**: 250–257
- Wang H, Wang AX, Aylor K, Barrett EJ** (2013a) Nitric oxide directly promotes vascular endothelial insulin transport. *Diabetes* **62**: 4030–4042

- Wang X, Ying W, Dunlap K a, Lin G, Satterfield MC, Burghardt RC, Wu G, Bazer FW** (2014) Arginine decarboxylase and agmatinase: an alternative pathway for de novo biosynthesis of polyamines for development of mammalian conceptuses. *Biol Reprod* **90**: 84
- Wang Y, Ries A, Wu K, Yang A, Crawford NM** (2010) The Arabidopsis Prohibitin Gene PHB3 Functions in Nitric Oxide – Mediated Responses and in Hydrogen Peroxide – Induced Nitric Oxide Accumulation. *Plant Cell* **22**: 249–259
- Wang Y, Yang L, Zheng Z, Grumet R, Loescher W, Zhu JK, Yang P, Hu Y, Chan Z** (2013b) Transcriptomic and Physiological Variations of Three Arabidopsis Ecotypes in Response to Salt Stress. *PLoS One* **8**: e69036
- Wardman P** (2007) Fluorescent and luminescent probes for measurement of oxidative and nitrosative species in cells and tissues: Progress, pitfalls, and prospects. *Free Radic Biol Med* **43**: 995–1022
- Weiner H, Kaiser WM** (1999) 14-3-3 Proteins Control Proteolysis of Nitrate Reductase in Spinach Leaves. *FEBS Lett* **455**: 75–78
- Weiner H, Kaiser WM** (2000) Binding to 14-3-3 proteins is not sufficient to inhibit nitrate reductase in spinach leaves. *FEBS Lett* **480**: 1–4
- Wimalasekera R, Villar C, Begum T, Scherer GFE** (2011) COPPER AMINE OXIDASE1 (CuAO1) of Arabidopsis thaliana Contributes to Abscisic Acid-and Polyamine-Induced Nitric Oxide Biosynthesis and Abscisic Acid Signal Transduction. *Mol Plant* **4**: 663–678
- Winter G, Todd CD, Trovato M, Forlani G, Funck D** (2015) Physiological implications of arginine metabolism in plants. *Front Plant Sci* **6**: 1–14
- Wojtera-Kwiczor J, Groß F, Leffers H-M, Kang M, Schneider M, Scheibe R** (2013) Transfer of a redox-signal through the cytosol by redox-dependent microcompartmentation of glycolytic enzymes at mitochondria and actin cytoskeleton. *Front Plant Sci* **3**: 1–19
- Yamasaki H, Sakihama Y** (2000) Simultaneous production of nitric oxide and peroxynitrite by plant nitrate reductase: In vitro evidence for the NR-dependent formation of active nitrosyl species. *FEBS Lett* **468**: 89–92
- Yanagisawa S** (2014) Transcription factors involved in controlling the expression of nitrate reductase genes in higher plants. *Plant Sci* **229**: 167–171
- Yoda H** (2006) Polyamine Oxidase Is One of the Key Elements for Oxidative Burst to Induce Programmed Cell Death in Tobacco Cultured Cells. *Plant Physiol* **142**: 193–206
- Yu X, Sukumaran S** (1998) Differential Expression of the Arabidopsis Nia1 and Cytokinin-Induced Nitrate Reductase Activity Is Correlated With Increased Nia1 Transcription and mRNA Levels. *Plant Cell* **10**: 1091–1096
- Yue J, Hu X, Sun H, Yang Y, Huang J** (2012) Widespread impact of horizontal gene transfer on plant colonization of land. *Nat Commun* **3**: 1152

- Zarei A, Trobacher CP, Cooke AR, Meyers AJ, Christopher Hall J, Shelp BJ** (2015) Apple fruit copper amine oxidase isoforms: Peroxisomal MdaO1 prefers diamines as substrates, whereas extracellular MdaO2 exclusively utilizes monoamines. *Plant Cell Physiol* **56**: 137–147
- Zeidler D, Zähringer U, Gerber I, Dubery I, Hartung T, Bors W, Hutzler P, Durner J** (2004) Innate immunity in *Arabidopsis thaliana*: lipopolysaccharides activate nitric oxide synthase (NOS) and induce defense genes. *Proc Natl Acad Sci U S A* **101**: 15811–15816
- Zhang Y, Wang L, Liu Y, Zhang Q, Wei Q, Zhang W** (2006) Nitric oxide enhances salt tolerance in maize seedlings through increasing activities of proton-pump and Na⁺/H⁺ antiport in the tonoplast. *Planta* **224**: 545–555
- Zhang Z, Naughton D, Winyard PG, Benjamin N, Blake DR, Symons MC** (1998) Generation of nitric oxide by a nitrite reductase activity of xanthine oxidase: a potential pathway for nitric oxide formation in the absence of nitric oxide synthase activity. *Biochem Biophys Res Commun* **249**: 767–772
- Zhao M-G, Chen L, Zhang L-L, Zhang W-H** (2009) Nitric reductase-dependent nitric oxide production is involved in cold acclimation and freezing tolerance in *Arabidopsis*. *Plant Physiol* **151**: 755–67
- Zhao S, Fernald RD** (2005) Comprehensive Algorithm for Quantitative Real-Time Polymerase Chain Reaction. *J Comput Biol* **12**: 1047–1064
- Zhu MY, Iyo A, Piletz JE, Regunathan S** (2004) Expression of human arginine decarboxylase, the biosynthetic enzyme for agmatine. *Biochim Biophys Acta - Gen Subj* **1670**: 156–164
- Zonia, L., Norm E. Stebbens JCP** (1995) Essential role of urease in germination of nitrogen-limited *Arabidopsis thaliana* seeds. *Plant Physiol* **107**: 1097–1103
- Zottini M, Costa A, De Michele R, Ruzzene M, Carimi F, Lo Schiavo F** (2007) Salicylic acid activates nitric oxide synthesis in *Arabidopsis*. *J Exp Bot* **58**: 1397–1405

Book:

- Weigel & Glazebrook** (2001) *Arabidopsis –A laboratory manual*. Cold Spring Harbor Laboratory (New York)

Danksagung

Zum Gelingen dieser Arbeit möchte ich folgenden Personen von ganzem Herzen danken:

Einen besonderen Dank möchte ich an Prof. Dr. Jörg Durner aussprechen, der mir die Möglichkeit gab an seinem Institut meine Doktorarbeit durchführen zu können. Die Freiheit eigenen Ideen nachzugehen und immer eine offene Tür vorzufinden war sehr wertvoll für mich. Auch die Möglichkeit zahlreiche Konferenzen zu besuchen, von denen vor allem auch die ICAR eine interessante Erfahrung war, hat die Doktorarbeit zu einer besonderen Erfahrung gemacht.

Ebenso möchte ich meinem Zweitprüfer und Thesis-Komitee Teilnehmer Prof. Dr. Erich Glawischnig danken, für hilfreiche Diskussionen und Anmerkungen in entspannter Atmosphäre was für einen erfolgreichen Dialog unersetzlich ist.

Prof. Dr. Schwechheimer möchte ich danken, dass er sich bereit erklärt hat, den Vorsitz meiner Verteidigung zu übernehmen.

Auch danken möchte ich Dr. Björn Thiele von Forschungszentrum Jülich, für die Messung der Aminosäuren in Arabidopsis.

Auch möchte ich mich bei Dr. Jeremy Astier für seine Unterstützung vor allem zu Beginn der Doktorarbeit bedanken. Die Hilfestellungen haben meine wissenschaftliche und persönliche Entwicklung gefördert, was mir in Zukunft sicher helfen wird. Sein Optimismus war immer wieder sehr erfrischend, bei dem Vortrag im NO-meeting unersetzlich, und hat mich bei Rückschlägen wieder aufgebaut.

Meiner Arbeitsgruppe möchte ich danken (Dr. Frank Gaupels, Dr. Jeremy Astier, Dr. Inonge Gross, Katharina Meier, Dörte Kasten, Claudia Scheler und Prof. Dr. Jörg Durner) für hilfreiche Diskussionen im Labormeeeting ohne die meine Doktorarbeit nicht so erfolgreich verlaufen wäre.

Ein großer Dank geht an Dörte Kasten, Jessica Lutterbach, Claudia Scheler, Eva König und Wei Zhang, für ihre Unterstützung im Labor aber auch im Privaten. Mit euch konnte ich immer lachen und das Aushelfen mit Süßigkeiten war lebenswichtig.

Auch allen anderen aktuellen und vergangenen Labormitgliedern möchte ich für eine entspannte Laboratmosphäre und eure Unterstützung danken.

Ein ganz besonderer Dank geht an dich Alexander. Dein Rückhalt in allen Lebenslagen, dein toller Humor und dein klares Denken waren und sind für mich von großer Bedeutung. Vor allem aber dein unerschütterlicher Glaube an mich war unersetzlich und leistete einen großen Beitrag zu dieser Doktorarbeit.

Am Ende geht auch ein großer Dank an meine Familie die mich immer unterstützt hat und die Entscheidung nach München zu gehen von Anfang an für gut und richtig befunden hat.

Curriculum

Felicitas Barbara Groß

D-Hörwarthstraße 33
80804 München
Mobil: 01737338974
E-Mail: felicitas.gross@gmail.com
geboren am 3. März 1986

Ausbildung

Studium:

- | | |
|-----------------|---|
| 01/2013-09/2016 | Technische Universität München, Helmholtz-Zentrum München

Promotion (Prof. Dr. Jörg Durner)

Institut für Biochemische Pflanzenpathologie

Titel: COPPER AMINE OXIDASE 8 (CuAO8) participates in the regulation of nitric oxide production during salt stress in seedlings of <i>Arabidopsis thaliana</i> |
| 10/2009-02/2012 | Universität Osnabrück

Studium: Biologie der Zellen, Master of Science (Note 1,2)

Schwerpunkt: Pflanzenphysiologie

Masterarbeit (Prof. Dr. Renate Scheibe): Einfluss von Redox-Modifikationen auf die Interaktion glykolytischer Enzyme mit dem Aktin-Zytoskelett (Note 1,0) |
| 10/2006-09/2009 | Universität Osnabrück

Studium: Biologie der Zellen, Bachelor of Science (Note: 2,2)

Bachelorarbeit (Prof. Dr. Renate Scheibe): Die spezifische Funktion der Isoform Ferredoxin 1 im zyklischen Elektronentransport von <i>Arabidopsis</i> (Note: 1,2) |

10/2005-09/2006

Westfälische Wilhelms-Universität Münster

Studium für Grund-, Haupt-, und Realschullehramt

Fächer: Biologie und Geographie

Schule

Juni 2005

Kopernikus-Gymnasium Rheine

Allgemeine Hochschulreife (Abitur)

Berufliche Erfahrung

03/2012-07/2012

wissenschaftliche Mitarbeiterin an der Universität Osnabrück

Abteilung Pflanzenphysiologie (Prof. Dr. Renate Scheibe),
Untersuchungen zu Protein-Interaktionen und der Einfluss von
Redoxstress, Etablierung neuer Methodik, Betreuung
studentischer Praktika

1/2011-08/2011

Studentische Hilfskraft an der Universität Osnabrück,

Abteilung Pflanzenphysiologie (Prof. Dr. Renate Scheibe),
Betreuung studentischer Praktika, Labor-Hilfsarbeiten

Konferenzbeiträge

07/2013: International Plant NO Club Meeting, München, Deutschland

Mündlicher Vortrag

08/2014: International Conference on Arabidopsis Research (ICAR), Vancouver, Kanada,

Poster Präsentation

06/2015: International Conference on Reactive Oxygen and Nitrogen Species in Plants from
model systems to field, Verona, Italien

Poster Präsentation

09/2015 Botanikertagung, Freising, Deutschland

Poster Präsentation

Publikationen

Wojtera-Kwiczor J, **Groß F**, Leffers HM, Kang M, Schneider M, Scheibe R. (2013) Transfer of a Redox-Signal through the Cytosol by Redox-Dependent Microcompartmentation of Glycolytic Enzymes at Mitochondria and Actin Cytoskeleton. *Front Plant Sci* **3**: 1–19

Groß F, Durner J, Gaupels F. (2013) Nitric oxide, antioxidants and prooxidants in plant defence responses. *Front Plant Sci* **4**: 419

Groß F, Rudolf EE, Thiele B, Durner J, Astier J. (2016) COPPER AMINE OXIDASE 8 (CuAO8) affects nitric oxide production in *Arabidopsis thaliana* seedlings by regulating arginase activity. (in preparation)

Eidstattliche Erklärung

Ich erkläre an Eides statt, dass ich die bei der promotionsführenden Einrichtung

**Wissenschaftszentrum Weihenstephan für Ernährung, Landnutzung und Umwelt
(WZW)**

Lehrstuhl für Biochemische Pflanzenpathologie

der TUM zur Promotionsprüfung vorgelegte Arbeit mit dem Titel:

**COPPER AMINE OXIDASE 8 (CuAO8) participates in the regulation of nitric oxide
production during salt stress in seedlings of *Arabidopsis thaliana***

unter der Anleitung und Betreuung durch Prof. Dr. Jörg Durner ohne sonstige Hilfe erstellt und bei der Abfassung nur die gemäß § 6 Abs. 6 und 7 Satz 2 angegebenen Hilfsmittel benutzt habe.

Ich habe keine Organisation eingeschaltet, die gegen Entgelt Betreuerinnen und Betreuer für die Anfertigung von Dissertationen sucht, oder die mir obliegenden Pflichten hinsichtlich der Prüfungsleistungen für mich ganz oder teilweise erledigt.

Ich habe die Dissertation in dieser oder ähnlicher Form in keinem anderen Prüfungsverfahren vorgelegt.

Ich habe den angestrebten Doktorgrad noch nicht erworben und bin nicht in einem früheren Promotionsverfahren für den angestrebten Doktorgrad endgültig gescheitert.

Die öffentlich zugängliche Promotionsordnung der TUM ist mir bekannt, insbesondere habe ich die Bedeutung von § 28 (Nichtigkeit der Promotion) und § 29 (Entzug des Doktorgrades) zur Kenntnis genommen. Ich bin mir der Konsequenzen einer falschen Eidesstaatlichen Erklärung bewusst.

Mit der Aufnahme meiner personenbezogenen Daten in die Alumni-Datei bei der TUM bin ich einverstanden.

München, den 22.9.2016

Felicitas Barbara Groß